doi : 10.17596/0003441

R/V Mirai MR22-03
Cruise Report

Distribution and impact of lithogenic materials from east Asia on the western Pacific ecosystem in spring

April 14–May 20, 2022

Japan Agency for Marine-Earth Science and Technology
(JAMSTEC)

Cover photo by Fumine Okada (NME)

CONTENTS

1. Outline of MR22-03

Cruise ID:	MR22-03
Name of vessel:	R/V Mirai
Title of cruise:	Distribution and impact of lithogenic materials from east Asia on the western Pacific ecosystem in spring
Captain:	Haruhiko Inoue (NME)
Chief Scientist:	Koji Sugie (RIGC, JAMSTEC)
Chief Technician:	Yutaro Murakami (NME)
	Daiki Ushiromura (MWJ)
Cruise period:	April 14–May 20, 2022
Port call:	Shimizu - Shimizu
Research area:	Western North Pacific

1.1 Objectives

1.1.1 Process study of the ecosystem in the western North Pacific

Phytoplankton in the ocean contribute approximately 40–50% of global primary production. However, phytoplankton productivity is often limited at least one macro- or micronutrient. In the western North Pacific, nitrate/phosphate- and iron-depletion limit phytoplankton productivity in the subtropical and subarctic region, respectively. Clarifying the biogeochemical cycling of those limiting nutrients is important to better understand the marine ecosystem. Here, we conducted multi-disciplinary cruise to quantify the flux of the multiple sources of limiting nutrients into the surface mixed layer, the impact of the addition of limiting nutrients on phytoplankton productivity, and the fate of organic carbon.

1.1.2 Ecosystem monitorings

The Station K2 is located at 47°00'N 160°00'E in the western subarctic Pacific, and ecosystem monitoring (including St. KNOT, 44°00'N 155°00'E) was started since 1997. Our monitoring efforts clarified the ecosystem processes and recent change in the ecosystem of the western subarctic Pacific such as warming and ocean acidification. In the aspect of long-term change in marine ecosystem, decadal and bi-decadal change are known to affect ecosystem status. This cruise contributes the continuous monitoring efforts by means of water samplings and recovery and deployment of moorings at St. K2. In addition, seawater samples were taken in the eastern Tsugaru Strait area where started ecosystem monitoring since 2010 to understand current change in local ecosystem.

1.2 List of research proposals

P22-04 Distribution and impact of lithogenic materials from east Asia on the western Pacific ecosystem in spring. (Koji Sugie, JAMSTEC)

Collaborative proposal

P22-04-1: Observational study of the spatiotemporal change in oceanic atmospheric aerosol. (Kazuma Aoki, Toyama University)

P22-04-2: Study of the interaction of atmosphere and ocean with respect to clouds and rain system. (Masaki Katsumata, JAMSTEC)

P22-04-3: In situ measurement of vertical profile and long-term mooring of pH with electrode sensors; Development of on-board measurement of toxic metal and iodine; Exploring useful microorganisms in the mesopelagic layer. (Kiminori Shitashima, Tokyo University of Marine Science and Technology)

JS22-03: Improvements of high-frequency radar and ship board ADCP data in the eastern Tsugaru Strait. (Hitoshi Kaneko, JAMSTEC)

1.3 List of participants

Table 1.3.1. Onboard participants

Name	Affiliation	Role
Koji Sugie	JAMSTEC	Chief Scientist
Tetsuichi Fujiki	JAMSTEC	2nd chief scientist
Katsunori Kimoto	JAMSTEC	3rd chef scientist
Masahide Wakita	JAMSTEC	Water sampling leader
Kazuhiko Matsumoto	JAMSTEC	
Fumikazu Taketani	JAMSTEC	
Minoru Kitamura	JAMSTEC	
Yoshiyuki Nakano	JAMSTEC	
Masatoshi Kishi	JAMSTEC	
Yoshinao Mino	Nagoya U.	
Takuhei Shiozaki	U. of Tokyo	
Qin Hong-wei	U. of Tokyo	
Yusuke Sasaki	U. of Tokyo	
Koki Shitashima	TUMST	
Mayu Ohi	TUMST	
Nanako Tonedachi	TUMST	
Miaka Yamaguchi	TUMST	
Yutararo Murakami	NME	Chief technician
Ryo Oyama	NME	
Fumino Okada	NME	
Daiki Ushiromura	MWJ	Chief technician
Hiroaki Sako	MWJ	
Masaki Furuhata	MWJ	
Nagisa Fujiki	MWJ	
Hiroyuki Nakajima	MWJ	
Masahiro Orui	MWJ	
Rei Ito	MWJ	
Misato Kuwahara	MWJ	
Yuta Oda	MWJ	
Yuko Miyoshi	MWJ	
Tun Htet Aung	MWJ	
Shiori Ariga	MWJ	
Airi Hara	MWJ	
Riho Fujioka	MWJ	

Abbreviations: JAMSTEC: Japan Agency for Marine-Earth Science and Technology; Nagoya U.: Nagoya University; U. of Tokyo: University of Tokyo; TUMST: Tokyo University of Marine Science and Technology; NME: Nippon Marine E

Table 1.3.2. Crew

Name	Title
Haruhiko Inoue	Master
Masato Chiba	Chief Officer
Takeshi Egashira	1st Officer
Shozo Fujii	Jr. 1st Officer
Yasuhito Iida	2nd Officer
Shoma Abe	3rd Officer
Tadashi Abe	Chief Engineer
Daisuke Gibu	1st Engineer
Yoshinobu Hiratsuka	2nd Engineer
Kenta Ikeguchi	3rd Engineer
Yoichi Inoue	Chief Radio Operator
Kazuyoshi Kudo	Boatswain
Tsuyoshi Sato	Quarter Master
Hideaki Tamotsu	Quarter Master
Hideaki Okubo	Quarter Master
Shinya Ueno	Quarter Master
Shohei Uehara	Quarter Master
Takuma Tokunaga	Sailor
Rin Yamaguchi	Sailor
Shin Ito	Sailor
Ryota Kume	Sailor
Kosei Hirai	Sailor
Hiroyuki Oishi	No. 1 Oiler
Kazuya Ando	Oiler
Daiki Sato	Oiler
Tamaki Fujishima	Assistant Oiler
Shion Narabe	Assistant Oiler
Fubuki Homma	Assistant Oiler
Kyotaro Maruyama	Assistant Oiler
Kiyotaka Kosuji	Chief Steward
Toshiyuki Asano	Steward
Kenichi Okumura	Steward
Tatsuya Shiraishi	Steward
Mizuki Nakano	Steward
Hayato Okada	Steward

Table 1.3.3. Non-boarding scientists and on-land supporters

Name	Affiliation
Yugo Kanaya	JAMSTEC
Nobuhisa Eguchi	JAMSTEC
Hiroshi Uchida	JAMSTEC
Shinya Koketsu	JAMSTEC
Minako Kurisu	JAMSTEC
Chunmao Zhu	JAMSTEC
Akihoko Murata	JAMSTEC
Masaki Katsumata	JAMSTEC
Kyoko Taniguchi	JAMSTEC
Shigeki Hosoda	JAMSTEC
Hitoshi Kaneko	JAMSTEC
Kenichi Sasaki	JAMSTEC
Takuma Miyakawa	JAMSTEC
Takashi Sekiya	JAMSTEC
Ichiro Yasuda	U. of Tokyo
Kazuma Aoki	Toyama University

Group photo of the MR22-03 cruise.

1.4 Cruise track and log

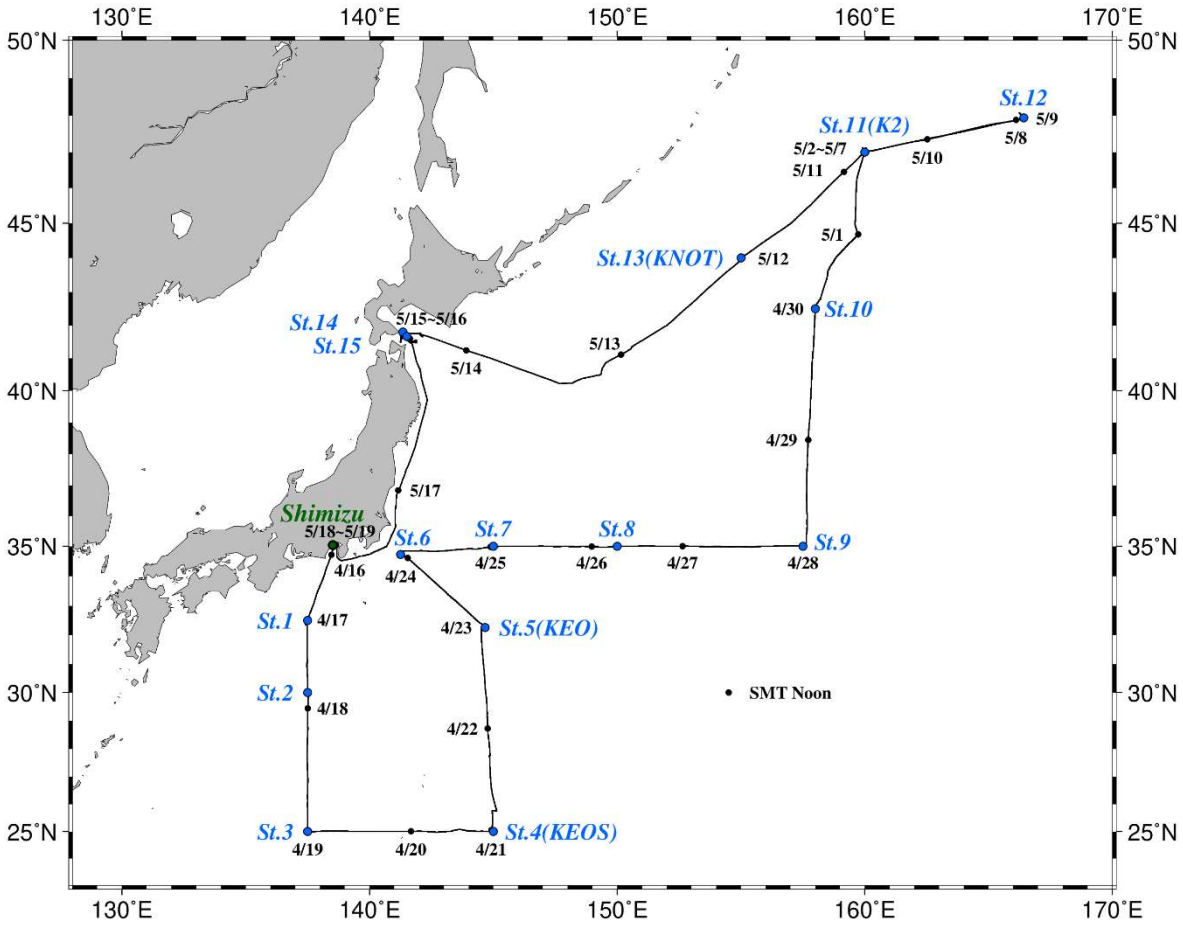

Figure 1.4-1 Whole track of MR22-03

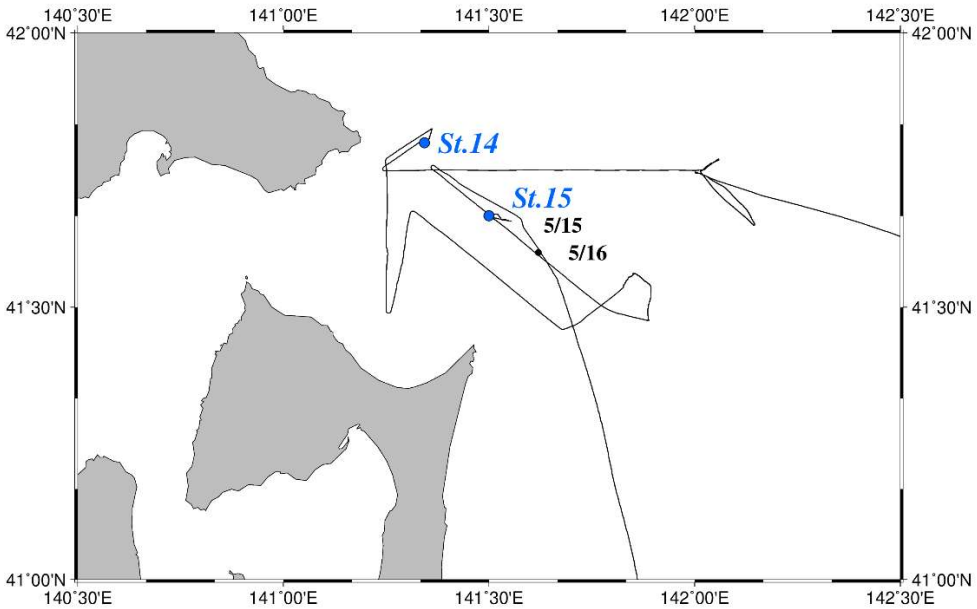

Figure 1.4-2 Part track of MR22-03

Cruise Log

U.T.C.		S.M.T.		Position		Event logs
Date	Time	Date	Time	Lat.	Lon.	
4.16	1:00	4.16	10:00	35-01.93N	138-30.30E	Departure from Shimizu
	7:17		16:17	33-56.39N	138-07.68E	Start sea water pump and SSV pump
	15:36	4.17	0:36	32-30.18N	137-29.52E	Arrival at St.1
	19:10		4:10	32-30.18N	137-30.05E	TVMP #1
	19:58		4:58	32-30.51N	137-29.88E	NORPAC net #1(150m)
	21:05		6:05	32-31.29N	137-29.85E	CTD cast #1 (200 m)
	22:08		7:08	32-31.22N	137-29.94E	Marine Snow Catcher #1
4.17	1:09		10:09	32-30.90N	137-30.08E	CTD cast #2 (3000 m)
	4:00		13:00	32-31.75N	137-29.35E	Departure from St.1
	7:00		16:00	32-00.53N	137-29.08E	Start C-band doppler radar observation
	18:30	4.18	3:30	30-01.99N	137-30.22E	Arrival at St.2
	19:07		4:07	29-59.98N	137-30.05E	TVMP #2
	20:14		5:14	30-00.13N	137-30.85E	NORPAC net #2 (150m)
	21:25		6:25	30-00.29N	137-31.25E	CTD cast #3 (3000 m)
4.18	0:06		9:06	30-00.08N	137-31.70E	Departure from St.2
	21:26	4.19	6:26	25-36.64N	137-29.90E	CTD cast #4 (200 m)
4.19	0:54		9:54	24-59.96N	137-29.87E	Arrival at St.3
	0:57		9:57	24-59.94N	137-29.91E	Marine Snow Catcher #2
	2:24		11:24	25-00.03N	137-29.70E	TVMP #3
	3:30		12:30	25-00.21N	137-29.21E	NORPAC net #3 (150m)
	4:33		13:33	25-00.33N	137-29.06E	CTD cast #5 (3000 m)
	7:31		16:31	25-00.37N	137-28.95E	Calibration for magnetometer #1
	8:00		17:00	24-59.94N	137-30.32E	Departure from St.3
	21:26	4.20	6:26	25-00.02N	140-29.68E	CTD cast #6 (300 m)
4.20	13:00		22:00	25-02.01N	143-53.75	Time adjustment +1 hour (SMT=UTC+10h)
	17:30	4.21	3:30	24-59.69N	144-53.63E	Arrival at St.4（KEOS）
	19:06		5:06	25-00.09N	144-59.27E	TVMP #4
	20:30		6:30	25-00.96N	144-57.04E	CTD cast #7 (300 m)
	21:19		7:19	25-01.39N	144-56.25E	NORPAC net #4 (150m)
	22:34		8:34	25-02.24N	144-55.16E	Marine Snow Catcher #3
4.21	0:48		10:48	25-02.73N	144-54.62E	CTD cast #8 (3000m)
	3:37		13:37	25-03.36N	144-55.88E	Niskin bottle clean sampling #1
	4:12		14:12	25-03.93N	144-56.40E	Departure from St.4 (KEOS)
	9:41		19:41	25-44.53N	145-08.41E	RINKO water sampling
	20:27	4.22	6:27	27-45.56N	144-51.06E	CTD cast #9 (200m)
4.22	19:48	4.23	5:48	32-15.33N	144-39.46E	Arrival at St.5（KEO）
	20:28		6:28	32-15.50N	144-40.43E	CTD cast #10 (300m)
	21:14		7:14	32-15.45N	144-40.27E	TVMP #5
	22:23		8:23	32-14.95N	144-40.86E	NORPAC net #5 (150m)
	23:32		9:32	32-15.00N	144-40.50E	Marine Snow Catcher #4
4.23	0:51		10:51	32-15.00N	144-40.61E	FRRF #1 (150m)
	3:29		13:29	32-15.10N	144-40.60E	CTD cast #11 (5575m)
	7:42		17:42	32-15.04N	144-41.13E	Departure from St.5 (KEO)

U.T.C.		S.M.T.		Position		Event logs
Date	Time	Date	Time	Lat.	Lon.	
4.24	3:24	4.24	13:24	34-43.63N	141-15.23E	Arrival at St.6
	3:31		13:31	34-43.57N	141-15.21E	CTD cast #12 (3000m)
	6:33		16:33	34-44.71N	141-15.94E	Marine Snow Catcher #5
	7:48		17:48	34-45.60N	141-16.39E	TVMP #6
	9:01		19:01	34-47.42N	141-17.79E	Niskin bottle clean sampling #2
	9:31		19:31	34-48.03N	141-18.29E	NORPAC net #6 (150m)
	10:47		20:47	34-49.78N	141-19.69E	CTD cast #13 (300m)
	11:24		21:24	34-50.68N	141-20.65E	Departure from St.6
4.25	2:24	4.25	12:24	34-59.48N	144-58.64E	Arrival at St.7
	3:29		13:29	35-00.07N	144-59.94E	CTD cast #14 (3000m)
	6:20		16:20	35-00.07N	144-59.99E	Marine Snow Catcher #6
	7:34		17:34	34-59.94N	145-00.23E	NORPAC net #7 (150m)
	8:32		18:32	34-59.39N	145-00.29E	TVMP #7
	10:01		20:01	34-58.96N	145-00.06E	Niskin bottle clean sampling #3
	10:36		20:36	34-59.31N	145-00.21E	Departure from St.7
4.26	3:18	4.26	13:18	34-59.86N	149-14.85E	Arrival at St.8
	3:30		13:30	34-59.81N	149-14.74E	CTD cast #15 (3000m)
	6:16		16:16	34-59.13N	149-11.71E	Marine Snow Catcher #7
	7:24		17:24	34-58.90N	149-10.05E	NORPAC net #8 (150m)
	8:20		18:20	34-58.50N	149-08.30E	TVMP #8
	9:48		19:48	34-58.40N	149-07.60E	Departure from St.8
4.27	12:00	4.27	22:00	34-59.15N	155-00.06E	Time adjustment +1 hour (SMT=UTC+11h)
	22:24	4.28	9:24	35-01.13N	157-30.89E	Arrival at St.9
	23:02		10:02	35-00.20N	157-30.16E	CTD cast #16 (5045m)
4.28	2:51		13:51	35-01.37N	157-31.44E	Marine Snow Catcher #8
	4:33		15:33	35-02.43N	157-32.98E	VMPS #1 (1000m)
	5:59		16:59	35-02.97N	157-34.00E	TVMP #9
	7:16		18:16	35-03.41N	157-36.55E	Niskin bottle clean sampling #4
	7:50		18:50	35-04.11N	157-37.16E	Calibration for magnetometer #2
	8:12		19:12	35-04.53N	157-37.65E	Departure from St.9
4.29	20:54	4.30	7:54	42-29.80N	158-00.01E	Arrival at St.10
	21:02		8:02	42-30.02N	158-00.09E	CTD cast #17 (3000m)
	23:41		10:41	42-30.27N	158-00.12E	Marine Snow Catcher #9
4.30	1:30		12:30	42-30.85N	158-00.53E	Departure from St.10
5.1	20:42	5.2	7:42	46-59.39N	160-00.69E	Arrival at St.11 (K2)
	21:00		8:00	46-59.48N	160-00.71E	CTD cast #18 (2000m)
	22:23		9:23	46-59.53N	160-00.72E	Marine Snow Catcher #10
5.2	0:25		11:25	46-59.98N	160-02.44E	ARGO float Deployment
	0:40		11:40	46-59.65N	160-00.80E	CTD cast #19 (5195m)
	4:35		15:35	46-59.67N	160-00.93E	TVMP #10
	5:42		16:42	46-59.87N	160-01.73E	Niskin bottle clean sampling #5
	21:02	5.3	8:02	47-00.38N	159-57.61E	Hybrid Mooring system Recovery

U.T.C.		S.M.T.		Position		Event logs
Date	Time	Date	Time	Lat.	Lon.	
5.3	17:01	5.4	4:01	47-00.03N	159-59.98E	FRRF #2 (100m)
	17:26		4:26	47-00.11N	160-00.07E	TVMP #11
	19:29		6:29	47-00.01N	159-59.96E	CTD cast #20 (300m)
	21:01		8:01	47-00.02N	160-00.05E	TVMP #12
	22:10		9:10	47-00.05N	160-00.67E	VMPS #2 (1000m)
5.4	1:01		12:01	46-59.99N	160-00.05E	FRRF #3 (100m)
	1:25		12:25	47-00.03N	160-00.20E	TVMP #13
	2:37		13:37	46-59.57N	160-00.68E	Niskin bottle clean sampling #6
	4:55		15:55	46-59.99N	160-00.03E	TVMP #14
	17:00	5.5	4:00	47-00.09N	160-00.22E	TVMP #15
	20:57		7:57	47-00.08N	159-59.89E	TVMP #16
5.5	1:00		12:00	47-00.26N	159-59.85E	TVMP #17
	4:57		15:57	46-59.96N	159-59.91E	TVMP #18
	8:58		19:58	47-00.00N	159-59.90E	NORPAC net #9 (150m)
	16:58	5.6	3:58	47-00.00N	159-59.81E	TVMP #19
	20:56		7:56	46-59.99N	159-59.93E	TVMP #20
5.6	1:00		12:00	46-59.92N	159-59.69E	TVMP #21
	2:28		13:28	46-59.84N	159-58.50E	CTD cast #21 (3000m)
	4:55		15:55	46-59.90N	159-58.63E	TVMP #22
	8:00		19:00	47-00.03N	160-00.00E	CTD cast #22 (3000m)
	21:05	5.7	8:05	47-04.25N	160-03.87E	Hybrid Mooring system Deployment
5.7	1:41		12:41	47-00.32N	159-58.38N	Mooring calibration (sinker fixed position)
	4:03		15:03	47-01.03N	160-02.62E	Calibration for magnetometer #3
	4:30		15:30	47-01.05N	160-04.02E	Departure from St.11 (K2)
5.8	2:00	5.8	13:00	47-56.69N	166-23.29E	Arrival at St.12
	2:12		13:12	47-57.14N	166-24.57E	CTD cast #23 (1000m)
	5:06		16:06	47-56.98N	166-24.42E	Marine Snow Catcher #11
	6:21		17:21	47-56.91N	166-24.00E	TVMP #23
	7:25		18:25	47-56.39N	166-24.58E	NORPAC net #10 (150m)
	19:12	5.9	6:12	47-57.10N	166-30.61E	Deep Ninja Recovery
5.9	2:00		13:00	47-56.03N	166-25.19E	CTD cast #24 (1000m)
	2:58		13:58	47-56.33N	166-25.16E	UVMP #1
	9:13		20:13	47-56.28N	166-29.77E	CTD cast #25 (1000m)
	10:00		21:00	47-56.03N	166-29.72E	Departure from St.12
5.10	9:42	5.10	20:42	47-02.09N	160-09.25E	Arrival at St.11 (K2)
	11:00		22:00	47-01.56N	160-05.26E	Time adjustment -1 hour (SMT=UTC+10h)
	19:45	5.11	5:45	46-59.99N	159-58.41E	Confirming operation of Top buoy (Mooring system)
	22:06		8:06	47-00.26N	159-58.21E	Departure from St.11 (K2)
5.11	21:30	5.12	7:30	44-00.47N	155-01.71E	Arrival at St.13 (KNOT)
	21:53		7:53	43-59.90N	155-00.17E	CTD cast #26 (3000m)
5.12	0:30		10:30	43-59.78N	155-00.38E	Marine Snow Catcher #12
	1:48		11:48	43-59.51N	155-00.93E	TVMP #24
	2:56		12:56	43-58.23N	155-01.91E	VMPS #3 (1000m)
	4:15		14:15	43-58.20N	155-02.35E	Niskin bottle clean sampling #7
	4:42		14:42	43-57.91N	155-02.31E	Departure from St.13 (KNOT)
	19:30	5.13	5:30	40-45.81N	145-44.27E	Stop C-band doppler radar observation

U.T.C.		S.M.T.		Position		Event logs
Date	Time	Date	Time	Lat.	Lon.	
5.13	12:00	5.14	22:00	41-42.25N	142-05.50E	Time adjustment -1 hour (SMT=UTC+9h)
5.14	21:45	5.15	6:45	41-44.98N	141-59.93E	ADCP Survay Line1
5.15	1:55		10:55	41-48.00N	141-20.47E	Arrival at St.14
	1:59		10:59	41-48.00N	141-20.45E	CTD cast #27 (264m)
	3:01		12:01	41-48.01N	141-20.51E	Marine Snow Catcher #13
	3:46		12:46	41-47.93N	141-20.74E	TVMP #25
	4:07		13:07	41-47.75N	141-20.84E	NORPAC net #11 (200m)
	4:46		13:46	41-47.60N	141-20.83E	NEUSTON net #1
	6:07		15:07	41-49.55N	141-21.67E	Departure from St.14
	6:53		15:53	41-45.35N	141-15.00E	ADCP Survay Line2～Line3-1
	20:45	5.16	5:45	41-34.01N	141-40.02E	ADCP Survay Line3-2
	21:43		6:43	41-39.96N	141-30.24E	Arrival at St.15
	21:57		6:57	41-40.01N	141-30.20E	CTD cast #28 (110m)
	22:33		7:33	41-40.19N	141-30.75E	NORPAC net #12 (100m)
	23:00		8:00	41-40.03N	141-31.41E	NEUSTON net #2
5.16	0:25		9:25	41-39.51N	141-32.69E	TVMP #26
	0:49		9:49	41-39.74N	141-31.05E	Departure from St.15
	0:54		9:54	41-40.11N	141-30.07E	ADCP Survay Line3-2
	6:31	5.17	15:31	40-53.19N	141-54.11E	Stop Sea water pump and SSV pump
5.19	23:40	5.20	8:40	35-01.93N	138-30.30E	Arrival at Shimizu

2. Observations
2.1 Meteorology
2.1.1 Surface meteorological observations

Koji SUGIE	**JAMSTEC PI**
Yutaro MURAKAMI	**NME**
Ryo OYAMA	**NME**
Fumine OKADA	**NME**
Yoichi INOUE	**MIRAI crew**

(1) Objectives
Surface meteorological parameters are observed as a basic dataset of the meteorology. These parameters provide the temporal variation of the meteorological condition surrounding the ship.

(2) Instruments and Methods
Surface meteorological parameters were observed during this cruise. In this cruise, we used two systems for the observation.

(2-1) MIRAI Surface Meteorological observation (SMet) system
Instruments of SMet system are listed in Table2.1.1-1 and measured parameters are listed in Table2.1.1-2. Data were collected and processed by KOAC-7800 weather data processor made by Koshin-Denki, Japan. The data set consists of 6 seconds averaged data.

(2-2) Shipboard Oceanographic and Atmospheric Radiation (SOAR) measurement system
SOAR system designed by BNL (Brookhaven National Laboratory, USA) consists of major five parts.
a) Analog meteorological data sampling with CR1000 logger manufactured by Campbell Inc., Canada - wind, pressure, and rainfall (by a capacitive rain gauge (CRG)) measurement.
b) Digital meteorological data sampling from individual sensors - air temperature, relative humidity and rainfall (by optical rain gauge (ORG)) measurement.
c) Radiation data sampling with CR1000X logger manufactured by Campbell Inc., Radiometers designed by Hukseflux Thermal Sensors B.V. Netherlands. – short and long wave downward radiation measurement.
d) Photosynthetically Available Radiation (PAR) and Ultraviolet Irradiance (UV) sensor manufactured by Biospherical Instruments Inc., USA. – PAR and UV measurement.
e) Scientific Computer System (SCS) developed by NOAA (National Oceanic and Atmospheric Administration, USA) - centralized data acquisition and logging of all data sets.SCS recorded radiation, air temperature, relative humidity, CR1000, ORG and PAR data. SCS composed Event data (JamMet) from these data and ship's navigation data every 6 seconds. Instruments and their locations are listed in Table 2.1.1-3 and measured parameters are listed in Table 2.1.1-4.

(2-3) Quality control
For the quality control as post processing, we checked the following sensors, before and after the cruise.
a) Young Rain Gauge (SMet and SOAR): Inspect of the linearity of output value from the rain gauge sensor to change input value by adding fixed quantity of test water.
b) Barometer (SMet and SOAR): Comparison with the portable barometer value, PTB220, VAISALA
c) Thermometer (air temperature and relative humidity) (SMet and SOAR): Comparison with the portable thermometer value, HMP70, VAISALA

(3) Preliminary results
Fig.2.1.1-1 show the time series of the following parameters;

Wind (SOAR)
Air temperature (SMet)
Relative humidity (SMet)
Precipitation (SOAR, ORG)
Short/long wave radiation (SOAR)
Barometric Pressure (SMet)
Sea surface temperature (SMet)
Significant wave height (SMet)

(4) Data archives
These obtained data will be submitted to JAMSTEC Data Management Group (DMG).

(5) Remarks (Times in UTC)
i) The following period, Sea surface temperature of SMet data were available.
07:18UTC 16 Apr. 2022 - 06:31UTC 17 May. 2022

ii) The following period, increasing of SMet capacitive rain gauge data were invalid due to transmitting for MF/HF or VHF radio.
04:26UTC 16 Apr. 2022
03:05UTC 01 May. 2022 - 03:06UTC 01 May. 2022
23:02UTC 07 May. 2022
00:28UTC 08 May. 2022
01:26UTC 12 May. 2022

iii) The following periods, SOAR ORG data were doubtful due to birds perching on the sensor.
12:37UTC 18 Apr. 2022 - 20:26UTC 18 Apr. 2022
12:56UTC 20 Apr. 2022 - 23:59UTC 20 Apr. 2022
00:00UTC 21 Apr. 2022 - 06:42UTC 21 Apr. 2022

iv) The following period, SOAR ORG sensor was not measured rainfall due to the sensor trouble.
21:41UTC 30 Apr. 2022 - 21:44UTC 30 Apr. 2022

Table 2.1.1-1. Instruments and installation locations of MIRAI Surface Meteorological observation system

Sensors	Type	Manufacturer	Location (altitude from surface)
Anemometer	KS-5900	Koshin Denki, Japan	Foremast (25 m)
Tair/RH	HMP155	Vaisala, Finland	Compass deck (21 m)
with aspirated radiation shield	43408 Gill	R.M. Young, USA	starboard side and port side
Thermometer: SST	RFN2-0	Koshin Denki, Japan	4th deck (-1m, inlet -5m)
Barometer	Model-370	Setra System, USA	Captain deck (13 m) weather observation room
Capacitive rain gauge	50202	R. M. Young, USA	Compass deck (19 m)
Optical rain gauge	ORG-815DS	Osi, USA	Compass deck (19 m)
Radiometer (short wave)	MS-802	Eko Seiki, Japan	Radar mast (28 m)
Radiometer (long wave)	MS-202	Eko Seiki, Japan	Radar mast (28 m)
Wave height meter	WM-2	Tsurumi-seiki, Japan	Bow (10 m) Stern (8 m)

Table 2.1.1-2. Parameters of MIRAI Surface Meteorological observation system

Parameter	Units	Remarks
1 Latitude	degree	
2 Longitude	degree	
3 Ship's speed	knot	MIRAI log
4 Ship's heading	degree	MIRAI gyro
5 Relative wind speed	m/s	6sec./10min. averaged
6 Relative wind direction	degree	6sec./10min. averaged
7 True wind speed	m/s	6sec./10min. averaged
8 True wind direction	degree	6sec./10min. averaged
9 Barometric pressure	hPa	adjusted to sea surface level 6sec. averaged
10 Air temperature (starboard)	degC	6sec. averaged
11 Air temperature (port)	degC	6sec. averaged
12 Dewpoint temperature (starboard)	degC	6sec. averaged
13 Dewpoint temperature (port)	degC	6sec. averaged
14 Relative humidity (starboard)	%	6sec. averaged
15 Relative humidity (port)	%	6sec. averaged
16 Sea surface temperature	degC	6sec. averaged
17 Precipitation intensity (optical rain gauge)	mm/hr	hourly accumulation
18 Precipitation (capacitive rain gauge)	mm/hr	hourly accumulation
19 Down welling shortwave radiation	W/m^2	6sec. averaged
20 Down welling infra-red radiation	W/m^2	6sec. averaged
21 Significant wave height (bow)	m	hourly
22 Significant wave height (stern)	m	hourly
23 Significant wave period (bow)	second	hourly
24 Significant wave period (stern)	second	hourly

Table 2.1.1-3. Instruments and installation locations of SOAR system

Sensors (Meteorological)	Type	Manufacturer	Location
Anemometer	05106	R.M. Young, USA	foremast (25 m)
Barometer with pressure port	PTB210 61002 Gill	Vaisala, Finland R.M. Young, USA	foremast (23 m)
Rain gauge	50202	R.M. Young, USA	foremast (24 m)
Tair/RH with aspirated radiation shield	HMP155 43408 Gill	Vaisala, Finland R.M. Young, USA	foremast (23 m)
Optical rain gauge	ORG-815DR	Osi, USA	foremast (24 m)

Sensors (Radiation)	Type	Manufacturer	Location *
Radiometer (short wave)	SR20	Hukseflux Thermal Sensors B.V., Netherlands	foremast (25 m)
Radiometer (long wave)	IR20	Hukseflux Thermal Sensors B.V., Netherlands	foremast (25 m)

Sensor (PAR&UV)	Type	Manufacturer	Location *
PAR&UV sensor	PUV-510	Biospherical Instruments Inc., USA	Navigation deck (18m)

*Location : Altitude from surface

Table 2.1.1-4. Parameters of SOAR system (JamMet)

Parameter	Units	Remarks
1 Latitude	degree	
2 Longitude	degree	
3 SOG	knot	
4 COG	degree	
5 Relative wind speed	m/s	
6 Relative wind direction	degree	
7 Barometric pressure	hPa	
8 Air temperature	degC	
9 Relative humidity	%	
10 Precipitation intensity (optical rain gauge)	mm/hr	
11 Precipitation (capacitive rain gauge)	mm/hr	reset at 50 mm
12 Down welling shortwave radiation	W/m^2	
13 Down welling infrared radiation	W/m^2	
14 PAR	$microE/cm^2/sec$	
15 UV 305 nm	$microW/cm^2/nm$	
16 UV 320 nm	$microW/cm^2/nm$	
17 UV 340 nm	$microW/cm^2/nm$	
18 UV 389 nm	$microW/cm^2/nm$	

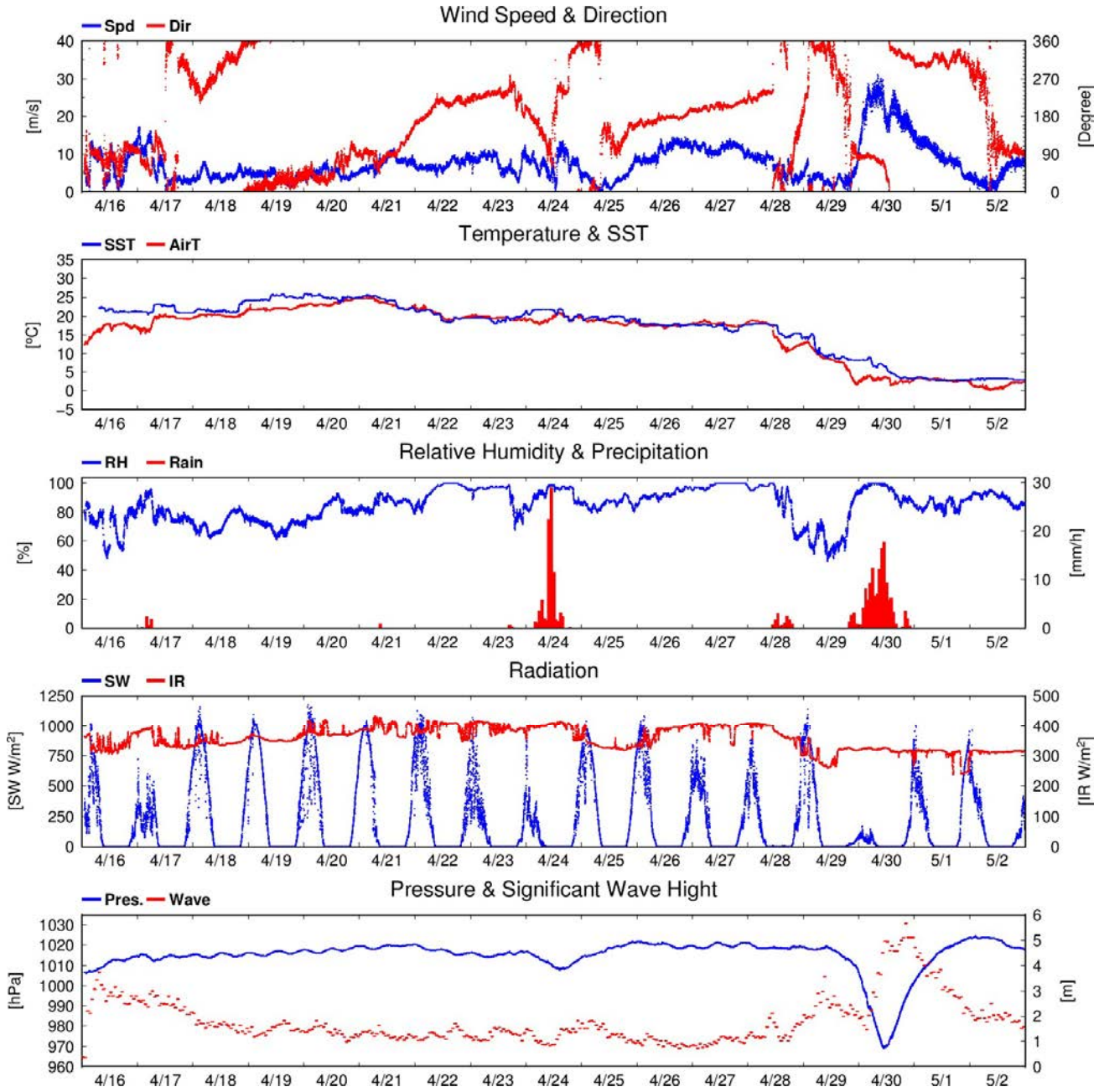

Fig. 2.1.1-1 Time series of surface meteorological parameters during MR22-03

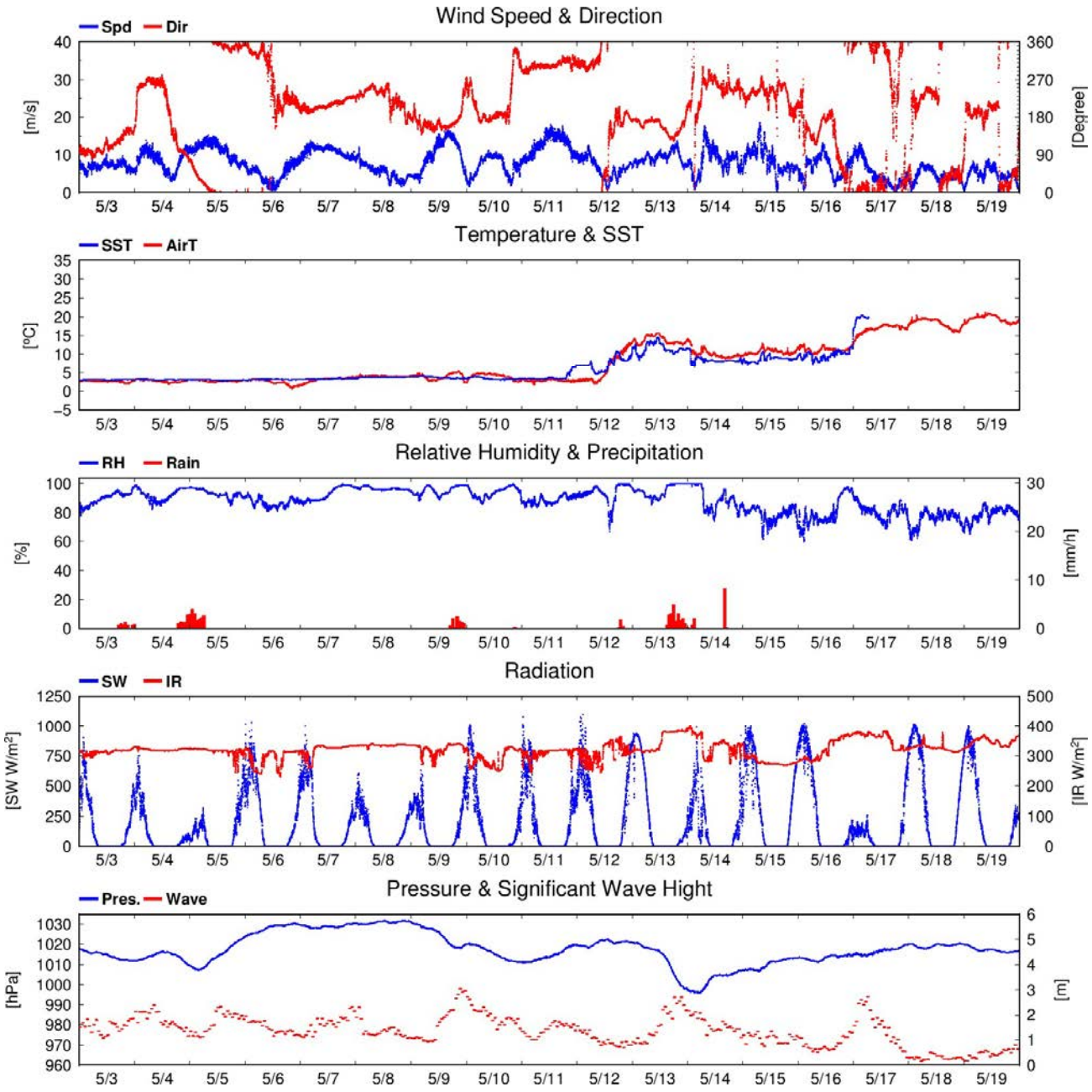

Fig. 2.1.1-1 (Continued)

2.1.2 Cloud base height observations by Ceilometer

Koji SUGIE	**JAMSTEC**	**PI**
Yutaro MURAKAMI	**NME**	
Ryo OYAMA	**NME**	
Fumine OKADA	**NME**	
Yoichi INOUE	**MIRAI crew**	

(1) Objectives

The information of cloud base height and the liquid water amount around cloud base is important to understand the process on formation of the cloud. As one of the methods to measure them, the ceilometer observation was carried out.

(2) Instruments and methods

Cloud base height and backscatter profile were observed by ceilometer (CL51, VAISALA, Finland). On the archive dataset, cloud base height and backscatter profile are recorded with the resolution of 10 m.

i). Parameters

a). Cloud base height [m].

b). Backscatter profile, sensitivity and range normalized at 10 m resolution.

c). Estimated cloud amount [oktas] and height [m]; Sky Condition Algorithm.

ii). The measurement configurations are shown in Table 2.1.1.2-1.

Table 2.1.1.2-1 The measurement configurations

Property	Description
Laser source	Indium Gallium Arsenide (InGaAs) Diode
Transmitting center wavelength	910±10 nm at 25 degC
Transmitting average power	19.5 mW
Repetition rate	6.5 kHz
Detector	Silicon avalanche photodiode (APD)
Responsibility at 905 nm	65 A/W
Cloud detection range	0 ~ 13 km
Measurement range	0 ~ 15 km
Resolution	10 m in full range
Sampling rate	36 sec.
Sky Condition	Cloudiness in octas (0 ~ 9) 0 Sky Clear 1 Few 3 Scattered 5-7 Broken 8 Overcast 9 Vertical Visibility

(3) Preliminary results

Figure 2.1.1.2-1 show the time-series of the lowest, second and third cloud base height during the cruise.

(4) Data archives

These obtained data will be submitted to JAMSTEC Data Management Group (DMG).

(5) Remarks (Times in UTC)
Window cleaning
23:51UTC 19 Apr. 2022
23:54UTC 27 Apr. 2022
22:00UTC 01 May. 2022
18:45UTC 10 May. 2022

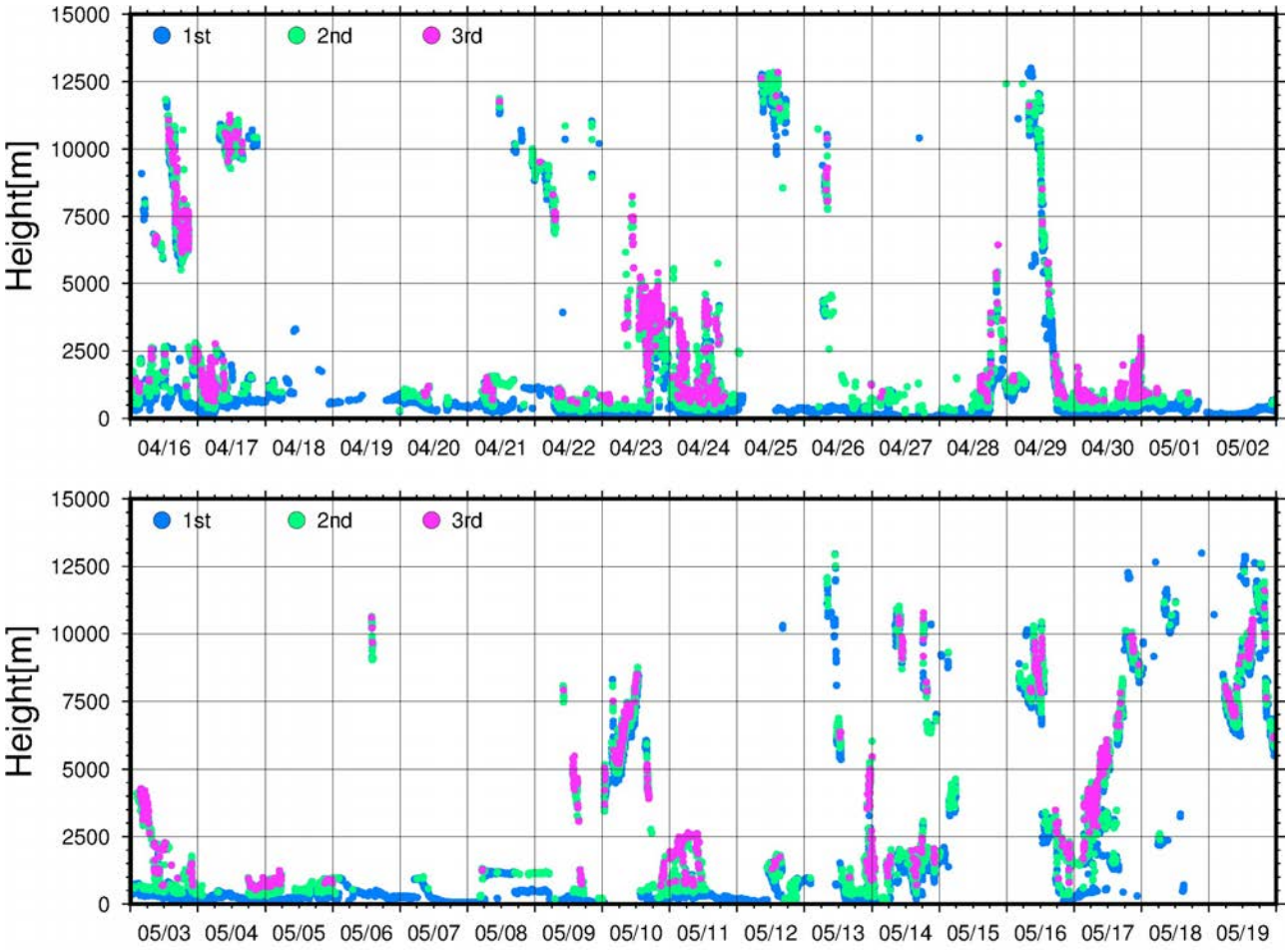

Figure 2.1.1.2-1 Time series of cloud base height during MR22-03

2.1.3 Trace gases and Aerosols in the marine boundary layer

Fumikazu TAKETANI **JAMSTEC**
Kazuhiko MATSUMOTO **JAMSTEC**
Minako KURISU **JAMSTEC**
Chunmao ZHU **JAMSTEC**
Kana NAGASHIMA **JAMSTEC**
Yugo KANAYA **JAMSTEC**
Observation was supported by Nippon Marine Enterprises, Ltd.

(1) Objectives
To investigate spatiotemporal behaviors and sources of trace elements in aerosol particles in Asian outflow.
To investigate the transport process of short-lived climate forcers from the Asian continent to the Northwestern Pacific Ocean during the spring season.
To investigate influence of the wet/dry deposition to the marine ecosystem over the Northwestern Pacific Ocean during the spring season.
To investigate the optical measurement requirement for direct identification of floating ocean debris over the sea surface.

(2) Parameters
Surface carbon monoxide (CO) and ozone(O_3) mixing ratios
Surface aerosol particle size distributions
Surface aerosol chemical composition of fine and coarse mode aerosols
Chemical composition of rain/fog water
Mineral grains in surface sea water
Optical images over the sea surface

(3) Instruments and methods
(3-1) Continuous surface aerosol/gas observations during the cruise:
(3-1-1) Particle size distributions
The size-resolved number concentration of particles was measured by a handheld optical particle counter (OPC) (KR-12A, RION) installed on the compass deck for the size range between 0.3 and 5 μm in diameter.
(3-1-2) CO and O_3:
Ambient air was continuously sampled on the compass deck and drawn through ~20-m-long Teflon tubes connected to a nondispersive infrared (NDIR) CO analyzer (Model 48i-TLE, Thermo Fisher Scientific) and a UV photometric ozone analyzer (model 205, 2B Technologies), located in the environmental research room. The data will be used for characterizing air mass origins.

(3-2) Aerosol sampling for the offline analyses:
Samplings of aerosol particles in the marine atmosphere for the chemical composition analyses were performed using High-volume air samplers on the compass deck.

Aerosol particles were collected on the filter along cruise track using two high-volume air samplers (HVS 1 and 2) located on the compass deck to analyze the chemical composition. To avoid collecting particles derived from the research vessel's own exhaust, the pumping by the samplers were automatically controlled using a "wind-direction selection system". All the samples will be analyzed in the laboratories at JAMSTEC. These sampling logs are listed in Tables 2.1.2-1 and 2.1.2-2.

HVS1: HV-700F (SIBATA Sci.) with a single-stage impactor for analyzing mode-segregated inorganic ions and carbonaceous species (elemental and organic carbon, organic molecular markers, etc.) of collected aerosols. Prebaked quartz fiber (QFF) filters (3 hrs at 900ºC) were used for the sampling. Fine (PM2.5) and Coarse (TSP - PM2.5) mode particles were separately collected on the two QFF filters at the sampling rate of approximately 500 L/min.

HVS2: 120SL (Kimoto Electric) with a single-stage impactor (TE231, Tisch Environmental, Inc.) for analyzing metallic elements and iron (Fe) isotope ratios of collected aerosols. A PTFE filters (PF050, Advantec, Japan) washed by soaking into 3 mol/L HCl overnight and rinsed carefully with ultrapure water before use were used for the sampling. Fine (PM2.5) and Coarse (TSP - PM2.5) mode particles were separately collected on the two PTFE filters at the sampling rate of approximately 1132 L/min.

(3-3) Rain/fog sampling:

Rain and fog samples were collected using rain and fog samplers, respectively. These samples were analyzed to investigate the chemical composition of rainwater and fog-water over Northwestern Pacific region. These sampling logs are listed in Table 2.1.2-3.

(3-4) Surface seawater sampling

Water samples at 10 m and 20 m depths were collected using Niskin-X bottles on a CTD-rosette system. Water samples at 0 m were collected using a bucket. All the samples will be analyzed to identify chemical/physical properties of mineral grains in the laboratories at JAMSTEC.

(3-5) Sea surface monitoring of floating ocean debris

Sea surface monitoring were performed by two cameras (Gopro Hero 9, Gopro Inc.) installed at the left and right sides of the research vessel on the bridge deck, respectively. Photos of the sea surface were taken every 30s. In each day, the cameras were running for approximately 4 hours. The taken photo will be analyzed for the floating ocean debris.

(4) Data archives

All data obtained during this cruise will be submitted to Data Management Group (DMG) of JAMSTEC after the sample analysis and validation. The data will be opened to the public via "Data Research System for Whole Cruise Information (DARWIN)" in JAMSTEC web site.

Tables 2.1.2-1 Sampling logs for aerosol composition analyses using HVS1

ID	Date Collected(UTC)				Latitude			Longitude		
	YYYY	MM	DD	hh : mm	Deg.	Min.	N/S	Deg.	Min.	E/W
MR22-03－HV-001	2022	4	16	2:40	34	47.75	N	138	28.19	E
MR22-03－HV-002	2022	4	17	23:48	30	0.42	N	137	31.65	E
MR22-03－HV-003	2022	4	19	1:03	24	59.92	N	137	29.88	E
MR22-03－HV-004	2022	4	20	0:03	25	59.95	N	140	59.56	E
MR22-03－HV-005	2022	4	20	23:09	25	2.33	N	144	55.07	E
MR22-03－HV-006	2022	4	22	1:29	28	38	N	144	46.37	E
MR22-03－HV-007	2022	4	22	23:53	32	15.02	N	144	40.45	E
MR22-03－HV-008	2022	4	24	23:43	34	54.55	N	144	20.32	E
MR22-03－HV-009	2022	4	26	23:36	34	59.87	N	152	5.09	E

Tables 2.1.2-2 Sampling logs for aerosol composition analyses using HVS2

ID	Date Collected(UTC)				Latitude			Longitude		
	YYYY	MM	DD	hh : mm	Deg.	Min.	N/S	Deg.	Min.	E/W
NO.1	2022	4	16	2:40	34	47.75	N	138	28.19	E
NO.2	2022	4	19	1:03	24	59.92	N	137	29.88	E
NO.3	2022	4	22	23:53	32	15.02	N	144	40.45	E
NO.4	2022	4	24	23:43	34	54.55	N	144	20.32	E
NO.5	2022	4	26	23:36	34	59.87	N	152	5.09	E
NO.6	2022	4	28	22:23	37	56.26	N	157	41.01	E
NO.7	2022	5	1	23:47	46	59.8	N	160	0.92	E
NO.8	2022	5	4	22:45	47	0.77	N	160	0.81	E
NO.9	2022	5	8	2:35	47	57.09	N	166	24.6	E
NO.10	2022	5	10	23:08	46	51.84	N	159	46.55	E
NO.11	2022	5	13	6:28	40	29.27	N	149	17.45	E

Tables 2.1.2-3 Sampling logs for rain/fog composition analyses using rain/fog sampler

ID	Date Collected(UTC)				Latitude			Longitude		
	YYYY	MM	DD	hh : mm	Deg.	Min.	N/S	Deg.	Min.	E/W
R001	2022	04	17	7:40	31	52.05	N	137	29.10	E
R002	2022	04	21	10:00	25	44.27	N	145	08.32	E
R-003	2022	04	23	0:02	32	15.03	N	144	40.47	E
R-004	2022	04	23	23:40	34	10.8	N	142	07.56	E
R-005	2022	04	24	6:56	34	10.8	N	142	07.56	E
R-006	2022	04	24	9:40	34	10.8	N	142	07.56	E
R-007	2022	04	24	22:40	34	55.01	N	144	05.96	E
fog-001	2022	04	27	22:30	35	0	N	155	20.00	E
R-008	2022	04	28	19:50	37	27.6	N	157	39.86	E
R-009	2022	04	29	21:43	42	30.07	N	158	00.21	E
R-010	2022	04	30	0:45	42	30.5	N	158	00.36	E
R-011	2022	05	01	21:30	46	59.48	N	160	00.70	E
R012	2022	05	03	19:00	47	0.9	N	159	59.92	E
R-013	2022	05	03	23:10	47	0.9	N	159	59.92	E
R-014	2022	05	05	7:00	46	59.99	N	160	00.00	E
Fog-002	2022	05	07	21:55	47	56.27	N	166	24.94	E
R-015	2022	05	10	0:33	47	22.34	N	162	39.49	E
R016	2022	05	10	23:10	46	50.53	N	159	44.75	E
Fog-003	2022	05	12	21:25	41	40.85	N	151	18.26	E
R-017	2022	05	12	21:25	41	40.85	N	151	18.26	E
R-018	2022	05	13	22:24	41	40.85	N	151	18.26	E
R-019	2022	05	14	1:03	41	10.72	N	144	09.62	E

2.1.4 Clouds, aerosols, water vapor and precipitation

2.1.4.1 Lidar observation

Masaki KATSUMATA	**JAMSTEC**
Kyoko TANIGUCHI	**JAMSTEC**
Yutaro MURAKAMI	**NME**
Ryo OYAMA	**NME**
Fumine OKADA	**NME**
Yoichi INOUE	**MIRAI Crew**

(1) Objective

The objective of this observation is to capture the vertical distribution of clouds, aerosols, and water vapor in high spatio-temporal resolution.

(2) Parameters

355nm Mie scattering signal
532nm Mie scattering signal
1064nm Mie scattering signal
387nm Raman nitrogen scattering signal (nighttime only)
408nm Raman water vapor scattering signal (nighttime only)
607nm Raman nitrogen scattering signal (nighttime only)
660nm Raman water vapor scattering signal (nighttime only)

(3) Instruments and methods

The Mirai Lidar system transmits a 10-Hz pulse laser in three wavelengths: 1064nm, 532nm, 355nm. For cloud and aerosol observation, the system detects Mie scattering at these wavelengths. The separate detections of polarization components at 532 nm and 355 nm obtain additional characteristics of the targets. The system also detects Raman water vapor signals at 660 nm and 408nm, Raman nitrogen signals at 607 nm and 387nm at nighttime. Based on the signal ratio of Raman water vapor to Raman nitrogen, the system offers water vapor mixing ratio profiles.

(4) Observation Period

16 April 2022 to 19 May 2022

(5) Preliminary Results

The lidar system observed the lower atmosphere throughout the cruise, except on EEZs and territorial waters without permission. All data will be reviewed after the cruise to maintain data quality.

(6) Data Archive

These data obtained in this cruise will be submitted to the Data Management Group of JAMSTEC, and will be opened to the public via “Data Research System for Whole Cruise Information in JAMSTEC (DARWIN)” in JAMSTEC web site. <http://www.godac.jamstec.go.jp/darwin/e>

2.1.4.2 C-band weather radar

Masaki KATSUMATA **JAMSTEC**
Biao GENG **JAMSTEC**
Yutaro MURAKAMI **NME**
Ryo OYAMA **NME**
Fumine OKADA **NME**
Yoichi INOUE **Mirai crew**

(1) Objectives
The objective of weather radar observations is to investigate the structures and evolutions of precipitating systems over the high-latitude region including arctic ocean.

(2) Instrumentation and methods
(a) Radar specifications
The C-band weather radar on board the R/V Mirai was used. Basic specifications of the radar are as follows:

Frequency:	5370 MHz (C-band)
Polarimetry:	Horizontal and vertical (simultaneously transmitted and received)
Transmitter:	Solid-state transmitter
Pulse Configuration:	Using pulse-compression
Output Power:	6 kW (H) + 6 kW (V)
Antenna Diameter:	4 meters
Beam Width:	1.0 degrees
Inertial Navigation Unit:	PHINS (IXBLUE S.A.S)

(b) Available radar variables
Radar variables, which were converted from the power and phase of the backscattered signal at vertically- and horizontally-polarized channels, were as follows:

Radar reflectivity:	Z
Doppler velocity:	Vr
Spectrum width of Doppler velocity:	SW
Differential reflectivity:	Z_{DR}
Differential propagation phase:	Φ_{DP}
Specific differential phase:	K_{DP}
Co-polar correlation coefficients:	ρ_{HV}

(c) Operation methodology
The antenna was controlled to point the commanded ground-relative direction, by controlling the azimuth and elevation to cancel the ship attitude (roll, pitch and yaw) detected by the laser gyro. The Doppler velocity was also corrected by subtracting the ship movement in beam direction.
For the maintenance, internal signals of the radar were checked and calibrated at the beginning and the end of the cruise. Meanwhile, the following parameters were checked daily; (1) frequency, (2) mean output power, (3) pulse width, and (4) PRF (pulse repetition frequency).
During the cruise, the radar was operated as in Table 2.1.4.2-1. A dual PRF mode was used for a volume scan. For RHI and surveillance PPI scans, a single PRF mode was used.

(3) Preliminary results

The C-band weather radar observations were conducted through the cruise, except in the area where the operations were prohibited by Japanese license. The observation periods are:

07:00 UTC on 16 Apr. 2022 to 21:00 UTC on 23 Apr. 2022

20:00 UTC on 24 Apr. 2022 to 19:30 UTC on 13 May 2022

Note that the observation was paused from 02:00 to 03:00 UTC on 18 Apr. 2022 due to system maintenance.

The obtained data will be analyzed after the cruise.

(4) Data archive

All data obtained during this cruise will be submitted to the JAMSTEC Data Management Group (DMG).

Table 2.1.4.2-1: Scan modes of C-band weather radar

	Survei-llance PPI Scan	Volume Scan						RHI Scan
Repeated Cycle (min.)	30	6						6
Times in One Cycle	1	1						3
PRF(s) (Hz)	400	dual PRF (ray alternative)						1250
		667	833	938	1250	1333	2000	
Azimuth (deg)	Full Circle							Option
Bin Spacing (m)	150							
Max. Range (km)	300	150		100		60		100
Elevation Angle(s) (deg.)	0.5	0.5		1.0, 1.8, 2.6, 3.4, 4.2, 5.1, 6.2, 7.6, 9.7, 12.2, 15.2		18.7, 23.0, 27.9, 33.5, 40.0		0.0 ~ 60.0

2.1.5 Aerosol optical characteristics measured by Shipborne Sky radiometer

Kazuma AOKI University of Toyama
Sky radiometer operation was supported by Nippon Marine Enterprises, Ltd.

(1) Objectives

Objective of this observation is to study distribution and optical characteristics of marine aerosols by using a ship-borne sky radiometer (POM-01 MK-III: PREDE Co. Ltd., Japan). Furthermore, collections of the data for calibration and validation to the remote sensing data were performed simultaneously.

(2) Instruments and methods

(2-1) Sky radiometer measurement

The sky radiometer measures the direct solar irradiance and the solar aureole radiance distribution with seven interference filters (0.315, 0.4, 0.5, 0.675, 0.87, 0.94, and 1.02 μm). Analysis of these data was performed by SKYRAD.pack version 4.2 developed by Nakajima et al. 1996 and 2020.

(3) Parameters

Aerosol optical thickness at five wavelengths (400, 500, 675, 870 and 1020 nm)
Ångström exponent
Single scattering albedo at five wavelengths
Size distribution of volume (0.01 μm – 20 μm)
GPS provides the position with longitude and latitude and heading direction of the vessel, and azimuth and elevation angle of the sun. Horizon sensor provides rolling and pitching angles.

(4) Data archive

Aerosol optical data are to be archived at University of Toyama (K.Aoki, SKYNET/SKY: http://skyrad.sci.u-toyama.ac.jp/sobs/) after the quality check and will be submitted to JAMSTEC.

(5) References

Nakajima,T., G. Tonna, R. Rao, P. Boi, Y. Kaufman and B. Holben (1996) Use of sky brightness measurements from ground for remote sensing of particulate polydispersions. Appl. Opt., 35, 2672–2686, doi: 10.1364/AO.35.002672.

Aoki. K., T. Takemura, K. Kawamoto and T. Hayasaka (2013) Aerosol climatology over Japan site measured by ground-based sky radiometer. AIP Conf. Proc., 1531, 284-287. doi:10.1063/1.4804762.

Nakajima,T., M. Campanelli, H. Che, V. Estellés, H. Irie, S.-W. Kim, et al. (2020) An overview and issues of the sky radiometer technology and SKYNET, Atmos. Meas. Tech., 13, 4195–4218. doi:10.5194/amt-13-4195-2020.

2.2 Physical Oceanography
2.2.1 CTD

Masahide WAKITA	**JAMSTEC**	
Hiroshi UCHIDA	**JAMSTEC**	
Hiroyuki NAKAJIMA	**MWJ**	***Operation Leader**
Tun Htet Aung	**MWJ**	
Airi HARA	**MWJ**	

(1) Objective
Investigation of oceanic structure and water sampling.

(2) Parameters
Temperature, Salinity, Pressure, Dissolved Oxygen, Fluorescence, Beam Transmission,
Turbidity, Photosynthetically Active Radiation, Chromophoric Dissolved Organic Matter (CDOM), Height above bottom (100 m range)

(3) Instruments and Methods
CTD/Carousel Water Sampling System was used for hydrographic observations and water samplings. Carousel system used in this cruise was a 36-positions Carousel Water Sampler (CWS), and sampling bottles used were 12-liter sampling bottles (Sea-Bird Electronics, Inc.). Normal type of sampling bottles with Viton O-ring were used in the CWS positions of from 1 to 10 while normal nitrile rubber O-ring were used in other 26 bottles. Viton O-rings used were not acid-cleaned.

Winch and cable
Traction winch system (4.5 ton) (Dynacon, Inc.)
Armored cable (φ = 9.53 mm) (Rochester Wire & Cable)
Compact underwater slip ring swivel (Hanayuu Co., Ltd.)

CTD: SBE911plus CTD system
Deck unit:
SBE11plus (S/N 11P54451-0872, Sea-Bird Electronics, Inc.)

Under water unit:
SBE9plus (S/N: 09P54451-1027, Sea-Bird Electronics, Inc.)
Pressure sensor: Digiquartz pressure sensor (S/N: 117457) Date of calibration: 08-Jul-2020

Carousel water sampler:
SBE32 (S/N: 3227443-0391, Sea-Bird Electronics, Inc.)

Temperature sensors:
Primary: SBE03F (S/N: 031525, Sea-Bird Electronics, Inc.) Date of calibration: 19-Jan-2022
Secondary: SBE03F (S/N: 031464, Sea-Bird Electronics, Inc.) Date of calibration: 05-Jun-2021
Deep ocean standards thermometer: SBE35 (S/N: 0022, Sea-Bird Electronics, Inc.)
Date of calibration: 10-Jun- 2021

Conductivity sensors:
Primary: SBE04C (S/N: 042240, Sea-Bird Electronics, Inc.) Date of calibration: 14-Oct-2021
(Casts used: 001M001~008M001, PE1M001~PE4M001)

Primary: SBE04C (S/N: 042435, Sea-Bird Electronics, Inc.) Date of calibration: 10-Feb-2022
(Casts used: 009M001~015M001)
Secondary: SBE04C (S/N: 041206, Sea-Bird Electronics, Inc.) Date of calibration: 16-Feb-2022

Dissolved oxygen sensors:
Primary: RINKOIII (S/N: 0287_163011BA, JFE Advantech Co., Ltd.) Date of calibration: 19-Oct-2021
Secondary: SBE43 (S/N: 432211, Sea-Bird Electronics, Inc.) Date of calibration: 19-Jun-2019

Transmissometer:
C-Star (S/N CST- 1727DR, WET Labs, Inc.)
Date of calibration: 05-Apr-2022

Fluorescence sensor:
Chlorophyll Fluorometer (S/N: 3618, Seapoint Sensors, Inc.) Date of calibration: None
Gain setting: 30X, 0-5 ug/l

Turbidity sensor:
Deep Ocean Turbidity Meter (ATUD-CAV-S50, S/N: 0002, JFE Advantech Co., Ltd.)
Date of calibration: 10-Mar-2022

Photosynthetically Active Radiation (PAR) Sensor:
PAR-Log ICSW (S/N: 2180, Sea-Bird Electronics, Inc.) Date of calibration: 14-Sep-2021

Chromophoric Dissolved Organic Matter (CDOM) Sensor:
Ultraviolet Fluorometer (S/N: 6246, Seapoint Sensors,Inc.) Gain setting: 30X, 0-50 QSU

Altimeter:
Benthos PSA-916T (S/N: 1100, Teledyne Benthos, Inc.)

Submersible pump:
Primary: SBE5T (S/N: 055816, Sea-Bird Electronics, Inc.)
Secondary: SBE5T (S/N: 054598, Sea-Bird Electronics, Inc.)

Bottom contact switch: (Sea-Bird Electronics, Inc.)

Other additional sensors
AFP07(micro temperature and conductivity sensors or two micro temperature sensors)
Lowered Acoustic Doppler Current Profilers (LADCP)
Gamma-ray sensor
pH/pCO_2 sensors
Configuration files: MR2203_A.xmlcon
(001M001~008M001, PE1M001~PE4M001)
MR2203_B.xmlcon
(009M001~015M001)

Data Collection
CTD was deployed from starboard side of the working deck. CTD raw data were acquired in real time by using Seasave-Win32 (ver.7.26.7.121, Sea-Bird Electronics, Inc.), and stored on the hard disk of the personal computer. Seawater was sampled during the upcast by sending fire (close) command from the operation PC. At each sampling

depth, fire command was sent after waiting for 30 seconds from the winch stop. After closing of water sampling bottle, the underwater unit of CTD/CWS system was stayed at the sampling depth at least 5 seconds for measurement of water temperature by SBE 35. For depths where vertical gradient of water properties was expected to be large (e.g. in thermocline), the bottle was exceptionally fired after waiting for 60 seconds from the winch stop to enhance exchanging the water between inside and outside of the bottle.

(5) Problems Encountered

From cast 001M001 to PE4M001, turbidity sensor was deployed in horizontal position on grating attached to CTD frame. During those casts, when CTD was being lowered at surface layer (0dbar~ 50dbar), the turbidity value was about -0.02FTU, then suddenly shifted to around 0.2～0.3FTU. The turbidity value was round 0.2～0.3FTU at medium layer. The same thing happened during up cast: turbidity value shifted suddenly from 0.2～0.3FTU to about -0.02FTU when it reached surface layer (around 50dbar or up). That negative value was considered to be caused by ambient light interference. Also, there was an LADCP battery case attached to CTD frame at about 21cm in straight direction from the sensor lens. Although that clearance was more than the recommended 20 cm clearance distance described in sensor manual, there was also a possibility of interference of reflection, so we tried changing the position of turbidity sensor, with the sensor lens in facing down. From next cast (005M001), the negative value at surface depth, which might be caused by ambient light interference was gone for the most of the cast, except for a couple of casts with turbidity value of -0.02FTU up to about 10db. Also, the 0.2～0.3FTU offset value at deeper depth, which was considered to be caused by some interference, was also gone.

At cast 005M002, at about 764～803dbar during downcast, there was a problem with data acquisition. Modulo Error Count (MEC) suddenly increased to 11 and spikes appeared in almost all sensor data. CTD was stopped at 825dbar and the cast was aborted. After CTD was brought back to deck, slip-ring swivel was changed and the cast conducted again with cast name 005M003.

From cast 001M001 to 008M001, during downcast, there was a difference in salinity data between primary and secondary conductivity sensors. The difference was largest at salinity minimum layer, with 0.004 PSU difference between primary and secondary sensors. There was no much difference between salinity data of primary and secondary sensors during up cast. The difference in upcast was 0.001PSU at largest. Compared with bottle analysis salinity measured by using AUTOSAL, the data of the secondary conductivity sensor were found to be closer to the bottle data. So, after the cast 008M001, primary sensor (S/N: 042240) was changed to S/N: 042435.

After changing the primary sensor, the difference in salinity during downcast was gone, but a linear difference of about 0.006PSU between primary and secondary sensor appeared in both downcast and upcast. The primary conductivity sensor (S/N: 2435) was kept on being used for the next casts.

(6) Data Processing

The procedure in processing of the obtained CTD data is herein described. In these processes, a utility software, SBE Data Processing-Win32 (ver.7.26.7.129) and some original modules were used.

(The process in order)

DATCNV converted the binary raw data to engineering unit data. DATCNV also extracts bottle information where scans were marked with the bottle confirm bit during acquisition. The scan duration to be included in bottle file was set to 4.4 seconds, and the offset was set to 0.0 seconds. . The hysteresis correction for the SBE 43 data (voltage) was applied for both profile and bottle information data.

TCORP (original module) corrected the pressure sensitivity of the temperature (SBE3) sensor.
1.714e-008 (degC/dbar) for S/N1525
-7.75293156e-009 (degC/dbar) for S/N1464

RINKOCOR (original module) corrected the time dependent, pressure induced effect (hysteresis) of the RINKOIII profile data.

Hysteresis correction: a= 0.0045, c= 5000.0, H= 2000.0

RINKOCORROS (original module) corrected the time dependent, pressure induced effect (hysteresis) of the RINKOIII bottle information data by using the hysteresis corrected profile data.

BOTTLESUM created a summary of the bottle data. The data were averaged over 4.4 seconds.

ALIGNCTD aligned parameter data in time, relative to pressure to ensure that all calculations were made using measurements from the same parcel of water.
For an SBE 9plus with TC-ducted temperature and conductivity sensors and a 3000-rpm pump, the typical lag of temperature to pressure is 0 second and lag of conductivity relative to temperature is 0.073 seconds. The Deck Unit was programmed to advance conductivity relative to pressure so conductivity alignment in ALIGNCTD was not needed. Dissolved oxygen data are systematically delayed with respect to pressure mainly because of the long time constant of the dissolved oxygen sensor and of an additional delay from the transit time of water in the pumped pluming line. This delay was compensated by 5 seconds advancing dissolved oxygen sensor (SBE43) output (dissolved oxygen voltage) relative to the temperature data. Delay of the RINKO data was also compensated by 1 second advancing sensor output (voltage) relative to the temperature data. Delay of the transmissometer data was also compensated by 2 seconds advancing sensor output (voltage) relative to the temperature data. Turbidity data (User polynomial 1 and voltage 4) was also advanced 1 second.

WILDEDIT marked extreme outliers in the data files. The first pass of WILDEDIT obtained the accurate estimate of the true standard deviation of the data. The data were read in blocks of 1000 scans. Data greater than 10 standard deviations were flagged. The second pass computed a standard deviation over the same 1000 scans excluding the flagged values. Values greater than 20 standard deviations were marked bad. This process was applied to pressure, depth, temperature (primary and secondary), conductivity (primary and secondary), and dissolved oxygen voltage (SBE43).

CELLTM used a recursive filter to remove conductivity cell thermal mass effects from the measured conductivity. Typical values for SBE 9plus with TC duct and 3000 rpm pump which were 0.03 for thermal anomaly amplitude alpha and 7.0 for the time constant 1/beta were used.

FILTER performed a low-pass filter on pressure and depth with a time constant of 0.15 second. In order to produce zero phase lag (no time shift) the filter runs forward first then backward.
WFILTER performed as a median filter to remove spikes in the output voltage of Transmissometer, beam transmission data, beam attenuation data, the fluorescence data, and turbidity data and turbidity sensor voltage, and CDOM data. A median value was determined by 49 scans of the window. For the CDOM data, an additional box-car filter with a window of 361 scans was applied to remove noise.

SECTIONU (original module of SECTION) selected a time span of data based on scan number in order to reduce a file size. The minimum number was set to be the starting time when the CTD package was beneath the sea-surface after activation of the pump. The maximum number of was set to be the end time when the package came up from the surface.

LOOPEDIT marked scans where the CTD was moving less than the minimum velocity of 0.0 m/s (traveling backwards due to ship roll).

DESPIKE (original module) removed spikes of the data. A median and mean absolute deviation was calculated in 1-dbar pressure bins for both down and up cast, excluding the flagged values. Values greater than 4 mean absolute

deviations from the median were marked bad for each bin. This process was performed twice for temperature, conductivity and dissolved oxygen (RINKOIII and SBE43) voltage.

DERIVE was used to compute dissolved oxygen (SBE43).

BINAVG averageed the data into 1 decibar pressure bins and 1 sec time bins.

BOTTOMCUT (original module) deleted the deepest pressure bin when the averaged scan number of the deepest bin was smaller than the average scan number of the bin just above.

DERIVE: was re-used to calculate salinity, potential temperature, and sigma-theta.

SPLIT was used to split data into downcast and upcast

Remaining spikes in the CTD data were manually eliminated from the 1-dbar-averaged data. The data gaps resulting from the elimination were linearly interpolated with a quality flag of 6.

(7) Station list
During the MR22-03 cruise, 28 casts of CTD were carried out. Date, time and locations of the CTD casts are listed in Table 2.2.1-1.

(8) Preliminary Results
During this cruise, we judged presence or absence of noise, spike or shift in the obtained hydro-cast data.

Definitions of these problems
(1) noise; not singly but continuously (mostly from several seconds to several minutes) detected outliers.
(2) spike; one-off outlier which is detected after data processing and is oceanographically impossible (e.g. reversal of density). Spike is not caused by a breaking down of sensor. Generally, we can detect spikes in the deep layer (e.g. below the thermocline).
(3) shift; continuous data under trend to collect values deviated from accurate ones. In most cases, the “shift” can be recognized from comparison of profiles between primary and secondary sensors or down and up casts. The “shift” may be caused by absorption of foreign substances into sensors, adhesion of substances on an optical sensor, crack in a part of sensor, characteristics in each sensor, etc.

Detected problems
001M001: Turbidity
Down 5~ Up 1 dbar: offset
001M002: Turbidity
Down 6~17 dbar, Up16~1dbar: ambient light interference
Down 18~Up 15 dbar: offset
002M001: Turbidity
Up 20~1 dbar: ambient light interference
Down 5~ Up 20 dbar: offset
PE1M001: Turbidity
Down 3~5 dbar, Up35~1dbar: ambient light interference
Down 5~ Up 34 dbar: offset
003M001: Turbidity
Down 4~52 dbar: ambient light interference
Down 53~ Up 1 dbar: offset

Up 33~32 dbar: spike

PE2M001: Turbidity
Down 1~14 dbar, Up11~0 dbar: ambient light interference
Down 15~ Up 12 dbar: offset
004M001: Turbidity
Up 10~1 dbar: ambient light interference
Down 3~ Up 11dbar: offset
004M002: Turbidity
Down 4~ 53 dbar, Up 56~1 dbar : ambient light interference
Down 54~Up 57 dbar: offset
PE4M001: Turbidity
Up2~1 db: ambient light interference
Down 4~ Up 2 dbar: offset
005M003: Turbidity
Down 3~4 dbar: ambient light interference
Beam Transmission
Down 356~983 dbar:noise, Down 1318~5689 dbar: noise, shift
006M002: Turbidity
Up 281~168 dbar: noise
007M001: Beam Transmission
Down 469~473 dbar, Down816~818 dbar: spike
CDOM
Down 3~ 10 dbar: ambient light interference
008M001: Turbidity
Down 4~10 dbar: ambient light interference
Beam Transmission
Down 650~652 dbar, Down 2515~2514 dbar: spike
010M001: Beam Transmission
Up 1284~1249 dbar : noise
011M001: Turbidity
Down 4~6 dbar, Up 10~1 dbar : ambient light interference
011M005: Beam Transmission
Down 668~671 dbar: spike
012M001: Beam Transmission
Down 231~233 dbar: spike

(9) Data archive

These data obtained in this cruise will be submitted to the Data Management Group of JAMSTEC, and will be opened to the public via “Data Research System for Whole Cruise Information in JAMSTEC (DARWIN)” in JAMSTEC web site.

Table 2.2.1-1 MR22-03 CTD cast table

MR22-03 CTD cast table													
Stnnbr	Castno	Date(UTC)	Time(UTC)		BottomPosition		Depth	Wire	HT Above	Max	Max	CTD	Remark
		(mmddyy)	Start	End	Latitude	Longitude	(m)	Out (m)	Bottom (m)	Depth (m)	Pressure	Filename	
001	1	041622	21:12	21:37	32-31.37N	137-29.80E	4038.0	196.4	-	201.5	203.0	001M001	
001	2	041722	01:15	03:46	32-31.21N	137-30.01E	4037.0	2961.8	-	2957.9	3000.0	001M002	
002	1	041722	21:32	23:57	30-00.42N	137-31.36E	4339.0	2962.3	-	2959.5	3001.0	002M001	
PE1	1	041822	21:31	21:45	25-36.56N	137-29.93E	5366.0	198.5	-	200.6	202.0	PE1M001	
003	1	041922	04:38	07:21	25-00.34N	137-28.87E	5166.0	2973.2	-	2961.6	3002.0	003M001	
PE2	1	041922	21:32	21:47	25-00.02N	140-29.94E	3149.0	205.8	-	199.6	201.0	PE2M001	
004	1	042022	20:35	21:08	25-01.05N	144-56.77E	5050.0	305.0	-	302.8	305.0	004M001	
004	2	042122	00:54	03:22	25-03.03N	144-54.80E	5007.0	3000.9	-	2962.6	3003.0	004M002	
PE4	1	042122	20:33	20:49	27-45.72N	144-51.36E	5758.0	204.7	-	203.5	205.0	PE4M001	
005	1	042222	20:33	21:03	32-15.47N	144-40.35E	5717.0	296.8	-	297.7	300.0	005M001	
005	3	042322	03:35	07:35	32-15.10N	144-40.81E	5596.0	5581.4	9.8	5575.4	5689.0	005M003	
006	1	042422	03:39	06:10	34-44.15N	141-15.58E	4444.0	2982.5	-	2959.3	3002.0	006M001	
006	2	042422	10:47	11:13	34-49.94N	141-19.86E	3440.0	296.6	-	297.6	300.0	006M002	
007	1	042522	03:34	06:04	35-00.00N	145-00.01E	5798.0	2964.7	-	2957.3	3000.0	007M001	
008	1	042622	03:35	06:01	34-59.54N	149-13.62E	6136.0	2994.1	-	2959.2	3002.0	008M001	
009	1	042722	23:07	02:33	35-00.86N	157-30.77E	5031.0	5055.1	9.0	5017.1	5114.0	009M001	
010	1	042922	21:07	23:32	42-30.08N	158-00.21E	5392.0	2962.3	-	2955.3	3000.0	010M001	
011	1	050122	21:05	22:18	46-59.47N	160-00.70E	5221.0	1978.1	-	1974.9	2001.0	011M001	
011	2	050222	00:44	04:26	46-59.56N	160-00.86E	5223.0	5205.1	10.2	5195.7	5304.0	011M002	
011	3	050322	19:35	20:22	46-59.98N	160-00.00E	5190.0	294.6	-	297.3	300.0	011M003	
011	4	050622	02:33	04:07	46-59.89N	159-58.51E	5220.0	2961.8	-	2956.0	3002.0	011M004	
011	5	050622	08:05	09:42	47-00.02N	159-59.94E	5186.0	2961.6	-	2955.0	3001.0	011M005	
012	1	050822	02:17	04:41	47-57.11N	166-24.54E	5901.0	2961.0	-	2953.8	3000.0	012M001	
012	2	050922	02:05	02:41	47-56.12N	166-25.34E	5835.0	994.3	-	991.2	1002.0	012M002	
012	3	050922	09:11	09:48	47-56.27N	166-29.96E	5958.0	992.5	-	989.2	1000.0	012M003	
013	1	051122	21:56	00:26	43-59.87N	155-00.25E	5313.0	2962.3	-	2955.9	3001.0	013M001	
014	1	051522	02:04	02:45	41-47.99N	141-20.42E	274.0	258.7	9.3	261.8	264.0	014M001	
015	1	051522	22:02	22:24	41-40.04N	141-30.32E	121.0	108.8	9.8	111.1	112.0	015M001	

2.2.2 Salinity

Masahide WAKITA JAMSTEC PI
Rei ITO MWJ Operation leader

(1) Objective
To provide calibrations for the measurements of salinity collected from CTD casts, bucket sampling, Clean CTD casts, Marine Snow Catcher, Mooring sample (Remote Access Sampler) and underway surface water monitoring system.

(2) Parameters
Salinity

(3) Instruments and methods
Seawater samples were collected with 12 Liter water sampling bottles, 12 Liter water clean sampling bottles, Marine Snow Catcher (large and small), RAS samples and underway surface water monitoring system. The salinity sample bottle of the 250ml brown glass bottle with screw cap (RAS samples used aluminum packs) was used for collecting the sample water. Each bottle was rinsed 3 times with the sample water, and was filled with sample water to the bottle shoulder. The salinity sample bottles for underway surface water monitoring system and MSC samples were sealed with a plastic septum and screw cap because we took into consideration the possibility of storage for about one month. The caps were rinsed 3 times with the sample seawater before its use. Each bottle was stored for more than 24 hours in the laboratory before the salinity measurement.
The kind and number of samples taken are shown as follows ;

Table 2.2.2.-1. Kind and number of samples

Kind of Samples	Number of Samples
Samples for CTD	501
Samples for underway surface water monitoring system	26
Sample for crean sampling bottol	30
Sample for Marine Snow Catcher	26
Sample for Mooring (RAS)	92
Total	675

The salinity analysis was carried out on R/V MIRAI during the cruise of MR22-03 using the salinometer (Model 8400B “AUTOSAL” ; Guildline Instruments Ltd.: S/N 62556) with an additional peristaltic-type intake pump (Ocean Scientific International, Ltd.). A pair of precision digital thermometers (1502A; FLUKE: S/N B78466 and B81549) were used for monitoring the ambient temperature and the bath temperature of the salinometer.

The specifications of the AUTOSAL salinometer and thermometer are shown as follows ;
Salinometer (Model 8400B “AUTOSAL” ; Guildline Instruments Ltd.)
Measurement Range : 0.005 to 42 (PSU)
Accuracy : Better than ±0.002 (PSU) over 24 hours
Maximum Resolution : Better than ±0.0002 (PSU) at 35 (PSU)
Thermometer (1502A: FLUKE)
Measurement Range : 16 to 30 deg C (Full accuracy)
Resolution : 0.001 deg C
Accuracy : 0.006 deg C (@ 0 deg C)

The measurement system was almost the same as Aoyama *et al.* (2002). The salinometer was operated in the air-conditioned ship's laboratory at a bath temperature of 24 deg C. The ambient temperature varied from approximately 22 deg C to 24 deg C, while the bath temperature was very stable and varied within +/- 0.002 deg C on rare occasion. The measurement for each sample was done with a double conductivity ratio and defined as the median of 34 readings of the salinometer. (Acquisition of the 34 readings took about 11 seconds when the function dial was turned to the 'read' setting) Data were taken after rinsed 5 (RAS samples were taken after rinsed 3) times with the sample water. The double conductivity ratio of sample was calculated from average value of two measurements. And it was used to calculate the bottle salinity with the algorithm for the practical salinity scale, 1978 (UNESCO, 1981). In the case of the difference between the double conductivity ratio of these two measurements being greater than or equal to 0.00003, continue to be measured up to 3 times. The difference between the double conductivity ratio of these two measurements being smaller than 0.00002 were selected. The measurement was conducted in about 8 hours per day and the cell was cleaned with neutral detergent after the measurement of the day.

(4) Station list

Table. 2.2.2-2 shows the sampling locations for the salinity analysis in this cruise.

Table. 2.2.2-2 List of sampling locations of the salinity samples collected from CTD

Stnnbr	Castno	Date(UTC)	Time(UTC)		BottomPosition		Depth
		(mmddyy)	Start	End	Latitude	Longitude	(m)
001	2	041722	01:15	03:46	32-31.21N	137-30.01E	4037.0
002	1	041722	21:32	23:57	30-00.42N	137-31.36E	4339.0
003	1	041922	04:38	07:21	25-00.34N	137-28.87E	5166.0
004	2	042122	00:54	03:22	25-03.03N	144-54.80E	5007.0
005	3	042322	03:35	07:35	32-15.10N	144-40.81E	5596.0
006	1	042422	03:39	06:10	34-44.15N	141-15.58E	4444.0
007	1	042522	03:34	06:04	35-00.00N	145-00.01E	5798.0
008	1	042622	03:35	06:01	34-59.54N	149-13.62E	6136.0
009	1	042722	23:07	02:33	35-00.86N	157-30.77E	5031.0
010	1	042922	21:07	23:32	42-30.08N	158-00.21E	5392.0
011	2	050222	00:44	04:26	46-59.56N	160-00.86E	5223.0
011	3	050322	19:35	20:22	46-59.98N	160-00.00E	5190.0
012	1	050822	02:17	04:41	47-57.11N	166-24.54E	5901.0
013	1	051122	21:56	00:26	43-59.87N	155-00.25E	5313.0
014	1	051522	02:04	02:45	41-47.99N	141-20.42E	274.0
015	1	051522	22:02	22:24	41-40.04N	141-30.32E	121.0

(5) Preliminary results

(5-1) Standard Seawater

Standardization control of the salinometer was set to 620 (17th Apr.) / 636 (8th May). The value of STANDBY was 24+5142 ~ 5143 / 24+5154 ~ 5155 and that of ZERO was 0.0±0000 ~ + 0001. The IAPSO Standard Seawater (SSW) batch P165 was used as the standard for salinity. 31 bottles of P165 were measured.

Fig. 2.2.2-1 shows the time series of the double conductivity ratio of the Standard Seawater batch P165. The average of the double conductivity ratio was 1.99972 and the standard deviation was 0.00001 which is equivalent to 0.0002 in salinity.

The specifications of SSW batch P165 used in this cruise are shown as follows ;

Batch	:	P165
Conductivity ratio	:	0.99972
Salinity	:	34.994
Use by	:	15th April. 2024

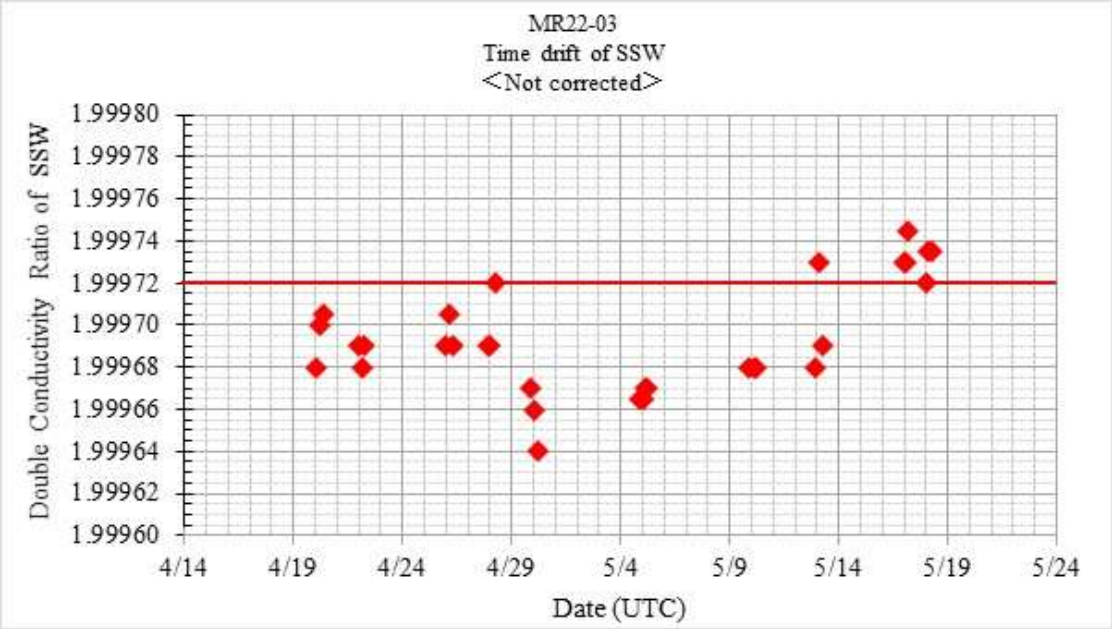

Fig. 2.2.2-1: Time series of double conductivity ratio for the Standard Seawater (before correction)

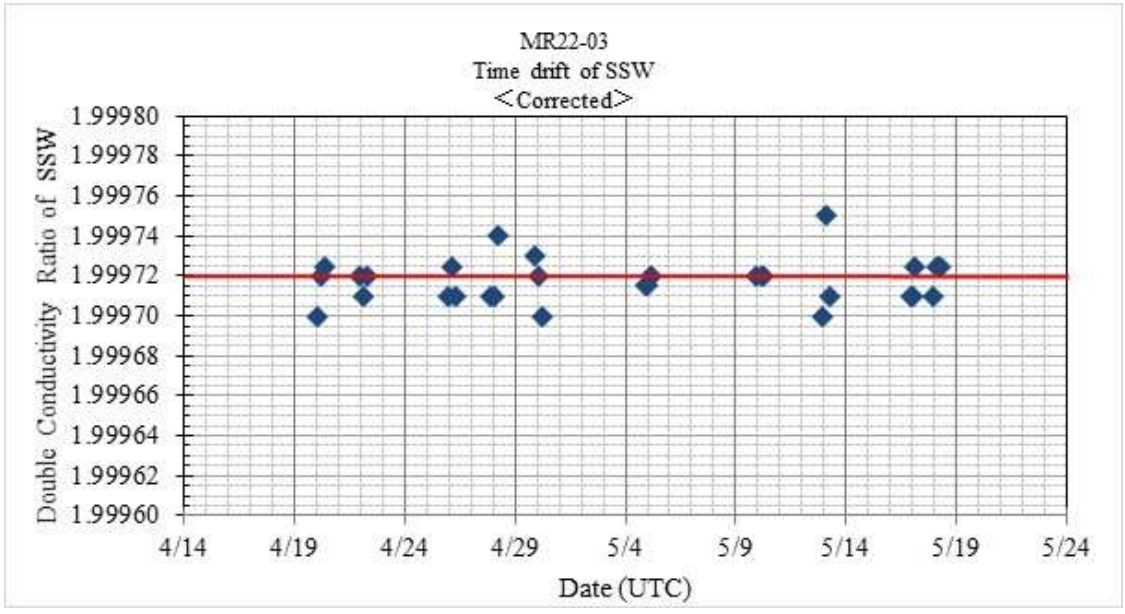

Fig. 2.2.2-2: Time series of double conductivity ratio for the Standard Seawater (after correction)

(5-2) Sub-Standard Seawater

Sub-standard seawater was made from surface sea water filtered by a pore size of 0.2 micrometer and stored in a 20 Liter container made of polyethylene and stirred for at least 24 hours before measuring. It was measured about every about 10 samples in order to check for the possible sudden drifts of the salinometer.

(5-3) Replicate Samples

We estimated the precision of this method using 46 pairs of replicate samples taken from the same water sampling bottle. Fig. 2.2.2-3 shows the histogram of the absolute difference between each pair of the replicate samples. The average and the standard deviation of absolute difference among 46 pairs of replicate samples were 0.0006 and 0.0007 in salinity, respectively.

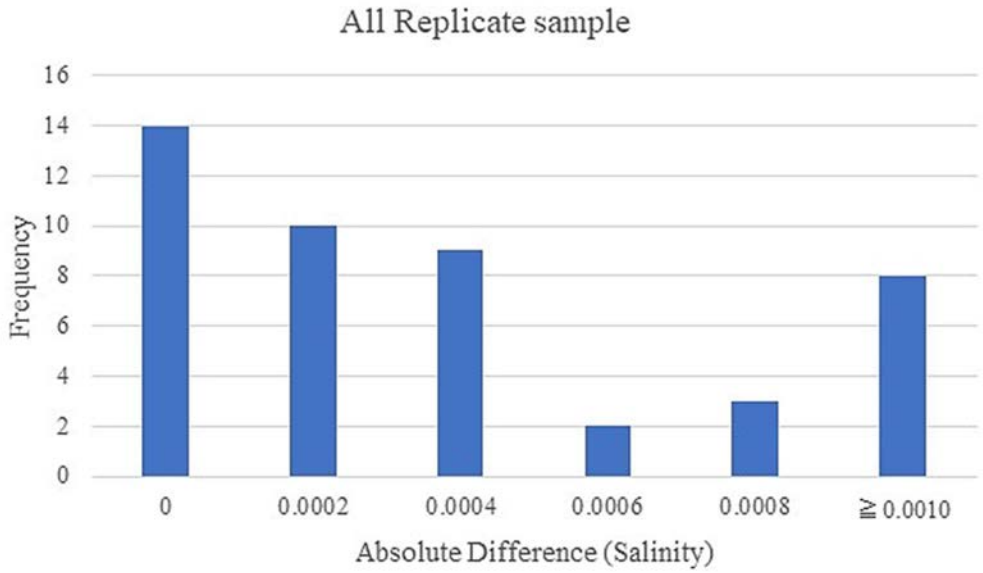

Fig. 2.2.2-3 The histogram of the salinity for the absolute difference of all replicate samples

(6) Data archive

These data obtained in this cruise will be submitted to the Data Management Group of JAMSTEC, and will be opened to the public via “Data Research System for Whole Cruise Information in JAMSTEC (DARWIN)” in JAMSTEC web site.

<http://www.godac.jamstec.go.jp/darwin/e>

(7) Reference

Aoyama, M., T. Joyce, T. Kawano and Y. Takatsuki (2002) Standard seawater comparison up to P129. Deep-Sea Research I, 49, 1103–1114.

UNESCO : Tenth report of the Joint Panel on Oceanographic Tables and Standards. UNESCO Tech. Papers in Mar. Sci., 36, 25 pp., 1981

2.2.3 Current and turbulence

2.2.3.1 Lowered Acoustic Doppler Current Profiler

Yusuke SASAKI	**Atmosphere and Ocean Research Institute, The University of Tokyo**	**PI**
Shinya KOUKETSU	**JAMSTEC**	
Ichiro YASUDA	**Atmosphere and Ocean Research Institute, The University of Tokyo**	

(1) Overview of the equipment

Two acoustic Doppler current profilers (ADCP) were integrated with the CTD/RMS package. The lowered ADCP (LADCP)s, Workhorse Monitor WHM300 and WHM600 (Teledyne RD Instruments, San Diego, California, USA), which has 4 facing transducers with 20-degree beam angles, rated to 6000 m, make direct current measurements at the depth of the CTD, thus providing a full profile of velocity. The LADCPs were powered during the CTD casts by a 48 volts battery pack. The LADCP unit was set for recording internally prior to each cast. After each cast the internally stored observed data were downloaded to the computer in the onboard laboratory. After the cruise, by combining the measured velocity of the sea water and ocean bottom relative to the instrument, shipboard navigation data, and pressure time series from the CTD, the absolute velocity profiles will be obtained with the software implemented by A.Thurnherr. The software is based on the method of Visbeck (2002) and available online at ftp://ftp.ldeo.columbia.edu/pub/LADCP.

The instruments used in this cruise were as follows.

WHM600(S/N 8694; downward), WHM300(S/N 22595; upward)

(2) Data collection

In this cruise, data were collected with the following configuration.

WHM600: Bin size: 2.0 m, Number of bins: 30

WHM300: Bin size: 4.0 m, Number of bins: 20

Some of the downloaded files were fragmented with occasional periods without data recordings (St. 1_2, 2_1, 3_1, 4_2). We suspected this was caused by overloaded battery power with two sensors with the ping intervals set to 1.4s. However, even after making the ping intervals longer (1.6s) for WHM600 and WHM300, fragmentations occurred again (St.3_1). After cleaning pings of power-supply cable, fragmentations did not occur (St.PE4 - 15_1).

Reference

Visbeck, M. (2002) Deep velocity profiling using Lowered Acoustic Doppler Current Profilers: Bottom track and inverse solutions. J. Atmos. Oceanic Technol., 19, 794-807.

2.2.3.2 Microstructure in temperature and conductivity

Yusuke SASAKI Atmosphere and Ocean Research Institute, The University of Tokyo PI
Ichiro YASUDA Atmosphere and Ocean Research Institute, The University of Tokyo

(1) Objective
The objective is to measure microstructure in temperature and conductivity to evaluate vertical mixing.

(2) Instruments and method
Microstructure observations were carried out by AFP07 (Rockland Scientific International Inc.), which were mounted on the CTD rosette and were powered from the CTD (SBE 9plus). On AFP07, which has two sensor sockets, FP07 thermistor or micro-conductivity sensor (SBE-7) can be installed. For the six casts (PE1, St.3_1, PE2, St.4_1, St.4_2, PE4), two FP07 thermistors were installed on both sockets of AFP07. For the other casts, one FP07 thermistor and one micro-conductivity sensor were installed on AFP07. We had to replace probes, as some of the probes failed during the cruise. AFP07 also measured high-frequency pressure and acceleration profiles. Low-frequency profiles of temperature and conductivity were recorded in the AFP07 with the input from the SBE-3 sensors on the CTD system. We downloaded the raw data from the instruments after each cast. We plan to examine methods for calibration and quality check of the data by comparing these micro temperature and conductivity with the CTD data and free fall micro shear structure data (VMP, see Section 2.2.3.3).

(3) Measurements
The probes installed on the instruments are described below:

AFP07
Sensor socket 1: T2120 (St.1_1-St.15_1)
Sensor socket 2: C293 (St.1_1), C302 (St.1_2 and 2_1), T1973 (PE1, St.3_1, PE2, St.4_1, St.4_2, and PE4) and C288 (St.5_1-St.15_1)

(4) Note for using data
The file included in the data ‘AFP07_MR2203.csv’ shows the correspondence between the station number and the data file name.

2.2.3.3 Vertical Microstructure Profiler (VMP)

Yusuke SASAKI	**Atmosphere and Ocean Research Institute, The University of Tokyo**	**PI**
Ichiro YASUDA	**Atmosphere and Ocean Research Institute, The University of Tokyo**	
Yutaro MURAKAMI	**NME**	
Ryo OYAMA	**NME**	
Fumine OKADA	**NME**	

(1) Objective

The objective is to measure microstructure in vertical shear of the horizontal velocity, temperature, and conductivity to evaluate vertical mixing.

(2) Instruments and method

Microstructure observations were carried out by VMP250-IR ("Internal Recording") manufactured by Rockland Scientific International Inc. We used the two sets of instruments (VMP250_SN354 and VMP250_SN271), which have different sensor configurations. The probes on each VMP250 sensor set are as follows:

VMP250_SN354
Vertical shear of the horizontal velocity (two sensors, 512Hz)
Fast thermistor temperature "FP07" (two sensors, 512Hz)
Micro-Conductivity "SBE-7" (512Hz)
Fine scale conductivity and temperature from JAC (JFE Advantech Co.) CT sensor (64Hz)
Pressure (512Hz)
Acceleration (512Hz)

VMP250_SN271
Vertical shear of the horizontal velocity (two sensors, 512Hz)
Fast thermistor temperature "FP07" (two sensors, 512Hz)
Fine scale conductivity and temperature from JAC (JFE Advantech Co.) CT sensor (64Hz)
Pressure (512Hz)
Acceleration (512Hz)
Chlorophyll and turbidity from JAC FLTU sensor (512Hz)

The microscale parameters were measured while the sensor descended without artificial acceleration/deceleration ("free fall"). A cable (12 strand Vectran rope with a diameter = 5 mm) was attached to the probe for recovery of the instrument. The cable was always kept slack to maintain the free fall. After the predetermined time had passed, we stopped feeding out the cable and recovered the instrument to the surface. We downloaded the raw data from the instrument after each cast and replaced damaged probes when necessary.

(3) Measurements

During the present cruise, 51 profiles were obtained. For the first five casts (St. V1_1, V2_1, V2_2, V3_1 and V3_2), the observations were operated using the VMP250_SN354. In the profiles of St. V3_1 and V3_2, the data of JAC_T sensor were drifted abnormally, and we suspected some damage in the JAC_T sensor itself or its electrical board. From the 6th cast (St. V4_1), we used the VMP250_SN271 instead. The serial number of sensor probes installed on the instruments are described below:

VMP250_SN354
Sensor socket S1: M1997 (St. V1_1-V3_2)
Sensor socket S2: M2002 (St. V1_1-V3_2)
Sensor socket T1: T1995 (St. V1_1-V3_2)
Sensor socket T2: F-T1975 (St. V1_1-V3_2)
Sensor socket C1: C288 (St. V1_1-V3_2)

VMP250_SN271
Sensor socket S1: M1815 (St. V4_1-V15_2)
Sensor socket S2: M1816 (St. V4_1-V15_2)
Sensor socket T1: T1609 (St. V4_1-V15_2)
Sensor socket T2: T1021 (St. V4_1-V15_2)

(5) Note for data use
The file included in the data 'TVMP_MR2203.csv' shows the information of each profile (the station location, date, time, and the file name).

2.2.3.4 Underway-VMP (UVMP)

Yusuke SASAKI	**Atmosphere and Ocean Research Institute, The University of Tokyo**	**PI**
Ichiro YASUDA	**Atmosphere and Ocean Research Institute, The University of Tokyo**	
Yutaro MURAKAMI	**NME**	
Ryo OYAMA	**NME**	
Fumine OKADA	**NME**	
Rei ITO	**MWJ**	
Airi HARA	**MWJ**	

(1) Objective

The purpose of this measurement is to explore the oceanic structure of temperature, salinity, and vertical mixing in the observation area. By using the Underway CTD (UCTD) on-deck unit and the vertical microstructure profiler (VMP), the microstructure in vertical shear of the horizontal velocity and temperature was obtained in horizontally high resolution.

(2) Instruments and method

The UVMP system consists of on-deck unit with a winch and davit (which is the same as used in Underway CTD observation), and a sensor probe unit (VMP250_IR manufactured by Rockland Scientific International Inc.). We used the VMP250_SN271 as a sensor probe, whose sensor configuration is described in detail in the section of “VMP”. The probe unit was released from the vessel with connection to the winch by a line, while the vessel was traveling with constant speed (The log speed at each cast is shown in Table 2.2.3.4). The probe unit measured temperature, conductivity, and microstructure during its descent with a speed of about 0.4-0.6 m/s in the water. After a predetermined time, we stopped feeding out the line and wound it up until the probe surfaced and approached the hull. The probe unit was on-deck only after all measurement casts on one observation section were finished. The data were internally recorded during the observation, which were retrieved after the probe was recovered.

Table 2.2.3.4 and Figure 2.2.3.4 show the time and location of each cast. The serial number of sensor probes installed on the instruments are described below:

VMP250_SN271
Sensor socket S1: M1815
Sensor socket S2: M1816
Sensor socket T1: T1609
Sensor socket T2: T1021

Table 2.2.3.4: The list of UVMP

Section	Towed time (UTC)		Towed position		Log speed (knot)	File name
	Date	Time	Lat	Lon		
Line UV1	2022/5/9	2:59	47-56.37N	166-25.17E	2.4	271_213
	2022/5/9	3:26	47-57.28N	166-25.18E	2	271_213
	2022/5/9	3:52	47-58.15N	166-25.18E	1.9	271_213
	2022/5/9	4:18	47-59.05N	166-25.17E	2.1	271_213
Line UV2	2022/5/9	5:29	47-56.39N	166-19.07E	1.8	271_214
	2022/5/9	5:55	47-56.33N	166-20.42E	2.2	271_214
	2022/5/9	6:21	47-56.35N	166-21.72E	2.1	271_214
	2022/5/9	6:47	47-56.32N	166-23.01E	2	271_214
	2022/5/9	7:12	47-56.33N	166-24.3E	2.1	271_214
	2022/5/9	7:38	47-56.32N	166-25.62E	2.1	271_214
	2022/5/9	8:03	47-56.32N	166-26.94E	2	271_214
	2022/5/9	8:29	47-56.31N	166-28.19E	2	271_214

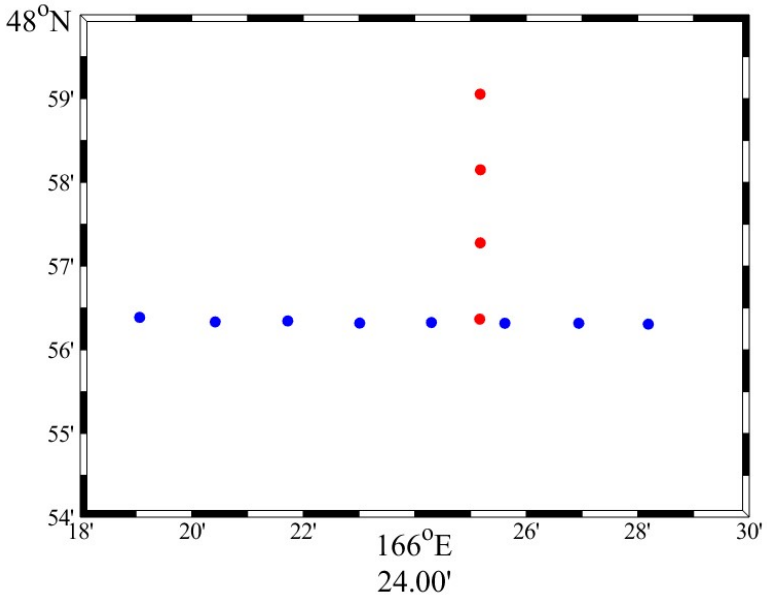

Fig 2.2.3.4: UVMP station locations. The red circles show the UVMP station along the observation section ‘Line_UV1’. The blue circles are for ‘Line_UV2’.

2.2.4 Shipboard ADCP

Hitoshi KANEKO	**JAMSTEC**	**PI**
Yutaro MURAKAMI	**NME**	
Ryo OYAMA	**NME**	
Fumine OKADA	**NME**	
Yoichi INOUE	**MIRAI crew**	

(1) Objectives

To obtain continuous measurement data of the current profile along the ship's track.

(2) Instruments and methods

Upper ocean current measurements were made during this cruise, using the hull-mounted Acoustic Doppler Current Profiler (ADCP) system. For most of its operation, the instrument was configured for water-tracking mode. Bottom-tracking mode, interleaved bottom-ping with water-ping, was made to get the calibration data for evaluating transducer misalignment angle in the shallow water. Major parameters for the measurement, Direct Command, are shown in Table 2.3.4-1. The system consists of following components;

(2-1) R/V MIRAI has installed the Ocean Surveyor for vessel-mount ADCP (frequency 76.8 kHz; Teledyne RD Instruments, USA). It has a phased-array transducer with single ceramic assembly and creates 4 acoustic beams electronically. We mounted the transducer head rotated to a ship-relative angle of 45 degrees azimuth from the keel.
(2-2) For heading source, we use ship's gyro compass (Tokyo Keiki, Japan), continuously providing heading to the ADCP system directory. Additionally, we have Inertial Navigation Unit (Phins, Ixblue, France) which provide high-precision heading, attitude information, pitch and roll. They are stored in ".N2R" data files with a time stamp.
(2-3) Differential GNSS system (StarPack-D, Fugro, Netherlands) providing precise ship's position.
(2-4) We used VmDas software version 1.50.19 (TRDI) for data acquisition.
(2-5) To synchronize time stamp of ping with Computer time, the clock of the logging computer is adjusted to GPS time server by using NTP (Network Time Protocol).
(2-6) Fresh water is charged in the sea chest to prevent bio fouling at transducer face.
(2-7) The sound speed at the transducer does affect the vertical bin mapping and vertical velocity measurement, and that is calculated from temperature, salinity (constant value; 35.0 PSU) and depth (6.5 m; transducer depth) by equation in Medwin (1975).
(2-8) Data were configured for "8 m" layer intervals starting about 19 m below sea surface. Data were recorded every ping as raw ensemble data (.ENR). Additionally, 30 seconds averaged data were recorded as short-term average (.STA). 300 seconds averaged data were long-term average (.LTA), respectively.

Table 2.3.4-1 Major parameters

Bottom-Track Commands	
BP = 001	Pings per Ensemble (almost less than 1,300m depth)
Environmental Sensor Commands	
EA = 04500	Heading Alignment (1/100 deg)
ED = 00065	Transducer Depth (0–65535 dm)
EF = +001	Pitch/Roll Divisor/Multiplier (pos/neg) [1/99–99]
EH = 00000	Heading (1/100 deg)
ES = 35	Salinity (0–40 pp thousand)
EX = 00000	Coordinate Transform (Xform: Type; Tilts; 3Bm; Map)
EZ = 10200010	Sensor Source (C; D; H; P; R; S; T; U)
	C (1): Sound velocity calculates using ED, ES, ET (temp.)
	D (0): Manual ED
	H (2): External synchro
	P (0), R (0): Manual EP, ER (0 degree)
	S (0): Manual ES
	T (1): Internal transducer sensor
	U (0): Manual EU
EV = 0	Heading Bias (1/100 deg)
Timing Commands	
TE = 00:00:02.00	Time per Ensemble (hrs:min:sec.sec/100)
TP = 00:02.00	Time per Ping (min:sec.sec/100)
Water-Track Commands	
WA = 255	False Target Threshold (Max) (0–255 count)
WC = 120	Low Correlation Threshold (0–255)
WD = 111 100 000	Data Out (V; C; A; PG; St; Vsum; Vsum^2; #G; P0)
WE = 1000	Error Velocity Threshold (0–5000 mm/s)
WF = 0800	Blank After Transmit (cm)
WN = 100	Number of depth cells (1–128)
WP = 00001	Pings per Ensemble (0–16384)
WS = 800	Depth Cell Size (cm)
WV = 0390	Radial Ambiguity Velocity (cm/s)

(3) Preliminary results

Horizontal velocity along the ship's track is presented in fig.2.3.4-1. In vertical direction, the data are averaged from 35 to 60m

(4) Data archives

These obtained data will be submitted to JAMSTEC Data Management Group (DMG).

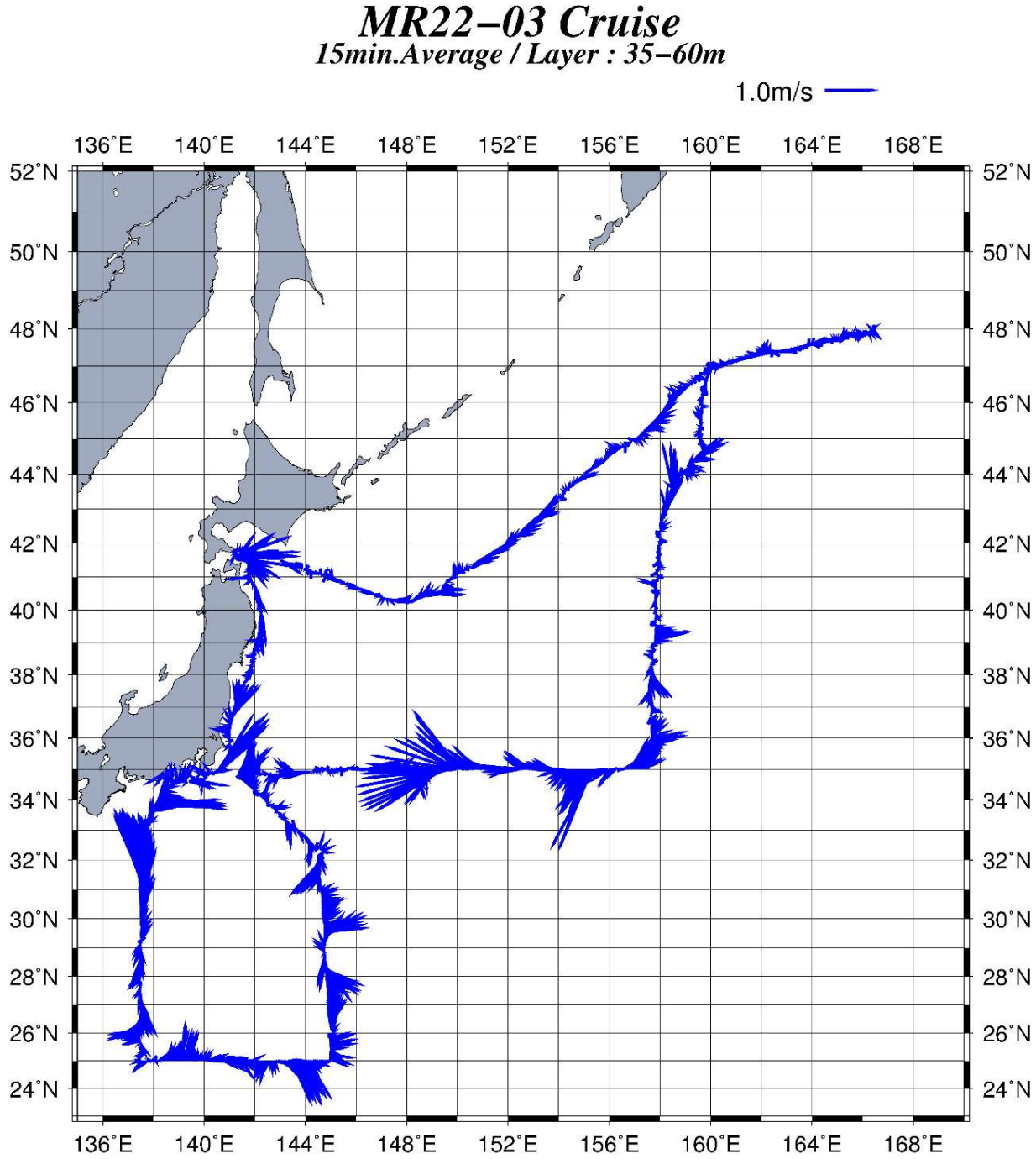

Fig.2.3.4. Horizontal Velocity along the ship's track in this cruise.
(15 min. Average / Layer: 35–60m)

2.3 Chemical oceanography
2.3.1 Dissolved oxygen

Masahide WAKITA JAMSTEC PI
Shiori ARIGA MWJ

(1) Objectives
Determination of dissolved oxygen in seawater by Winkler titration.

(2) Parameters
Dissolved Oxygen

(3) Instruments and Methods
Following procedure is based on winkler method (Dickson, 1996; Culberson, 1991).

Instruments
Burette for sodium thiosulfate and potassium iodate;
Automatic piston burette (APB-510 / APB610 / APB-620) manufactured by Kyoto Electronics Manufacturing Co., Ltd. / 10 cm^3 of titration vessel
Detector;
Automatic photometric titrator (DOT-15X) manufactured by Kimoto Electric Co., Ltd.
Software; DOT_Terminal Ver. 1.3.1

Reagents
Pickling Reagent I: Manganese(II) chloride solution (3 mol dm^{-3})
Pickling Reagent II:
Sodium hydroxide (8 mol dm^{-3}) / Sodium iodide solution (4 mol dm^{-3})
Sulfuric acid solution (5 mol dm^{-3})
Sodium thiosulfate (0.025 mol dm^{-3})
Potassium iodate (0.001667 mol dm^{-3})

Sampling
Seawater samples were collected with Niskin bottle attached to the CTD/Carousel Water Sampling System (CTD system). Seawater for oxygen measurement was transferred from the bottle to a volume calibrated flask (ca. 100 cm^3), and three times volume of the flask was overflowed. Temperature was simulteneously measured by digital thermometer during the overflowing. After transfering the sample, two reagent solutions (Reagent I and II) of 1 cm^3 each were added immediately and the stopper was inserted carefully into the flask. The sample flask was then shaken vigorously to mix the contents and to disperse the precipitate finely throughout. After the precipitate has settled at least halfway down the flask, the flask was shaken again vigorously to disperse the precipitate. The sample flasks containing pickled samples were stored in a laboratory until they were titrated.
Sample measurement
For over two hours after the re-shaking, the pickled samples were measured on board. Sulfuric acid solution with its volume of 1 cm^3 and a magnetic stirrer bar were put into the sample flask and the sample was stirred. The samples were titrated by sodium thiosulfate solution whose morality was determined by potassium iodate solution. Temperature of sodium thiosulfate during titration was recorded by a digital thermometer. Dissolved oxygen concentration (μmol kg^{-1}) was calculated by sample temperature during seawater sampling, salinity of the sensor on CTD system, flask volume, and titrated volume of sodium thiosulfate solution without the blank. During this cruise, 2 sets of the titration apparatus were used.

Standardization and determination of the blank

Concentration of sodium thiosulfate titrant was determined by potassium iodate solution. Pure potassium iodate was dried in an oven at 130 ºC, and 1.7835 g of it was dissolved in deionized water and diluted to final weight of 5 kg in a flask. After 10 cm^3 of the standard potassium iodate solution was added to an another flask using a volume-calibrated dispenser, 90 cm^3 of deionized water, 1 cm^3 of sulfuric acid solution, and 1 cm^3 of pickling reagent solution II and I were added in order. Amount of titrated volume of sodium thiosulfate for this diluted standard potassium iodate solution (usually 5 times measurements average) gave the morality of sodium thiosulfate titrant.

The oxygen in the pickling reagents I (1 cm^3) and II (1 cm^3) was assumed to be 7.6×10^{-8} mol (Murray et al., 1968). The blank due to other than oxygen was determined as follows. First, 1 and 2 cm^3 of the standard potassium iodate solution were added to each flask using a calibrated dispenser. Then 100 cm^3 of deionized water, 1 cm^3 of sulfuric acid solution, 1 cm^3 of pickling II reagent solution, and same volume of pickling I reagent solution were added into the flask in order. The blank was determined by difference between the first (1 cm^3 of potassium iodate) titrated volume of the sodium thiosulfate and the second (2 cm^3 of potassium iodate) one. The titrations were conducted for 3 times and their average was used as the blank value.

(4) Observation log

(4-1) Standardization and determination of the blank

Table 2.3.1-1 shows results of the standardization and the blank determination during this cruise.

Table 2.3.1-1 Results of the standardization and the blank determinations during cruise

Date (yyyy/mm/dd)	Potassium iodate ID	Sodium thiosulfate ID	DOT-15X (No.9)		DOT-15X (No.10)		Stations
			E.P. (cm^3)	Blank (cm^3)	E.P. (cm^3)	Blank (cm^3)	
2022/04/17	K21E08	T-21F	-	-	3.969	0.001	001M002#23~36,0,002M001#9~22,003M001#23~36,0,004M002#0
2022/04/17	K21F04	T-21F	3.966	0.002	-	-	001M002#9~22,002M001#23~36,0,003M001#9~22
2022/04/21	K21E09	T-21F	3.966	0.003	3.968	0.001	004M002#9~36,005M003,006M001
2022/04/25	K21E11	T-21F	3.966	0.002	3.969	0.004	007M001,008M001,009M001
2022/04/29	K21F07	T-21F	3.965	0.002	3.968	0.001	010M001,011M002
2022/05/03	K21C04	T-21F	3.969	0.004	3.970	0.001	011M003
2022/05/07	K21C08	T-21F	3.970	0.004	3.970	0.001	012M001
2022/05/10	K21C07	T-21F	3.970	0.003	3.972	0.003	-
2022/05/10	K21C07	T-21G	3.970	0.003	3.969	-0.001	013M001
2022/05/14	K21C06	T-21G	3.968	0.003	3.971	0.003	014M001#24~30 015M001#28~32
2022/05/14	K21C06	T-21G	-	-	3.971	0.001	014M001#31~36,0,015M001#33~36,0
2022/05/16	K21C05	T-21G	3.968	0.002	3.971	0.001	-

(4-2) Repeatability of sample measurement

Replicate samples were taken at every CTD casts. The standard deviation of the replicate measurement (Dickson et al., 2007) was 0.08 μmol kg^{-1} (n = 44).

(5) Data archives

These data obtained in this cruise will be submitted to the Data Management Group (DMG) of JAMSTEC, and will opened to the public via “Data Research System for Whole Cruise Information in JAMSTEC (DARWIN)” in JAMSTEC web site.

<http://www.godac.jamstec.go.jp/darwin/e>

(6) References

Culberson, C. H. (1991). Dissolved Oxygen. WHPO Publication 91-1.

Dickson, A. G. (1996). Determination of dissolved oxygen in sea water by Winkler titration. In WOCE Operations Manual, Part 3.1.3 Operations & Methods, WHP Office Report WHPO 91-1.

Dickson, A. G., Sabine, C. L., & Christian, J. R.(Eds.), (2007). Guide to best practices for ocean CO_2 measurements, PICES Special Publication 3: North Pacific Marine Science Organization.

Murray, C. N., Riley, J. P., & Wilson, T. R. S. (1968). The solubility of oxygen in Winklerreagents used for the determination of dissolved oxygen. Deep Sea Res., 15, 237-238.

2.3.2 Nutrients

Masahide WAKITA	**JAMSTEC**	**PI**
Michio AOYAMA	**JAMSTEC/University of Tsukuba**	
Yuko MIYOSHI	**MWJ**	**Operation Leader**
Yuta ODA	**MWJ**	

(1) Objectives

The objective of this document is to show the present status of the nutrient concentrations during the R/V Mirai MR22-03 cruise (EXPOCODE: 49NZ20220416) in the Pacific Ocean, and then evaluate the comparability of this obtained data set during this cruise using the certified reference materials of the nutrients in seawater.

(2) Parameters

The parameters are nitrate, nitrite, silicate, phosphate and ammonia in seawater.

(3) Instruments and methods

(3.1) Analytical detail using QuAAtro 39 systems (BL TEC K.K.)

The analytical systems were replaced from QuAAtro 2-HR to QuAAtro 39 in March 2021.

Nitrate + nitrite and nitrite were analyzed by the following methodology that was modified from the original method of Grasshoff (1976). The flow diagrams were shown in Figure 2.3.2-1 for nitrate + nitrite and Figure 2.3.2-2 for nitrite. For the nitrate + nitrite analysis, the sample were mixed with the alkaline buffer (Imidazole) and then the mixture was pushed through a cadmium coil which was coated with a metallic copper. This step was conducted due to reduce from nitrate to nitrite in the sample, which allowed us to determine nitrate + nitrite in the seawater sample. For the nitrite analysis, the sample was mixed with reagents without this reduction step. In the flow system, seawater sample with or without the reduction step was mixed with an acidic sulfanilamide reagent through a mixing coil to produce a diazonium ion. And then, the mixture was mixed with the N-1-naphthylethylenediamine dihydrochloride (NED) to produce a red azo dye. The azo dye compound was injected into the spectrophotometric detection to monitor the signal at 545 nm. Thus, for the nitrite analysis, sample was determined without passing thought the Cd coil. Nitrate was computed by the difference between nitrate+nitrite concentration and nitrite concentration.

The silicate method is analogous to that described for phosphate (see below). The method is essentially that of Grasshoff et al. (1999). The flow diagrams were shown in Figure 2.3.2-3. Silicomolybdic acid compound was first formed by mixing silicate in the sample with the molybdic acid. The silicomolybdic acid compound was then reduced to silicomolybdous acid, "molybdenum blue," using L-ascorbic acid as the reductant. And then the signal was monitored at 630 nm.

The methodology for the phosphate analysis is a modified procedure of Murphy and Riley (1962). The flow diagrams were shown in Figure 2.3.2-4. Molybdic acid was added to the seawater sample to form the phosphomolybdic acid compound, and then it was reduced to phosphomolybdous acid compound using L-ascorbic acid as the reductant. And then the signal was monitored at 880 nm.

The ammonia in seawater was determined using the flow diagrams shown in Figure 2.3.2-5. Sample was mixed with an alkaline solution containing EDTA, which ammonia as gas state was formed from seawater. The ammonia (gas) is absorbed in a sulfuric acid by way of 0.5 μm pore size membrane filter (ADVANTEC PTFE) at the dialyzer attached to the analytical system. And then the ammonia absorbed in sulfuric acid was determined by coupling with phenol and hypochlorite to form indophenols blue, and the signal was determined at 630 nm.

The details of a modification of analytical methods for four parameters, nitrate, nitrite, silicate and phosphate, are also compatible with the methods described in nutrients section in the new GO-SHIP repeat hydrography nutrients manual (Becker et al., 2019). This manual is a revised version of the GO-SHIP repeat hydrography nutrients manual (Hydes et al., 2010). The analytical method of ammonium is compatible with the determination of ammonia in seawater using a vaporization membrane permeability method (Kimura, 2000).

(3.2) Nitrate + Nitrite reagents
50 % Triton solution
50 mL of Triton™ X-100 (CAS No. 9002-93-1) were mixed with 50 mL of ethanol (99.5 %).

Imidazole (buffer), 0.06 M (0.4 % w/v)
Dissolved 4 g of the imidazole (CAS No. 288-32-4) in 1000 mL ultra-pure water, and then added 2 mL of the hydrogen chloride (CAS No. 7647-01-0). After mixing, 1 mL of the 50 % triton solution was added.

Sulfanilamide, 0.06 M (1 % w/v) in 1.2 M HCl
Dissolved 10 g of 4-aminobenzenesulfonamide (CAS No. 63-74-1) in 900 mL of ultra-pure water, and then add 100 mL of the hydrogen chloride (CAS No. 7647-01-0). After mixing, 2 mL of the 50 % triton solution was added.

NED, 0.004 M (0.1 % w/v)
Dissolved 1 g of N-(1-naphthalenyl)-1,2-ethanediamine dihydrochloride (CAS No. 1465-25-4) in 1000 mL of ultra-pure water and then added 10 mL of hydrogen chloride (CAS No. 7647-01-0). After mixing, 1 mL 50 % of the Triton solution was added. This reagent was stored in a dark bottle.

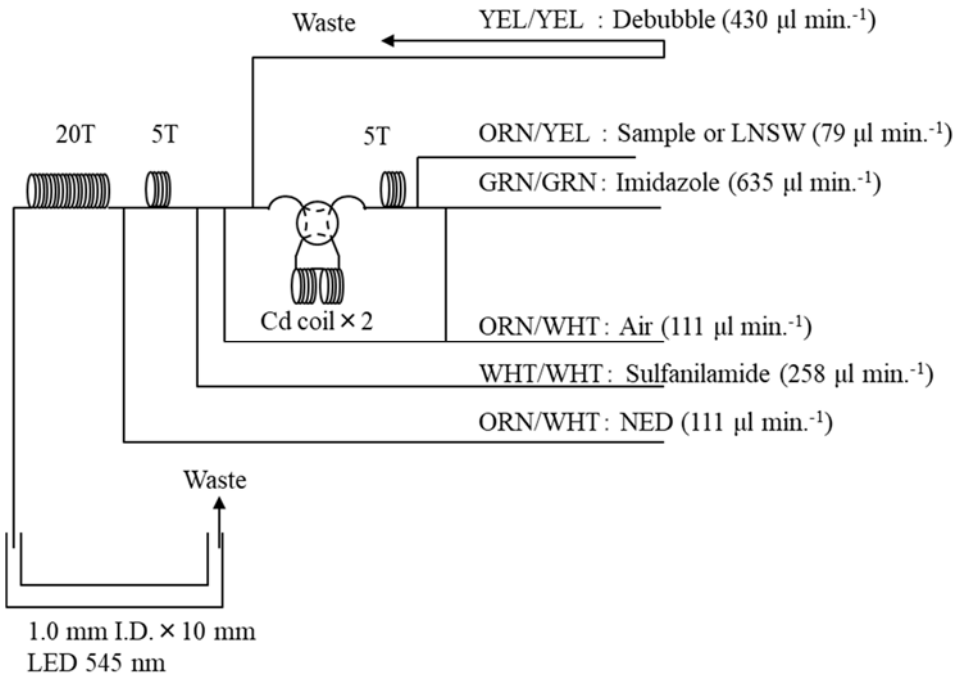

Figure 2.3.2-1 NO_3+NO_2 (1ch.) flow diagram.

(3.3) Nitrite reagents
50 % Triton solution
50 mL of the Triton™ X-100 (CAS No. 9002-93-1) were mixed with 50 mL ethanol (99.5 %).

Sulfanilamide, 0.06 M (1 % w/v) in 1.2 M HCl
Dissolved 10 g of 4-aminobenzenesulfonamide (CAS No. 63-74-1) in 900 mL of ultra-pure water, and then added 100 mL of hydrogen chloride (CAS No. 7647-01-0). After mixing, 2 mL of the 50 % triton solution were added.

NED, 0.004 M (0.1 % w/v)
Dissolved 1 g of N-(1-naphthalenyl)-1,2-ethanediamine dihydrochloride (CAS No. 1465-25-4) in 1000 mL of ultra-pure water and then added 10 mL of hydrogen chloride (CAS No. 7647-01-0). After mixing, 1 mL of the 50 % triton solution was added. This reagent was stored in a dark bottle.

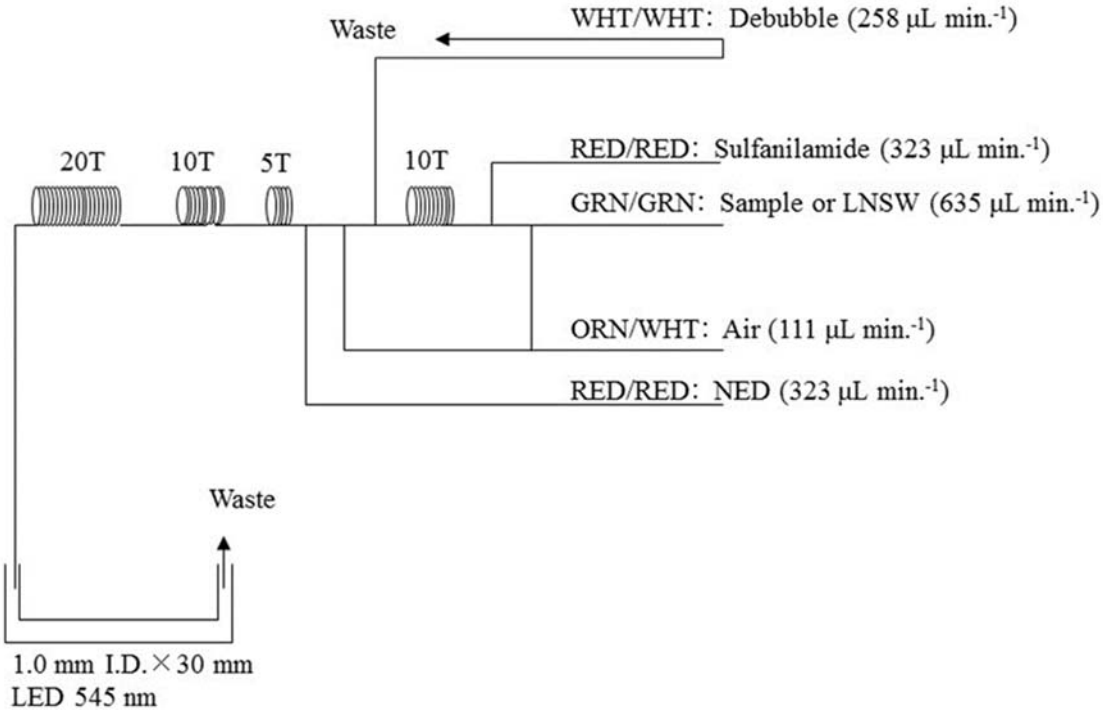

Figure 2.3.2-2 NO_2 (2ch.) flow diagram.

(3.4) Silicate reagents
15 % Sodium dodecyl sulfate solution
75 g of sodium dodecyl sulfate (CAS No. 151-21-3) was mixed with 425 mL ultra-pure water.

Molybdic acid, 0.03 M (1 % w/v)
Dissolved 7.5 g of sodium molybdate dihydrate (CAS No. 10102-40-6) in 980 mL ultra-pure water, and then added 12 mL of a 4.5M sulfuric acid. After mixing, 20 mL of the 15 % sodium dodecyl sulfate solution was added. Note that the amount of sulfuric acid was reduced from the previous report (MR19-03C) since we have modified the method of Grasshoff et al. (1999).

Oxalic acid, 0.6 M (5 % w/v)
Dissolved 50 g of oxalic acid (CAS No. 144-62-7) in 950 mL of ultra-pure water.

Ascorbic acid, 0.01 M (3 % w/v)
Dissolved 2.5 g of L-ascorbic acid (CAS No. 50-81-7) in 100 mL of ultra-pure water. This reagent was freshly prepared every day.

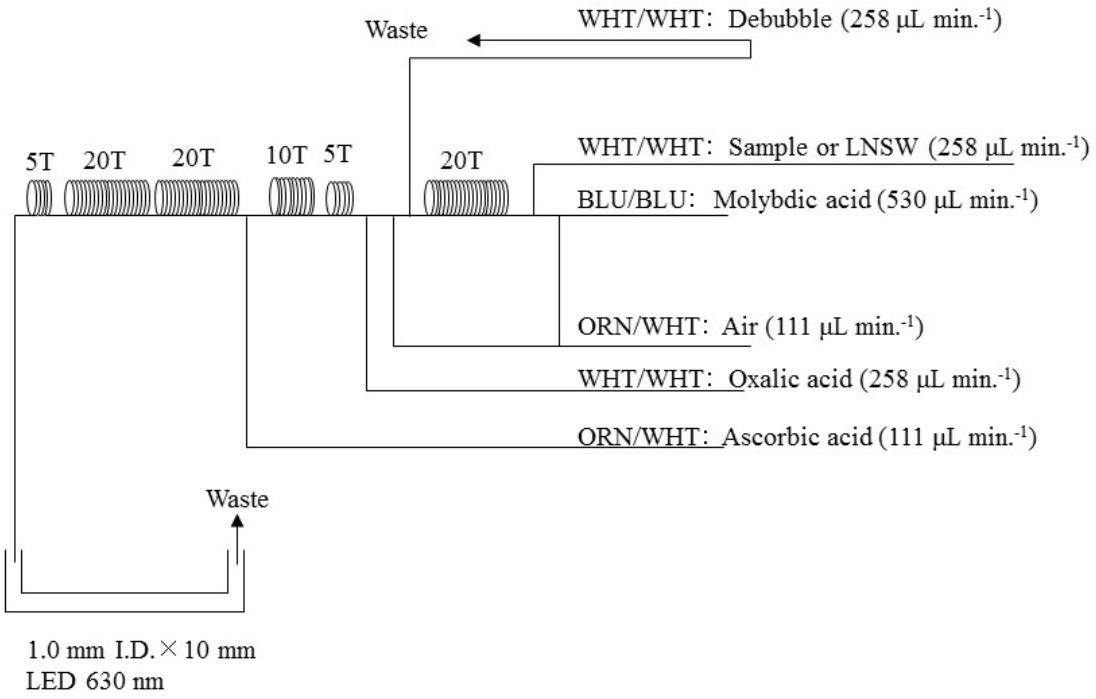

Figure 2.3.2-3 SiO_2 (3ch.) flow diagram.

(3.5) Phosphate reagents
15 % Sodium dodecyl sulfate solution
75 g of sodium dodecyl sulfate (CAS No. 151-21-3) were mixed with 425 mL of ultra-pure water.

Stock molybdate solution, 0.03 M (0.8 % w/v)
Dissolved 8 g of sodium molybdate dihydrate (CAS No. 10102-40-6) and 0.17 g of antimony potassium tartrate trihydrate (CAS No. 28300-74-5) in 950 mL of ultra-pure water, and then added 50 mL of sulfuric acid (CAS No. 7664-93-9).

PO_4 color reagent
Dissolved 1.2 g of L-ascorbic acid (CAS No. 50-81-7) in 150 mL of the stock molybdate solution. After mixing, 3 mL of the 15 % sodium dodecyl sulfate solution was added. This reagent was freshly prepared before every measurement.

(3.6) Ammonia reagents
30 % Triton solution
30 mL of a Triton™ X-100 (CAS No. 9002-93-1) were mixed with 70 mL ultra-pure water.

EDTA
Dissolved 41 g of a tetrasodium; 2-[2-[bis(carboxylatomethyl)amino]ethyl- (carboxylatemethyl)amino] acetate;tetrahydrate (CAS No. 13235-36-4) and 2 g of a boric acid (CAS No. 10043-35-3) in 200 mL of ultra-pure water. After mixing, a 1 mL of the 30 % triton solution was added. This reagent is prepared every week.

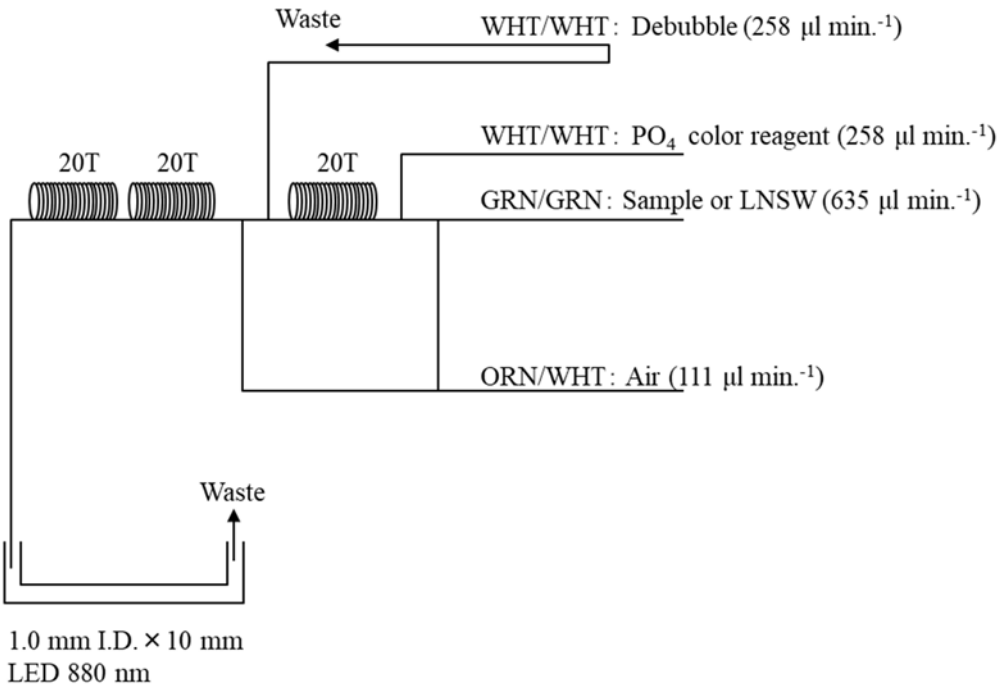

Figure 2.3.2-4 PO_4 (4ch.) flow diagram.

NaOH liquid

Dissolved 1.5 g of a sodium hydroxide (CAS No. 1310-73-2) and 16 g of a tetrasodium; 2-[2-[bis(carboxylatomethyl) amino]ethyl - (carboxylatomethyl) amino]acetate; tetrahydrate (CAS No. 13235-36-4) in 100 mL of ultra-pure water. This reagent was prepared every week. Note that we reduced the amount of a sodium hydroxide from 5 g to 1.5 g because pH of C standard solutions has been lowered 1 pH unit due to the change of recipe of B standards solution (the detailed of those standard solution, see 6.2.4).

Stock nitroprusside

Dissolved 0.25 g of a sodium nitroferricyanide dihydrate (CAS No. 13755-38-9) in 100 mL of ultra-pure water, and then added 0.2 mL of a 1M sulfuric acid. Stored in a dark bottle and prepared every month.

Nitroprusside solution

Added 4 mL of the stock nitroprusside and 4 mL of a 1M sulfuric acid in 500 mL of ultra-pure water. After mixing, 2 mL of the 30 % triton solution was added. This reagent was stored in a dark bottle and prepared every 2 or 3 days.

Alkaline phenol

Dissolved 10 g of a phenol (CAS No. 108-95-2), 5 g of a sodium hydroxide (CAS No. 1310-73-2) and 2 g of a sodium citrate dihydrate (CAS No. 6132-04-3) in 200 mL of ultra-pure water. Stored in a dark bottle and prepared every week.

NaClO solution

Mixed 3 mL of a sodium hypochlorite (CAS No. 7681-52-9) in 47 mL of ultra-pure water. Stored in a dark bottle and fleshly prepared before every measurement. This reagent need be 0.3 % available chlorine.

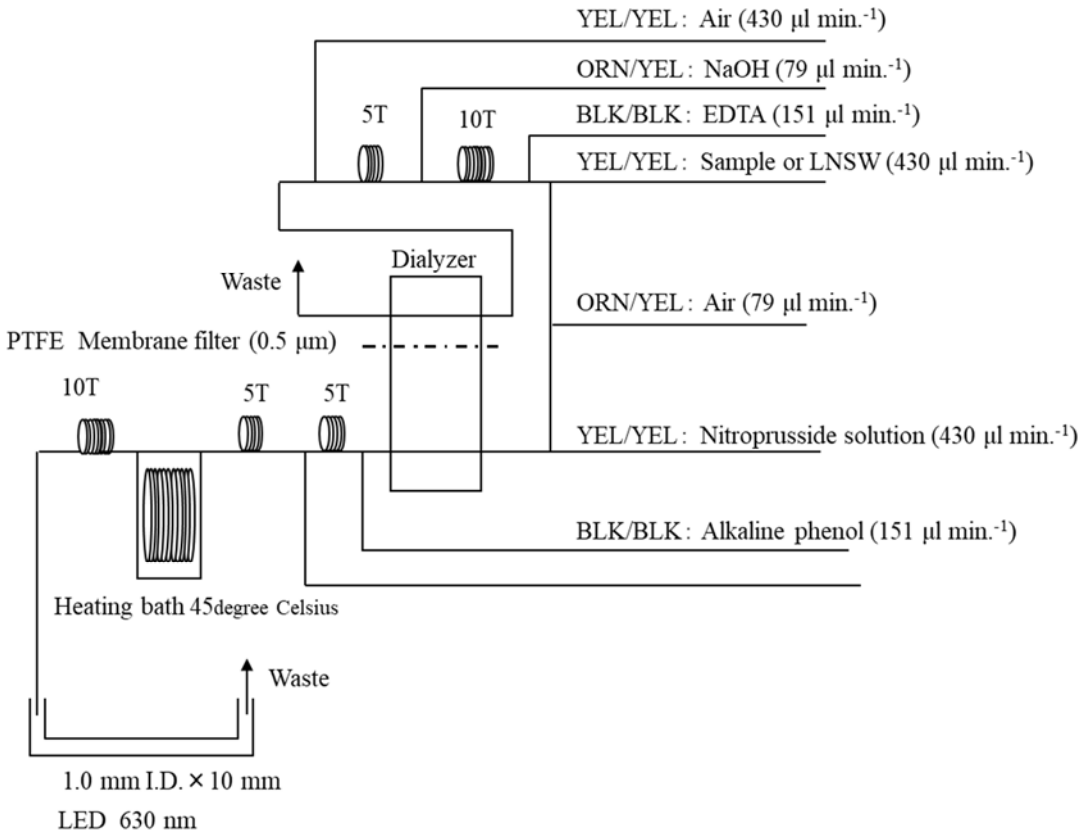

Figure 2.3.2-5 NH_4 (5ch.) flow diagram.

(3.7) Sampling procedures

Sampling for nutrient samples was conducted right after the sampling for other parameters (oxygen, trace gases and salinity). Samples were collected into two new 10 mL polyacrylates vials without any sample drawing tube that usually used for the oxygen samples. Each vial was rinsed three times before filling and then was sealed without any head-space immediately after the collection. The vials were put into a water bath that was adjusted to the ambient temperature at 22.0 ± 0.6 degree Celsius, for more than 30 minutes to keep the constant temperature of samples before measuring.

No transfer from the vial to another container was made and the vials were set an autosampler tray directly. Samples were analyzed after collection within 24 hours.

(3.8) Data processing

Raw data from QuAAtro 39 were treated as follows:

- Checked if there were any baseline shift.
- Checked the shape of each peak and positions of peak values. If necessary, a change was made for the positions of peak values.
- Conducted carry-over correction and baseline drift correction followed by sensitivity correction to apply to the peak height of each sample.
- Conducted baseline correction and sensitivity correction using the linear regression.
- Using the pressure from uncalibrated CTD data, the salinity (from CTD data or determined on the ship) and the laboratory room temperature (20 degree Celsius), the density of each sample had been calculated tentatively. The obtained density was used to calculate the final nutrient concentration with the unit of umol kg^{-1}.
- Calibration curves to obtain the nutrients concentrations were assumed second order equations.

(3.9) Summary of nutrients analysis

During this cruise, 20 runs were conducted to obtain the values for the samples collected by 23 casts at 18 stations. The total number of the seawater samples were 935. For each sample depth, we basically collected duplicate samples, and then determined all of the samples. The sampling locations for the nutrients was shown in Figure 2.3.2-6.

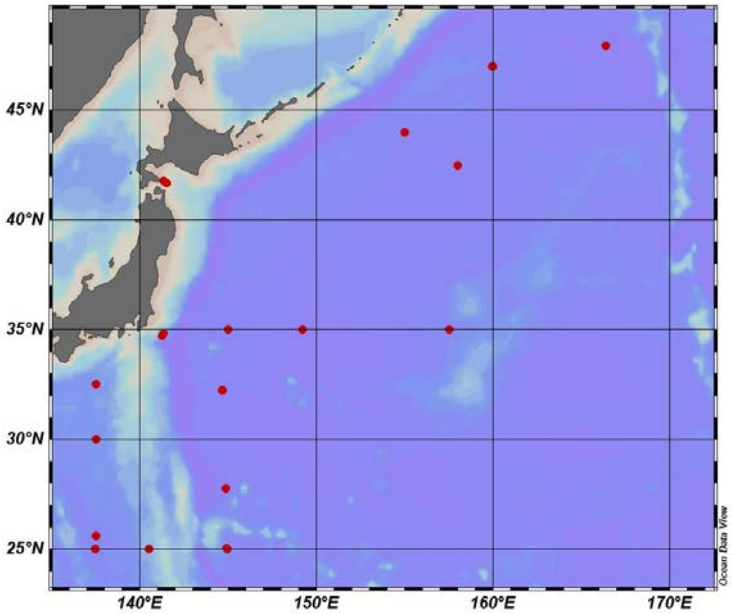

Figure 2.3.2-6 Sampling positions of nutrients sample in the Pacific Ocean.

(4) Station list

The sampling stations were listed as shown in Table 2.3.2-1.

Table 2.3.2-1 List of stations

Station	Cast	Date (UTC)	Position*		Depth (m)
		(mmddyy)	Latitude	Longitude	
001	1	041622	32-31.37N	137-29.81E	4038
001	2	041722	32-31.22N	137-30.02E	4037
002	1	041722	30-00.43N	137-31.36E	4339
PE1	1	041822	25-36.56N	137-00.00E	5366
003	1	041922	25-00.35N	137-28.88E	5166
PE2	1	041922	25-00.02N	140-29.95E	3149
004	1	042022	25-01.06N	144-56.78E	5050
004	2	042122	25-03.04N	144-54.80E	5007
PE4	1	042122	27-45.73N	144-51.37E	5758
005	1	042222	32-15.47N	144-40.36E	5717
005	3	042322	32-15.11N	144-40.82E	5596
006	1	042422	34-00.00N	141-15.59E	4444
006	2	042422	34-49.94N	141-19.87E	3440
007	1	042522	35-00.01N	145-00.01E	5798

008	1	042622	34-59.54N	149-00.00E	6136
009	1	042822	35-00.87N	157-30.77E	5031
010	1	042922	42-30.08N	158-00.21E	5392
011	2	050222	46-59.56N	160-00.87E	5223
011	3	050322	46-59.99N	160-00.01E	5190
012	1	050822	47-57.11N	166-24.55E	5901
013	1	051122	43-59.87N	155-00.25E	5313
014	1	051522	41-47.99N	141-20.43E	274
015	1	051522	41-40.04N	141-30.32E	121

* Position indicates latitude and longitude where CTD reached maximum depth at the cast.

(5) Certified Reference Material of nutrients in seawater

KANSO certified reference materials (CRMs, Lot: CE, CL, CG, CM, CF) were used to ensure the comparability and traceability of nutrient measurements during this cruise. The details of CRMs are shown below.

Production

KANSO CRMs for inorganic nutrients in seawater were produced by KANSO Co.,Ltd. This CRM has been produced using autoclaved natural seawater based on the quality control system under ISO Guide 34 (JIS Q 0034).

KANSO Co.,Ltd. has been accredited under the Accreditation System of National Institute of Technology and Evaluation (ASNITE) as a CRM producer since 2011. (Accreditation No.: ASNITE 0052 R)

Property value assignment

The certified values were the arithmetic means of the results of 30 bottles from each batch (measured in duplicates) analyzed by both KANSO Co.,Ltd. and Japan Agency for Marine-Earth Science and Technology (JAMSTEC) using the colorimetric method (continuous flow analysis, CFA, method). The salinity of the calibration standards solution to obtain each calibration curve was adjusted to the salinity of the used CRMs within ± 0.5.

Metrological Traceability

Each certified value of nitrate, nitrite, and phosphate of KANSO CRMs were calibrated using one of Japan Calibration Service System (JCSS) standard solutions for each nitrate ions, nitrite ions, and phosphate ions. JCSS standard solutions were calibrated using the secondary solution of JCSS for each of these ions. The secondary solution of JCSS was calibrated using the specified primary solution produced by Chemicals Evaluation and Research Institute (CERI), Japan. CERI specified primary solutions were calibrated using the National Metrology Institute of Japan (NMIJ) primary standards solution of nitrate ions, nitrite ions and phosphate ions, respectively.

For the certified value of silicate of KANSO CRM was calibrated using a newly established silicon standards solution named “exp96” produced by JAMSTEC and KANSO. This silicon standard solution was produced by a dissolution technique with an alkaline solution. The mass fraction of Si in the produced solution was calibrated based on NMIJ CRM 3645-a03 Si standard solution by a technology consulting system of National Institute of Advanced Industrial Science and Technology (AIST), and this value is traceable to the International System of Units (SI).

The certified values of nitrate, nitrite, and phosphate of KASNO CRM are thus traceable to the SI through the unbroken chain of calibrations, JCSS, CERI and NMIJ solutions as stated above, each having stated uncertainties. The certified values of silicate of KANSO CRM are traceable to the SI through the unbroken chain of calibrations, NMIJ CRM 3645-a03 Si standard solution, having stated uncertainties.

As stated in the certificate of NMIJ CRMs, each certified value of dissolved silica, nitrate ions, and nitrite ions was determined by more than one method using one of NIST SRM of silicon standard solution and NMIJ primary standards solution of nitrate ions and nitrite ions. The concentration of phosphate ions as stated information value in the certificate was determined NMIJ primary standards solution of phosphate ions. Those values in the certificate of NMIJ CRMs are traceable to the SI.

One of the analytical methods used for certification of NMIJ CRM for nitrate ions, nitrite ions, phosphate ions and dissolved silica was a colorimetric method (continuous mode and batch mode). The colorimetric method is the same as the analytical method (continuous mode only) used for certification of KANSO CRM. For certification of dissolved silica, exclusion chromatography/isotope dilution-inductively coupled plasma mass spectrometry and ion exclusion chromatography with post-column detection was used. For certification of nitrate ions, ion chromatography by direct analysis and ion chromatography after halogen-ion separation was used. For certification of nitrite ions, ion chromatography by direct analysis was used.

NMIJ CRMs were analyzed at the time of certification process for CRM and the results were confirmed within expanded uncertainty stated in the certificate of NMIJ CRMs.

(5.1) CRM for this cruise

20 sets of CRM lots CE, CL, CG, CM and CF were used, which almost cover a range of nutrients concentrations in the Pacific Ocean. Each CRM's serial number was randomly selected. The CRM bottles were stored at a room named "BIOCHEMICAL LABORATORY" on the ship, where the temperature was maintained around 20.16 degree Celsius – 23.33 degree Celsius.

(5.2) CRM concentration

Nutrients concentrations for the CRM lots CE, CL, CG, CM and CF were shown in Table 2.3.2-2.

Table 2.3.2-2 Certified concentration and the uncertainty (k=2) of CRMs. unit in μmol kg^{-1}

Lot	Nitrate	Nitrite**	Silicate	Phosphate	Ammonia***
CE*	0.01 ± 0.03	0.031 ± 0.03	0.06 ± 0.09	0.012 ± 0.006	0.69
CL	5.47 ± 0.15	0.016 ± 0.006	13.8 ± 0.3	0.425 ± 0.019	1.68
CG	23.7 ± 0.2	0.071 ± 0.03	56.4 ± 0.5	1.70 ± 0.02	0.61
CM	33.2 ± 0.3	0.018 ± 0.006	100.5 ± 0.5	2.38 ± 0.03	0.59
CF	43.4 ± 0.4	0.091 ± 0.02	159.7 ± 1.0	3.06 ± 0.03	0.46

*Nitrate, silicate and phosphate values of CRM lot CE are below quantifiable detection limit and shown as only reference values.

**Nitrite concentration values of CRM lot CE, CL, CG and CF are measured on the ship before MR21-04 cruise in July 2021.

***Ammonia values are not certified and shown as only reference values.

(6) Nutrients standards

(6.1) Volumetric laboratory-ware of in-house standards

All volumetric glassware and polymethylpentene (PMP)-ware used were gravimetrically calibrated. Plastic volumetric flasks were gravimetrically calibrated at the temperature of use within 2 K at around 22 degree Celsius.

(6.1.1) Volumetric flasks

Volumetric flasks of Class quality (Class A) are used because their nominal tolerances are 0.05 % or less over the size ranges likely to be used in this work. Since Class A flasks are made of borosilicate glass, the standard solutions were transferred to plastic bottles as quickly as possible after the solutions were made up to volume and well mixed in order to prevent the excessive dissolution of silicate from the glass. PMP volumetric flasks were gravimetrically calibrated and used only within 3 K of the calibration temperature.

The computation of volume contained by the glass flasks at various temperatures other than the calibration temperatures were conducted by using the coefficient of linear expansion of borosilicate crown glass.

The coefficients of cubical expansion of each glass and PMP volumetric flask was determined by actual measurement in 2018 and 2019. The coefficients of cubical expansion of glass volumetric flask (SHIBATA HARIO) was 0.0000110 to 0.0000172 K^{-1} and that of PMP volumetric flask (NALGEN PMP) was 0.00039 to 0.00045 K^{-1}. The weights obtained in the calibration weightings were corrected for the density of water and air buoyancy.

(6.1.2) Pipettes

All glass pipettes have nominal calibration tolerances of 0.1 % or better. These were gravimetrically calibrated to verify and improve upon this nominal tolerance.

(6.2) Reagents, general considerations

(6.2.1) Specifications

For nitrate standard, “potassium nitrate 99.995 suprapur®” provided by Merck, Batch B1706365, CAS No. 7757-79-1, was used. For nitrite standard solution, we used a nitrite ion standard solution (NO_2^- 1000) provided by Wako, Lot ESG1055, Code. No. 146-06453. This standard solution was certified by Wako using the ion chromatography method. Calibration result is 1004 mg L^{-1} at 20 degree Celsius. Expanded uncertainty of calibration (k=2) is 0.8 % for the calibration result. For the silicate standard solution, we used our in-house Si standard solution “exp96” which was produced by alkali fusion technique from 5N SiO_2 powder produced jointly by JAMSTEC and KANSO. The mass fraction of Si in the “exp96” solution was calibrated based on NMIJ CRM 3645-a03 Si standard solution. For phosphate standard, we used a potassium dihydrogen phosphate anhydrous 99.995 suprapur®” provided by Merck, Batch B1871308, CAS No.: 7778-77-0, was used. For ammonia standard, ammonium chloride (CRM 3011-a) provided by NMIJ, CAS No. 12125-02-9 was used. The purity of this standard was reported as >99.9 % by the manufacture. Expanded uncertainty of calibration (k = 2) was 0.026 %.

(6.2.2) Ultra-pure water

Ultra-pure water (Milli-Q water) freshly drawn was used for the preparation of reagents, standard solutions and for measurements of the reagent and the system blanks.

(6.2.3) Low nutrients seawater (LNSW)

Nutrients concentrations in LNSW were measured on August 2020. The averaged nutrient concentrations in the LNSW were 0.004 μmol L^{-1} for nitrate, 0.001 μmol L^{-1} for nitrite, 1.931 μmol L^{-1} for silicate and 0.002 μmol L^{-}

[1] for ammonia. We observed phosphate concentration values were different in each cardboard box, so we measured the values for each box. The phosphate concentration value in the LNSW we used in this cruise was 0.081 to 0.093 μmol L^{-1}. The concentrations of nitrate, nitrite and ammonia were lower than detection limit as stated in chapter (7.5).

(6.2.4) Concentrations of nutrients for A, D, B and C standards

Concentrations of nutrients for A, D, B and C standards were adjusted as shown in Table 2.3.2-3. We used JAMSTEC-KANSO in-house Si standard solution for A standard of silicate, which doesn't need to neutralize by the hydrochloric acid. B standard was diluted from A standard with the following recipes shown in Table 2.3.2-4. In order to match the salinity and the density of the stock solution (B standard) to the LNSW, during this dilution step, 15.30 g of a sodium chloride powder was dissolved in B standard, and then the final volume was adjusted to 500 mL. The C standard solution was prepared in the LNSW following the recipes shown in Table 2.3.2-5. All volumetric laboratory tools were calibrated prior the cruise as stated in chapter (6.1). Then the actual concentrations of nutrients in each fresh standard solution were calculated based on the solution temperature, together with the determined factors of volumetric laboratory wares. The calibration curves for each run for nitrate, nitrite, silicate and phosphate were obtained using 6 levels, C-2, C-3, C-4, C-5, C-6 and C-7. For ammonia, that was obtained using 3 levels, C-1, C-4, C-7. C-2, C-3, C-5 and C-6 were the CRM of nutrients in seawater. C-1 was LNSW, and C-4 and C-7 were diluting using the B standard. The D standard solutions were made to calculate the reduction rate of Cd coil. The D standard was diluted from the A standard solution into the pure water.

Table 2.3.2-3 Nominal concentrations of nutrients for A, D, B and C standards. Unit in μmol kg^{-1}

	A	B	D	C-1	C-2	C-3	C-4	C-5	C-6	C-7
NO_3	45000	900	900	-	CE	CL	27	CM	CF	54
NO_2	21800	26	870	-	CE	CL	0.8	CM	CF	1.6
SiO_2	35500	2850		-	CE	CL	87	CM	CF	172
PO_4	6000	60		-	CE	CL	1.9	CM	CF	3.7
NH_4	4000	40		LNSW	-	-	1.2	-	-	2.4

Table 2.3.2-4 B standard recipes. Final volume was 500 mL.

	A Std.
NO_3	10 mL
NO_2*	15 mL
SiO_2	40 mL
PO_4	5 mL
NH_4	5 mL

*NO_2 was D standard solution which was diluted from A standard.

Table 2.3.2-5 Working calibration standard recipes. Final volume was 500 mL.

C Std.	B Std.
C-4	15 mL
C-7	30 mL

(6.2.5) Renewal of in-house standard solutions

In-house standard solutions as stated in paragraph (6.2.4) were remade by each “renewal time” shown in Table 2.3.2-6(a) to (c).

Table 2.3.2-6(a) Timing of renewal of in-house standards.

NO_3, NO_2, SiO_2, PO_4, NH_4	Renewal time
A-1 Std. (NO_3)	maximum a month
A-2 Std. (NO_2)	commercial prepared solution
A-3 Std. (SiO_2)	JAMSTEC-KANSO Si standard solution
A-4 Std. (PO_4)	maximum a month
A-5 Std. (NH_4)	maximum a month
D-1 Std.	maximum 8 days
D-2 Std.	maximum 8 days
B Std. (mixture of A-1, D-2, A-3, A-4 and A-5 std.)	maximum 8 days

Table 2.3.2-6(b) Timing of renewal of working calibration standards.

Working standards	Renewal time
C Std. (diluted from B Std.)	every 24 hours

Table 2.3.2-6(c) Timing of renewal of in-house standards for reduction estimation.

Reduction estimation	Renewal time
36 μM NO_3 (diluted D-1 Std.)	when C Std. renewed
35 μM NO_2 (diluted D-2 Std.)	when C Std. renewed

(7) Quality control

(7.1) The precision of the nutrient analyses during the cruise

The highest standard solution (C-7) was repeatedly determined every 4 to 18 samples to obtain the analytical precision of the nutrient analyses during this cruise. During each run, the total number of the C-7 determination was 7 to 14 times depending on the run. Each run, we obtained the analytical precision based on this C-7 results, shown in Figures 2.3.2-7 to 2.3.2-11. In this cruise, there was total 20 runs. The analytical precisions were less than 0.2% for nitrate, silicate, and phosphate.

The overall precisions throughout this cruise were calculated based on the analytical precisions obtained from all of the runs, and shown in Table 2.3.2-7. During this cruise, overall median precisions were 0.14 % for nitrate, 0.22 % for nitrite, 0.15 % for silicate, 0.15 % for phosphate and 0.43 % for ammonia, respectively. The overall median precision for each parameter during this cruise was comparable to the previously published the precisions during the R/V Mirai cruises conducted in 2009 - 2021.

Table 2.3.2-7 Summary of overall precision based on the replicate analyses (k = 1)

	Nitrate CV %	Nitrite CV %	Silicate CV %	Phosphate CV %	Ammonia CV %
Median	0.15	0.24	0.16	0.16	0.44
Mean	0.14	0.22	0.15	0.15	0.43
Maximum	0.19	0.34	0.19	0.19	0.77
Minimum	0.07	0.11	0.08	0.07	0.20
N	20	20	20	20	20

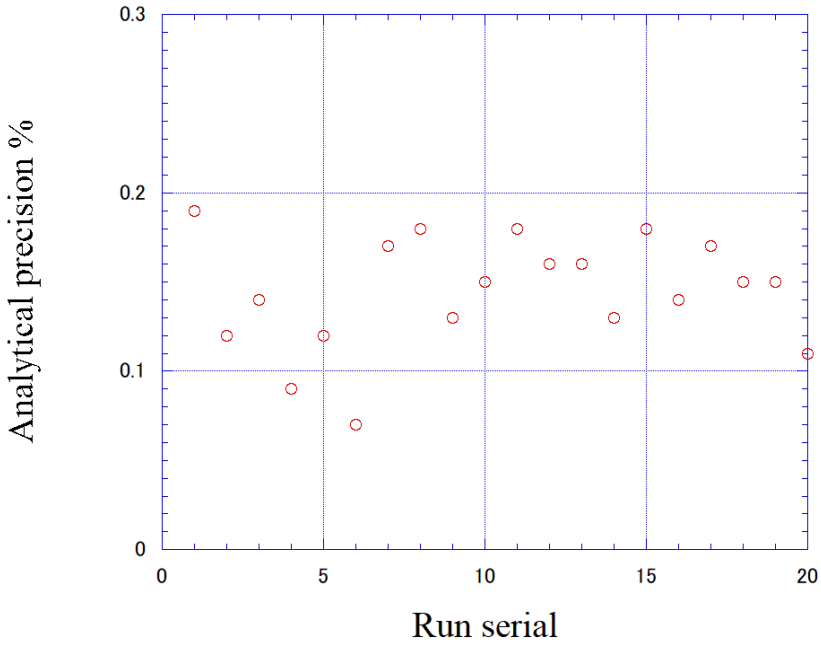

Figure 2.3.2-7 Time series of precision of nitrate in MR22-03.

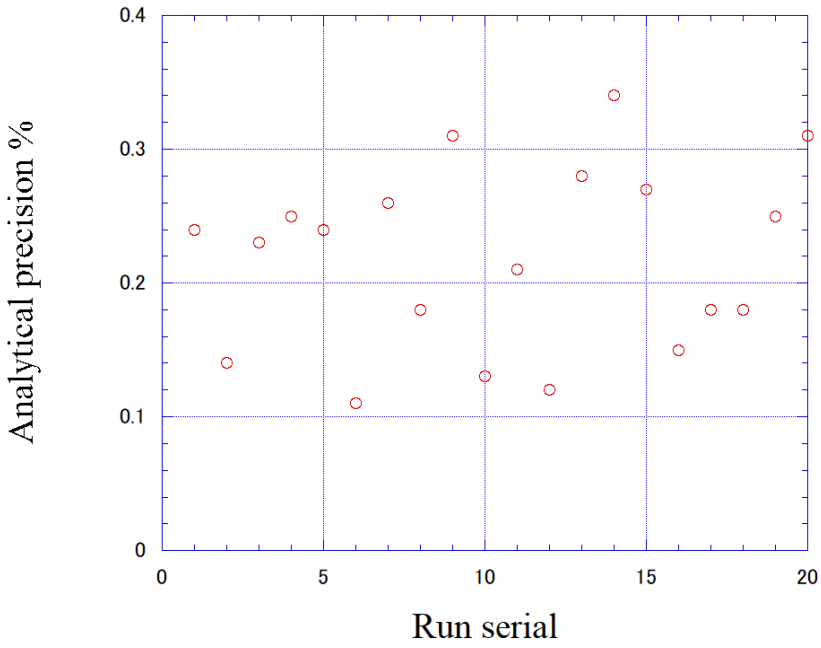

Figure 2.3.2-8 Same as 2.3.2-7 but for nitrite.

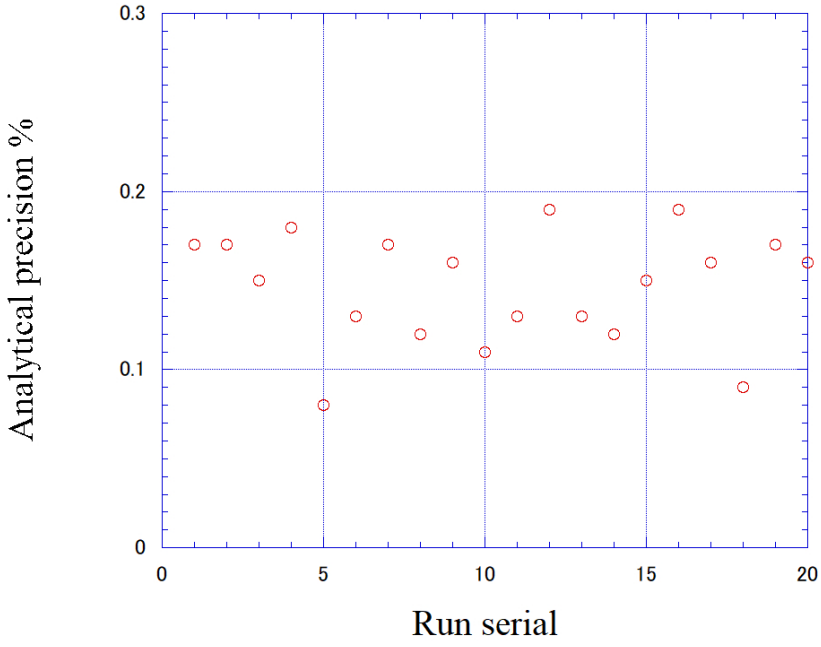

Figure 2.3.2-9 Same as 2.3.2-7 but for silicate.

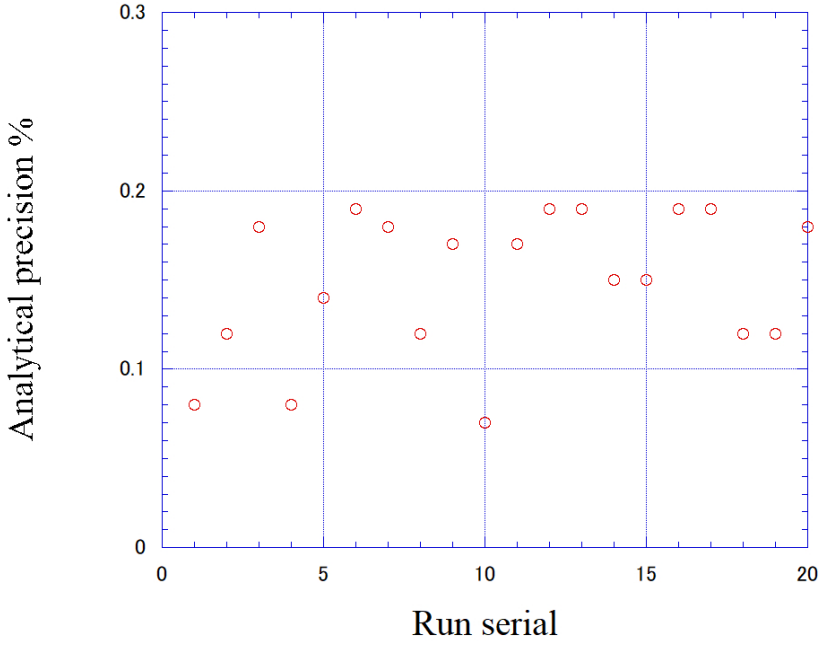

Figure 2.3.2-10 Same as 2.3.2-7 but for phosphate.

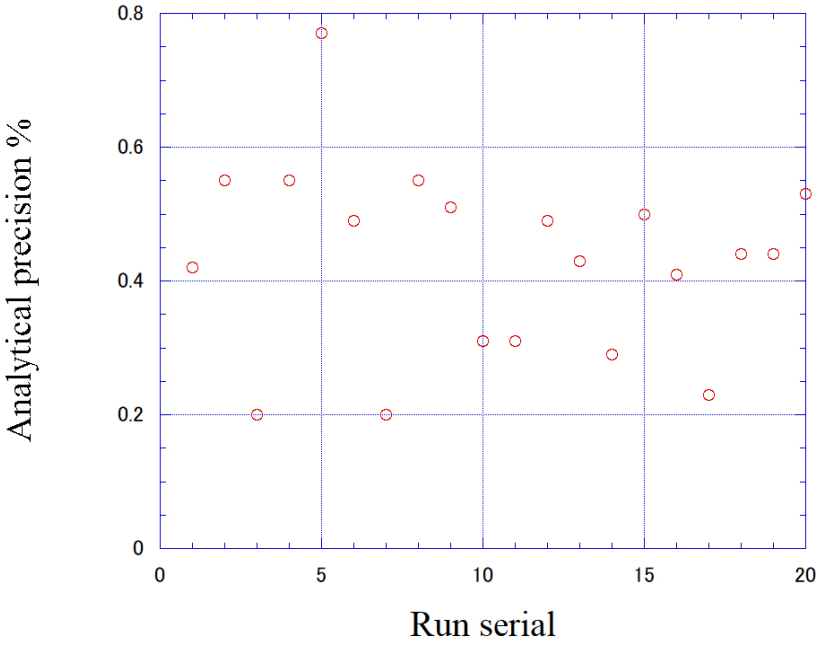

Figure 2.3.2-11 Same as 2.3.2-7 but for ammonia.

(7.2) CRM lot. CG measurement during this cruise

CRM lot. CG was measured every run to evaluate the comparability throughout the cruise. The all of the results of lot. CG during this cruise were shown as Figures 2.3.2-12 to 2.3.2-16. All of the measured concentrations of CRM lot. CG was within the uncertainty of certified values for nitrate, nitrite, silicate and phosphate. The reported CRM values were shown in Table 2.3.2-2.

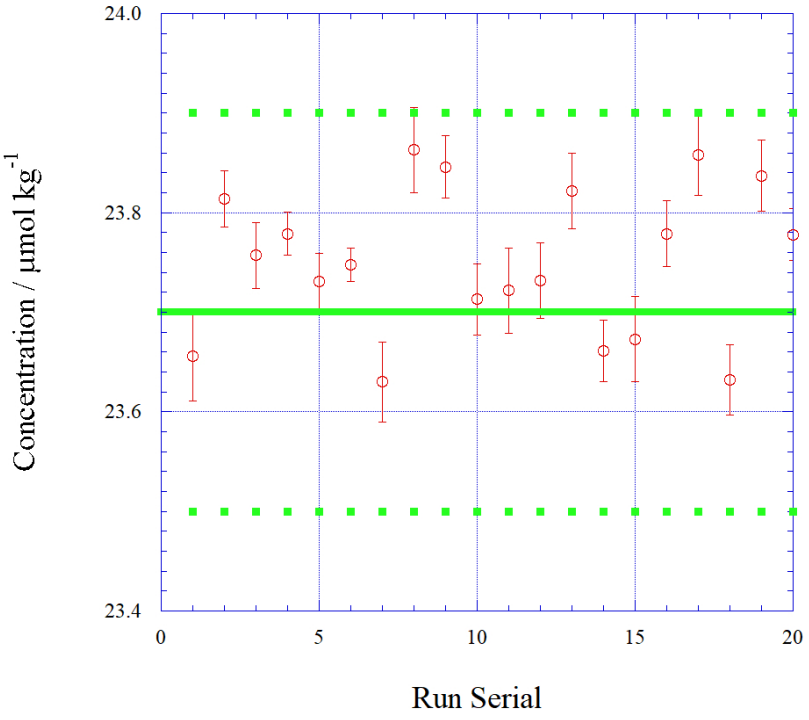

Figure 2.3.2-12 Time series of CRM-CG of nitrate in MR22-03. Solid green line is certified nitrate concentration of CRM and broken green line show uncertainty of certified value at $k = 2$.

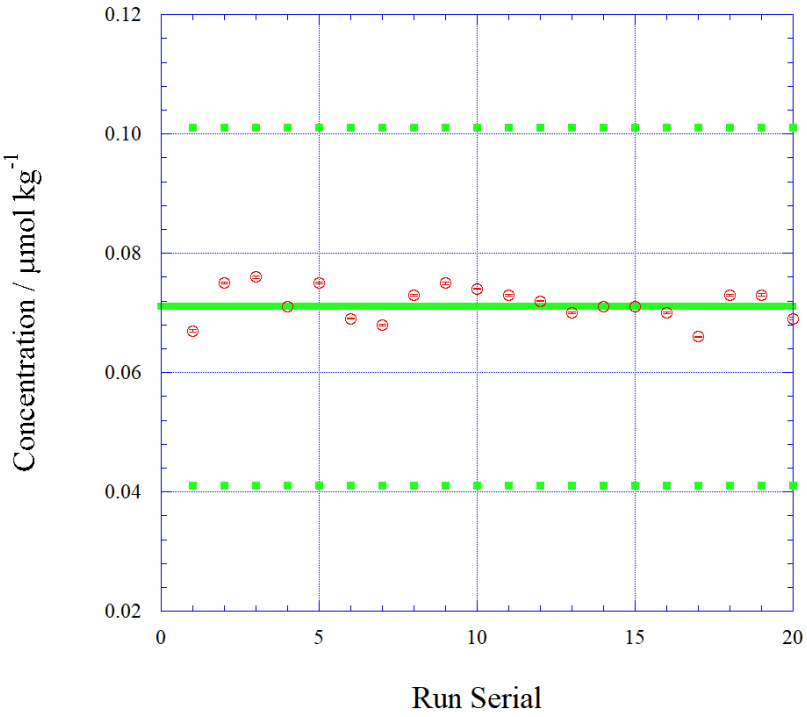

Figure 2.3.2-13 Same as Figure 2.3.2-12, but for nitrite.

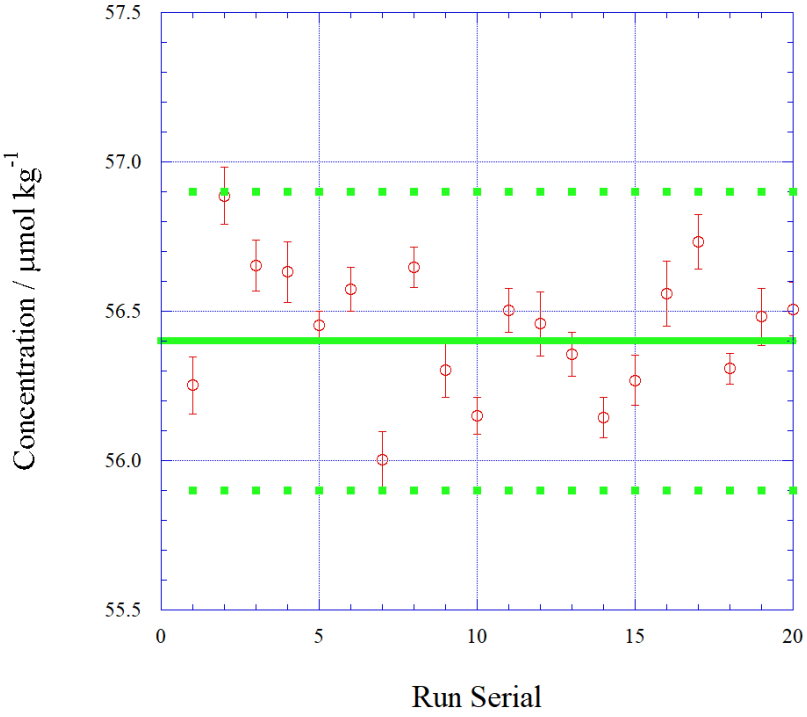

Figure 2.3.2-14 Same as Figure 2.3.2-12, but for silicate.

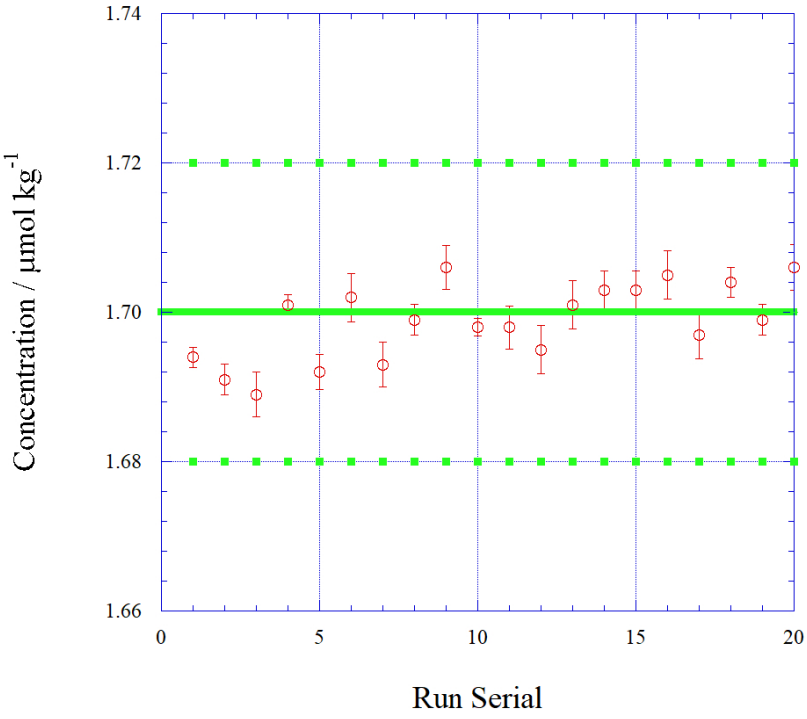

Figure 2.3.2-15 Same as Figure 2.3.2-12, but for phosphate.

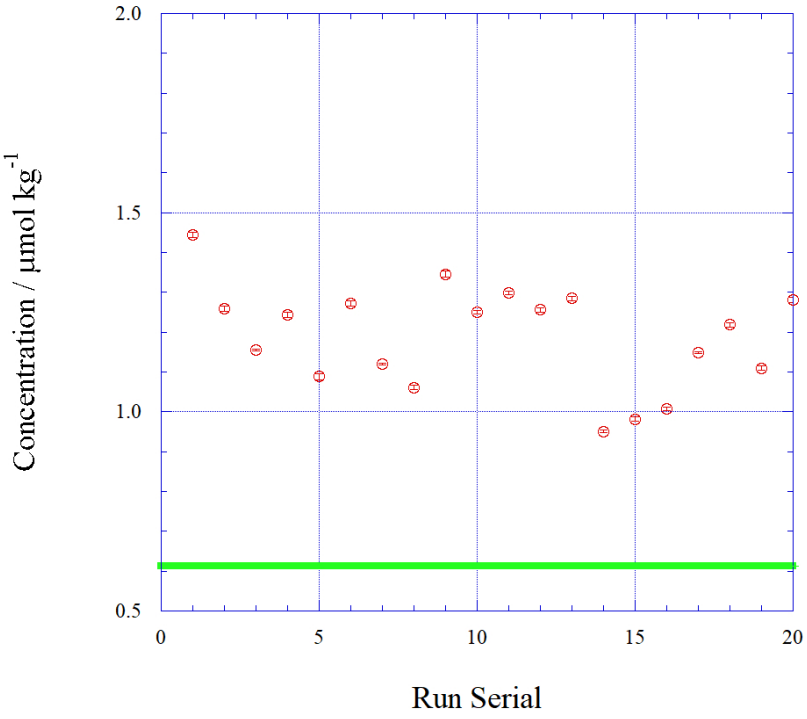

Figure 2.3.2-16 Time series of CRM-CG of ammonia in MR22-03. Solid green line is reference value for ammonia concentration of CRM-CG.

(7.3) Carryover

We also summarized the magnitudes of carry over throughout the cruise. In order to evaluate carryover in each run, we conducted determinations of C-7 followed by determination of LNSW twice. The difference from LNSW-1 to LNSW-2 was obtained and used for this “carryover” evaluation. The Carryover (%) was obtained from the following equation.

Carryover (%) = (LNSW-1 – LNSW-2) / (C-7 – LNSW-2) * 100 (%)

The summary of the carryover (%) was shown in Table 2.3.2-8 and Figure 2.3.2-17 to 2.3.2-21. The results were low % (<0.2 % for nitrite and phosphate; <0.3% for nitrate and silicate; <1% for ammonia). The low % indicates that there is no significant issue during this cruise.

Table 2.3.2-8 Summary of carryover throughout MR22-03.

	Nitrate %	Nitrite %	Silicate %	Phosphate %	Ammonia %
Median	0.28	0.13	0.23	0.17	1.02
Mean	0.29	0.14	0.23	0.17	1.06
Maximum	0.39	0.33	0.26	0.32	2.07
Minimum	0.18	0.00	0.18	0.00	0.46
N	20	20	20	20	20

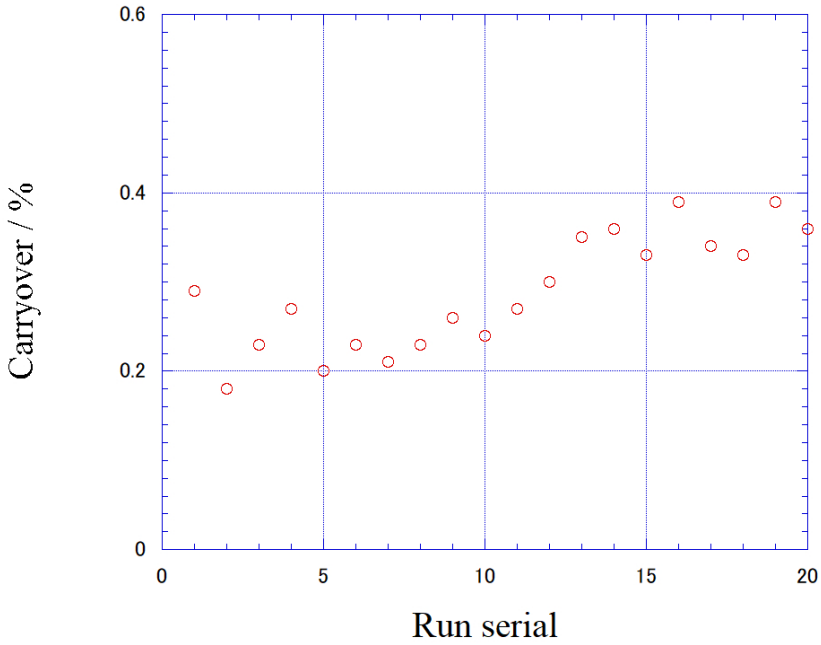

Figure 2.3.2-17 Time series of carry over of nitrate in MR22-03.

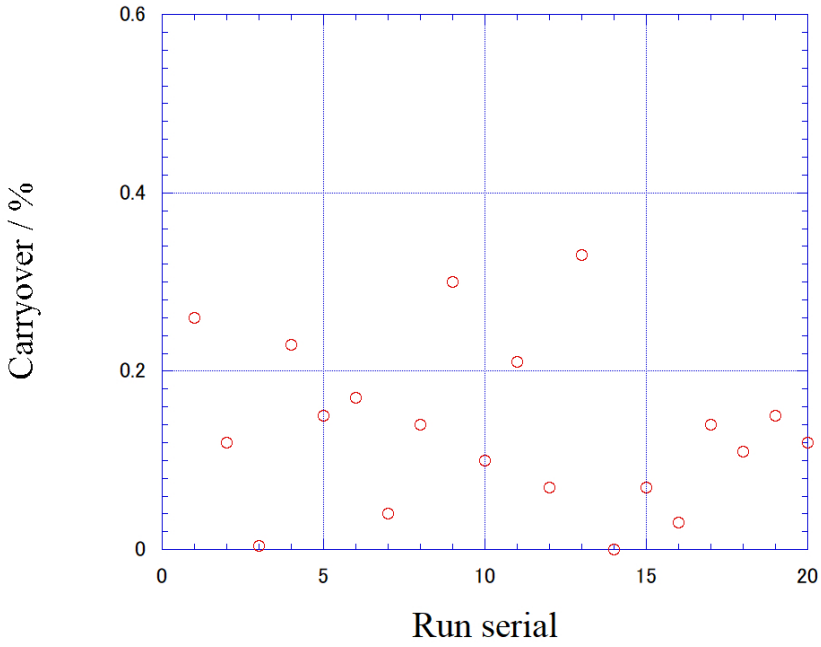

Figure 2.3.2-18 Same as 2.3.2-17 but for nitrite.

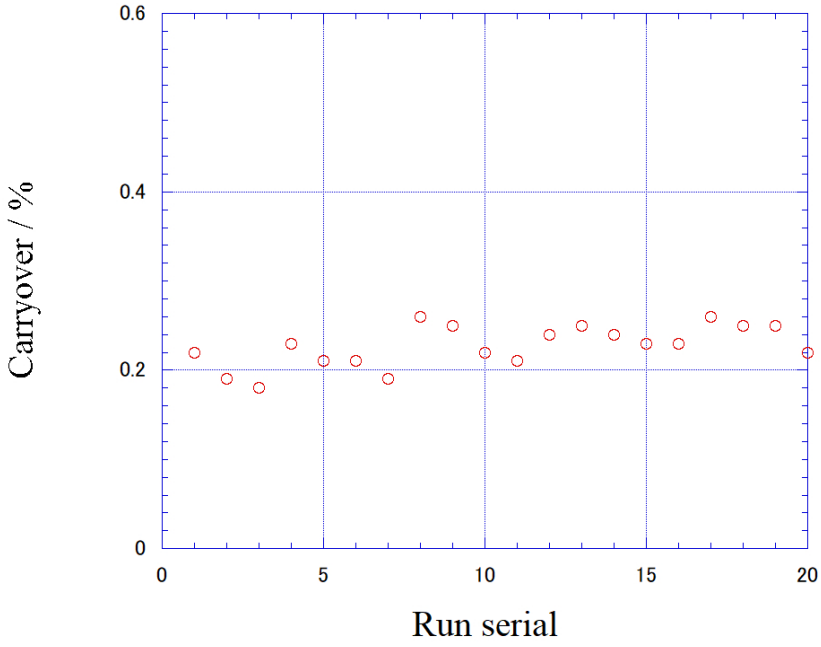

Figure 2.3.2-19 Same as 2.3.2-17 but for silicate

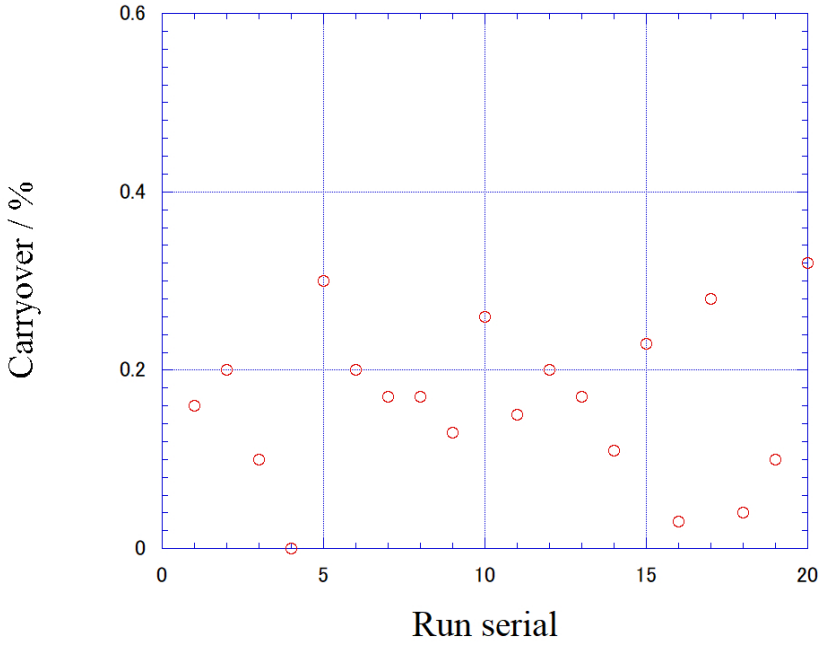

Figure 2.3.2-20 Same as 2.3.2-17 but for phosphate.

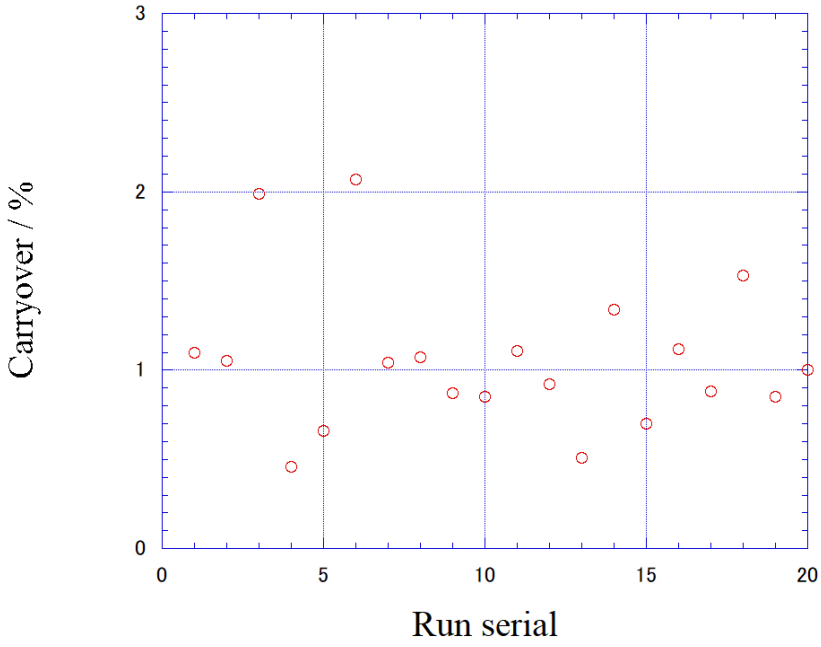

Figure 2.3.2-21 Same as 2.3.2-17 but for ammonia.

(7.4) Estimation of uncertainty of nitrate, silicate, phosphate, nitrite and ammonia concentrations

Empirical equations, eq. (1), (2) and (3) to estimate the uncertainty of measurement of nitrate, silicate and phosphate were obtained based on 20 measurements of 20 sets of CRMs (Table 2.3.2-2). These empirical equations are as follows, respectively.

Nitrate Concentration C_{NO3} in μmol kg^{-1}:

Uncertainty of measurement of nitrate (%) = 0.26949 + 0.94173 * (1 / C_{NO3}) --- (1)

where C_{NO3} is nitrate concentration of sample.

Silicate Concentration C_{SiO2} in µmol kg^{-1}:
Uncertainty of measurement of silicate (%) = 0.26862 + 3.06000 * (1 / C_{SiO2}) --- (2)
where C_{SiO2} is silicate concentration of sample.

Phosphate Concentration C_{PO4} in µmol kg^{-1}:
Uncertainty of measurement of phosphate (%) = 0.23096 + 0.29200 * (1 / C_{PO4}) --- (3)
where C_{PO4} is phosphate concentration of sample.

Empirical equations, eq. (4) and (5) to estimate the uncertainty of measurement of nitrite and ammonia were obtained based on duplicate measurements of the samples.

Nitrite Concentration C_{NO2} in µmol kg^{-1}:
Uncertainty of measurement of nitrite (%) =
– 0.49755 + 0.35453 * (1 / C_{NO2}) – 0.000096543 * (1 / C_{NO2}) * (1 / C_{NO2}) --- (4)
where C_{NO2} is nitrite concentration of sample.

Ammonia Concentration C_{NH4} in µmol kg^{-1}:
Uncertainty of measurement of ammonia (%) =
1.922 + 0.93249 * (1 / C_{NH4}) + 0.00008772 * (1 / C_{NH4}) * (1 / C_{NH4}) --- (5)
where C_{NH4} is ammonia concentration of sample.

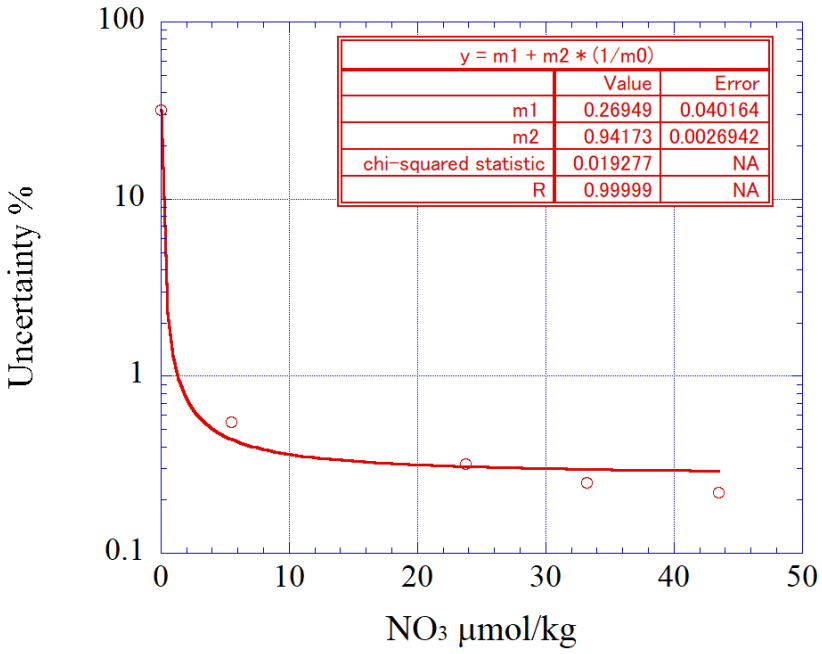

Figure 2.3.2-22 Estimation of uncertainty for nitrate.

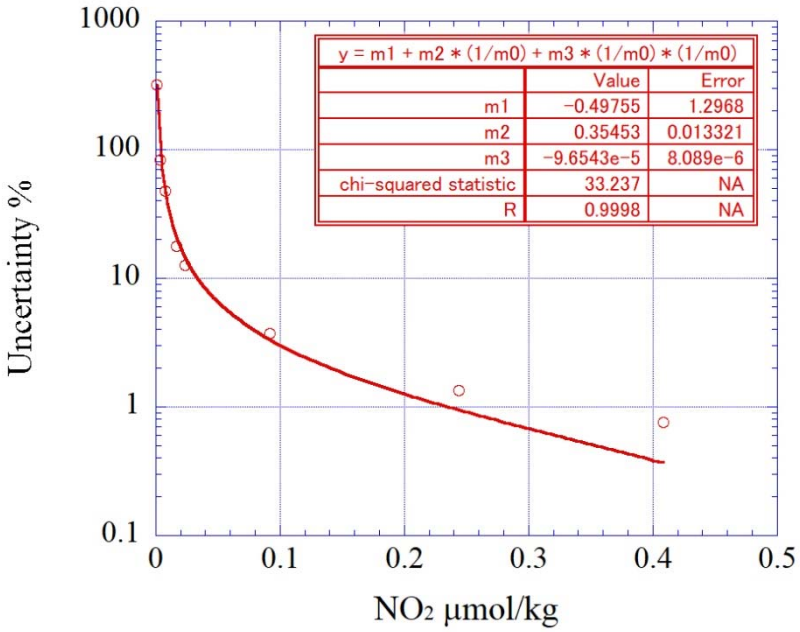

Figure 2.3.2-23 Estimation of uncertainty for nitrite.

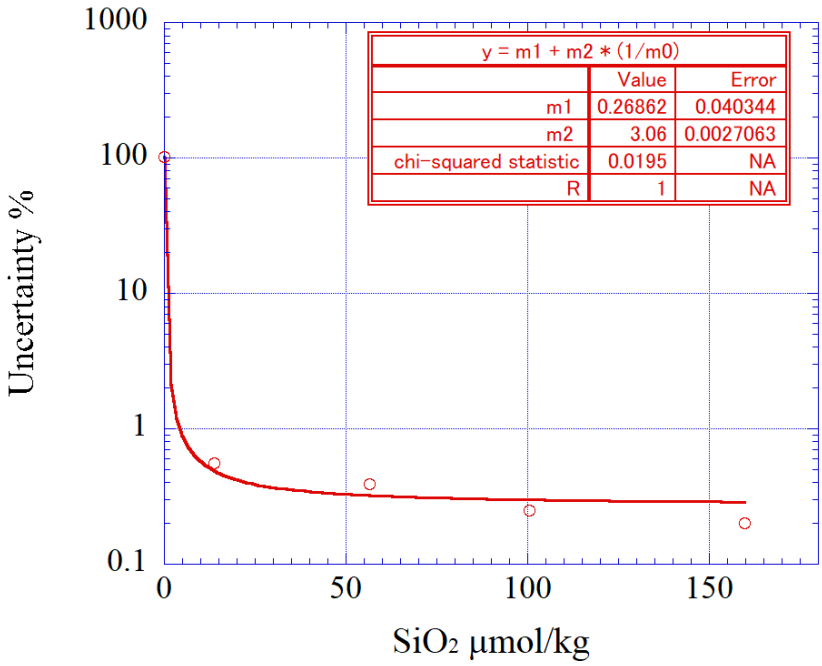

Figure 2.3.2-24 Estimation of uncertainty for silicate.

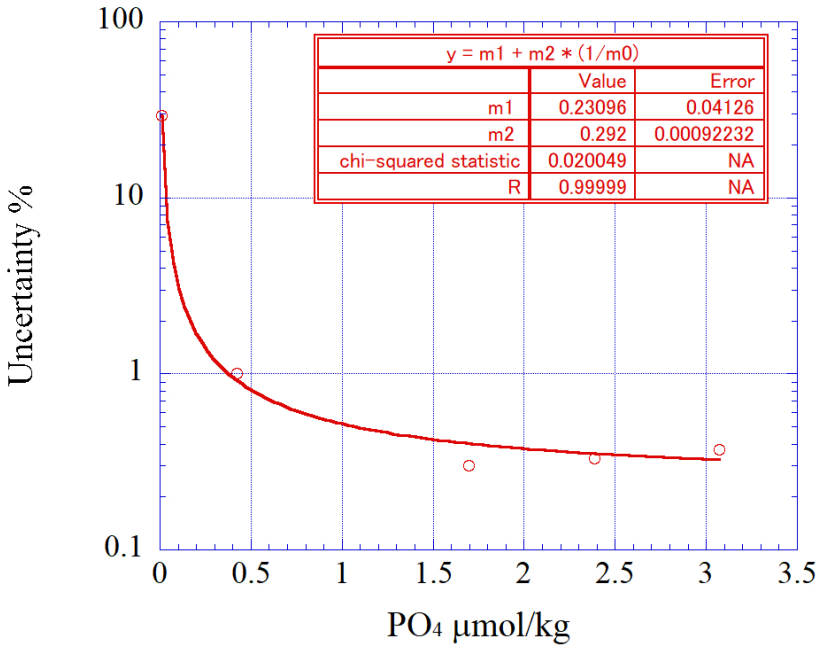

Figure 2.3.2-25 Estimation of uncertainty for phosphate.

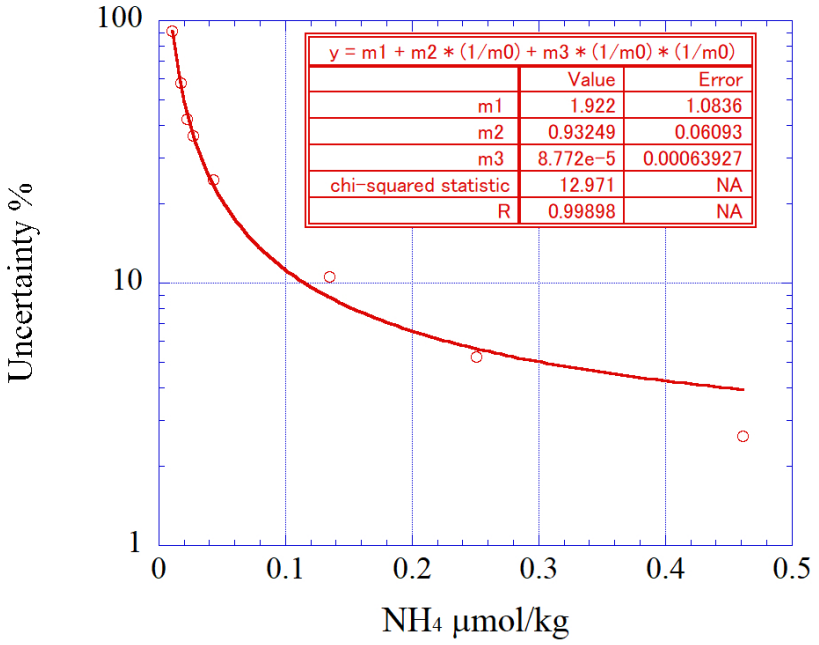

Figure 2.3.2-26 Estimation of uncertainty for ammonia.

(7.5) Detection limit and quantitative determination of nutrients analyses during the cruise

The LNSW was determined every 4 to 18 samples to obtain detection limit of the nutrient analyses during this cruise. During each run, the total number of the LNSW determination was 6-13 times depending on the run. The detection limit was calculated based on the LNSW results obtained from all the runs by the following equation.

Detection limit = 3 * standard deviation of repeated measurement of LNSW,

The summary of detection limit is shown in Table 2.3.2-9. During in this cruise, detection limit is 0.05 μmol kg^{-1} for nitrate, 0.006 μmol kg^{-1} for nitrite, 0.13 μmol kg^{-1} for silicate, 0.006 μmol kg^{-1} for phosphate and 0.02 μmol kg^{-1} for ammonia, respectively. The quantitative determination of nutrient analyses is the concentration of which uncertainty is 33 % in the empirical equations, eq. (1) to (5) in chapter (7.4). The summary of quantitative determination is shown in Table 2.3.2-9. During in this cruise, the quantitative determination was 0.03 μmol kg^{-1} for nitrate, 0.01 μmol kg^{-1} for nitrite, 0.09 μmol kg^{-1} for silicate, 0.009 μmol kg^{-1} for phosphate and 0.03 μmol kg^{-1} for ammonia, respectively.

Replicate samples were taken at most of the layers. The summary of average and standard deviation of the difference between each pair of analysis was shown in Table 2.3.2-10. During this cruise, average of the difference between each pair of analyses were 0.04 μmol kg^{-1} for nitrate, 0.005μmol kg^{-1} for nitrite, 0.12 μmol kg^{-1} for silicate, 0.005 μmol kg^{-1} for phosphate and 0.02 μmol kg^{-1} for ammonia, respectively. Standard deviation of the difference between each pair of analyses were 0.04 μmol kg^{-1} for nitrate, 0.004 μmol kg^{-1} for nitrite, 0.13 μmol kg^{-1} for silicate, 0.004 μmol kg^{-1} for phosphate and 0.01 μmol kg^{-1} for ammonia, respectively.

Table 2.3.2-9 Summary of detection limit and quantitative determination.

	Nitrate μmol kg^{-1}	Nitrite μmol kg^{-1}	Silicate μmol kg^{-1}	Phosphate μmol kg^{-1}	Ammonia μmol kg^{-1}
Detection limit	0.05*	0.006	0.13*	0.006	0.02
Quantitative determination	0.03	0.01	0.09	0.009	0.03

* Due to the large baseline variability over the daily analysis, the detection limit was calculated to be greater than the calculated quantitative determination.

Table 2.3.2-10 Summary of average and standard deviation of the difference between each pair of analysis.

	Nitrate μmol kg^{-1}	Nitrite μmol kg^{-1}	Silicate μmol kg^{-1}	Phosphate μmol kg^{-1}	Ammonia μmol kg^{-1}
Average	0.04	0.005	0.12	0.005	0.02
Standard deviation	0.04	0.004	0.13	0.004	0.01
N	458	455	454	455	466

(8) Problems and our actions/solutions

The precision of the nutrient analysis using QuAAtro 39 systems is decreasing from 2021 to 2022. This is due to wrong performances of the pumps. Then in this cruise, we tried improving the precision by having sampler extend the suction time of samples and getting reaction time longer. At the beginning of the cruise, we compared the precisions on condition that suction time of samples is 60 seconds (we set usually), 70 seconds and 80 seconds, and the precision in case of 70 seconds was the best. Therefore, we set the suction time to 70 seconds thorough this cruise (except for station1 and 2). The precision in case of 80 seconds wasn't the best because the length of sample lines might not be adequate.

(9) List of reagents

Table 2.3.2-11 List of reagents in MR22-03.

IUPAC name	CAS Number	Formula	Compound Name	Manufacture	Grade
4-Aminobenzenesulfonamide	63-74-1	$C_6H_8N_2O_2S$	Sulfanilamide	FUJIFILM Wako Pure Chemical Corporation	JIS Special Grade
Ammonium chloride	12125-02-9	NH_4Cl	Ammonium Chloride	FUJIFILM Wako Pure Chemical Corporation	JIS Special Grade
Antimony potassium tartrate trihydrate	28300-74-5	$K_2(SbC_4H_2O_6)_2 \cdot 3H_2O$	Bis[(+)-tartrato]diantimonate(III) Dipotassium Trihydrate	FUJIFILM Wako Pure Chemical Corporation	JIS Special Grade
Boric acid	10043-35-3	H_3BO_3	Boric Acid	FUJIFILM Wako Pure Chemical Corporation	JIS Special Grade
Hydrogen chloride	7647-01-0	HCl	Hydrochloric Acid	FUJIFILM Wako Pure Chemical Corporation	JIS Special Grade
Imidazole	288-32-4	$C_3H_4N_2$	Imidazole	FUJIFILM Wako Pure Chemical Corporation	JIS Special Grade
L-Ascorbic acid	50-81-7	$C_6H_8O_6$	L-Ascorbic Acid	FUJIFILM Wako Pure Chemical Corporation	JIS Special Grade
N-(1-Naphthalenyl)-1,2-ethanediamine, dihydrochloride	1465-25-4	$C_{12}H_{16}Cl_2N_2$	N-1-Naphthylethylenediamine Dihydrochloride	FUJIFILM Wako Pure Chemical Corporation	for Nitrogen Oxides Analysis
Oxalic acid	144-62-7	$C_2H_2O_4$	Oxalic Acid	FUJIFILM Wako Pure Chemical Corporation	Wako Special Grade
Phenol	108-95-2	C_6H_6O	Phenol	FUJIFILM Wako Pure Chemical Corporation	JIS Special Grade
Potassium nitrate	7757-79-1	KNO_3	Potassium Nitrate	Merck KGaA	Suprapur®
Potassium dihydrogen phosphate	7778-77-0	KH_2PO_4	Potassium dihydrogen phosphate anhydrous	Merck KGaA	Suprapur®
Sodium chloride	7647-14-5	NaCl	Sodium Chloride	FUJIFILM Wako Pure Chemical Corporation	TraceSure®
Sodium citrate dihydrate	6132-04-3	$Na_3C_6H_5O_7 \cdot 2H_2O$	Trisodium Citrate Dihydrate	FUJIFILM Wako Pure Chemical Corporation	JIS Special Grade
Sodium dodecyl sulfate	151-21-3	$C_{12}H_{25}NaO_4S$	Sodium Dodecyl Sulfate	FUJIFILM Wako Pure Chemical Corporation	for Biochemistry
Sodium hydroxide	1310-73-2	NaOH	Sodium Hydroxide for Nitrogen Compounds Analysis	FUJIFILM Wako Pure Chemical Corporation	for Nitrogen Analysis
Sodium hypochlorite	7681-52-9	NaClO	Sodium Hypochlorite Solution	Kanto Chemical co., Inc.	Extra pure
Sodium molybdate dihydrate	10102-40-6	$Na_2MoO_4 \cdot 2H_2O$	Disodium Molybdate(VI) Dihydrate	FUJIFILM Wako Pure Chemical Corporation	JIS Special Grade
Sodium nitroferricyanide dihydrate	13755-38-9	$Na_2[Fe(CN)_5NO] \cdot 2H_2O$	Sodium Pentacyanonitrosylferrate(III) Dihydrate	FUJIFILM Wako Pure Chemical Corporation	JIS Special Grade
Sulfuric acid	7664-93-9	H_2SO_4	Sulfuric Acid	FUJIFILM Wako Pure Chemical Corporation	JIS Special Grade
tetrasodium;2-[2-[bis(carboxylatomethyl)amino]ethyl-(carboxylatomethyl)amino]acetate;tetrahydrate	13235-36-4	$C_{10}H_{12}N_2Na_4O_8 \cdot 4H_2O$	Ethylenediamine-N,N,N',N'-tetraacetic Acid Tetrasodium Salt Tetrahydrate (4NA)	Dojindo Molecular Technologies, Inc.	-
Synonyms: t-Octylphenoxypolyethoxyethanol 4-(1,1,3,3-Tetramethylbutyl)phenyl-polyethylene glycol Polyethylene glycol tert-octylphenyl ether	9002-93-1	$(C_2H_4O)_nC_{14}H_{22}O$	Triton™ X-100	MP Biomedicals, Inc.	-

(10) Data archives

These data obtained in this cruise will be submitted to the Data Management Group of JAMSTEC, and will be opened to the public via “Data Research System for Whole Cruise Information in JAMSTEC (DARWIN)” in JAMSTEC web site. <http://www.godac.jamstec.go.jp/darwin/e>

(11) References

Susan Becker, Michio Aoyama E. Malcolm S. Woodward, Karel Bakker, Stephen Coverly, Claire Mahaffey, Toste Tanhua, (2019) The precise and accurate determination of dissolved inorganic nutrients in seawater, using Continuous Flow Analysis methods, n: The GO-SHIP Repeat Hydrography Manual: A Collection of Expert Reports and Guidelines. Available online at: http://www.go-ship.org/HydroMan.html. DOI: http://dx.doi.org/10.25607/OBP-555

Grasshoff, K. 1976. Automated chemical analysis (Chapter 13) in Methods of Seawater Analysis. With contribution by Almgreen T., Dawson R., Ehrhardt M., Fonselius S. H., Josefsson B., Koroleff F., Kremling K. Weinheim, New York: Verlag Chemie.

Grasshoff, K., Kremling K., Ehrhardt, M. et al. 1999. Methods of Seawater Analysis. Third, Completely Revised and Extended Edition. WILEY-VCH Verlag GmbH, D-69469 Weinheim (Federal Republic of Germany).

Hydes, D.J., Aoyama, M., Aminot, A., Bakker, K., Becker, S., Coverly, S., Daniel, A., Dickson, A.G., Grosso, O., Kerouel, R., Ooijen, J. van, Sato, K., Tanhua, T., Woodward, E.M.S., Zhang, J.Z., 2010. Determination of Dissolved Nutrients (N, P, Si) in Seawater with High Precision and Inter-Comparability Using Gas-Segmented Continuous Flow Analysers, In: GO-SHIP Repeat Hydrography Manual: A Collection of Expert Reports and Guidelines. IOCCP Report No. 14, ICPO Publication Series No 134.

Kimura, 2000. Determination of ammonia in seawater using a vaporization membrane permeability method. 7th auto analyzer Study Group, 39-41.

Murphy, J., and Riley, J.P. 1962. Analytica Chimica Acta 27, 31-36.

2.3.3 Dissolved inorganic carbon

Masahide WAKITA	**JAMSTEC**	**PI**
Masahiro ORUI	**MWJ**	**Operation Leader**
Nagisa FUJIKI	**MWJ**	

(1) Objective

To discuss CO_2 dynamics in seawater of the western subtropical Pacific, total dissolved inorganic carbon was measured on board during the MR22-03 cruise.

(2) Methods, Apparatus and Performance

(2-1) Seawater sampling

Seawater samples were collected by 12 liter sampling bottles mounted on the CTD/Carousel Water Sampling System and a bucket at 19 stations. Seawater was sampled in a 250 mL glass bottle (SCHOTT DURAN) that was previously soaked in 5 % alkaline detergent solution (decon 90, Decon Laboratories Limited) at least 3 hours and was cleaned by fresh water for 5 times and Milli-Q deionized water for 3 times. A sampling silicone rubber tube with PFA tip was connected to the sampling bottle when sampling was carried out. The glass bottles were filled from its bottom gently, without rinsing, and were overflowed for 20 seconds. They were sealed using the polyethylene inner lids with its diameter of 29 mm with care not to leave any bubbles in the bottle. Within about one hour after collecting the samples on the deck, the glass bottles were carried to the laboratory to be poisoned. Small volume (3 mL) of the sample (1 % of the bottle volume) was removed from the bottle and 100 μL of over saturated solution of mercury (II) chloride was added. Then the samples were sealed by the polyethylene inner lids with its diameter of 31.9 mm and stored in a refrigerator at approximately 5 °C. About one hour before the analysis, the samples were taken from refrigerator and put in the water bath kept about 25 °C.

(2-2) Seawater analysis

Measurements of DIC were made with total CO_2 measuring system (Nihon ANS Inc.). The system comprise of seawater dispensing unit, a CO_2 extraction unit, and a coulometer (Model 3000, Nihon ANS Inc.).

The seawater dispensing unit has an auto-sampler (6 ports), which dispenses the seawater from a glass bottle to a pipette of nominal 15 mL volume. The pipette was kept at 25.00 °C ± 0.05 °C by a water jacket, in which water circulated through a thermostatic water bath (NESLAB RTE10, Thermo Fisher Scientific).

The CO_2 dissolved in a seawater sample is extracted in a stripping chamber of the CO_2 extraction unit by adding 10 % phosphoric acid solution. The stripping chamber is made approx. 25 cm long and has a fine frit at the bottom. First, a constant volume of acid is added to the stripping chamber from its bottom by pressurizing an acid bottle with nitrogen gas (99.9999 %). Second, a seawater sample kept in a pipette is introduced to the stripping chamber by the same method. The seawater and phosphoric acid are stirred by the nitrogen bubbles through a fine frit at the bottom of the stripping chamber. The stripped CO_2 is carried to the coulometer through two electric dehumidifiers (kept at 2 °C) and a chemical desiccant (magnesium perchlorate) by the nitrogen gas (flow rate of 140 mL min^{-1}).

Measurements of system blank (phosphoric acid blank), 1.5 % CO_2 standard gas in a nitrogen base, and seawater samples (6 samples) were programmed to repeat. The variation of our own made JAMSTEC DIC reference material was used to correct the signal drift results from chemical alternation of coulometer solutions.

(3) Preliminary results

A few replicate samples were taken at most of the stations and difference between each pair of analyses was plotted on a range control chart (fig. 2.3.3-1). The average of the differences was 1.1 μmol kg^{-1}, with its standard deviation of 1.0 μmol kg^{-1} (n = 43).

(4) Data archive

These data obtained in this cruise will be submitted to the Data Management Group (DMG) of JAMSTEC, and will opened to the public via “Data Research System for Whole Cruise Information in JAMSTEC (DARWIN)” in JAMSTEC web site. <http://www.godac.jamstec.go.jp/darwin/e>

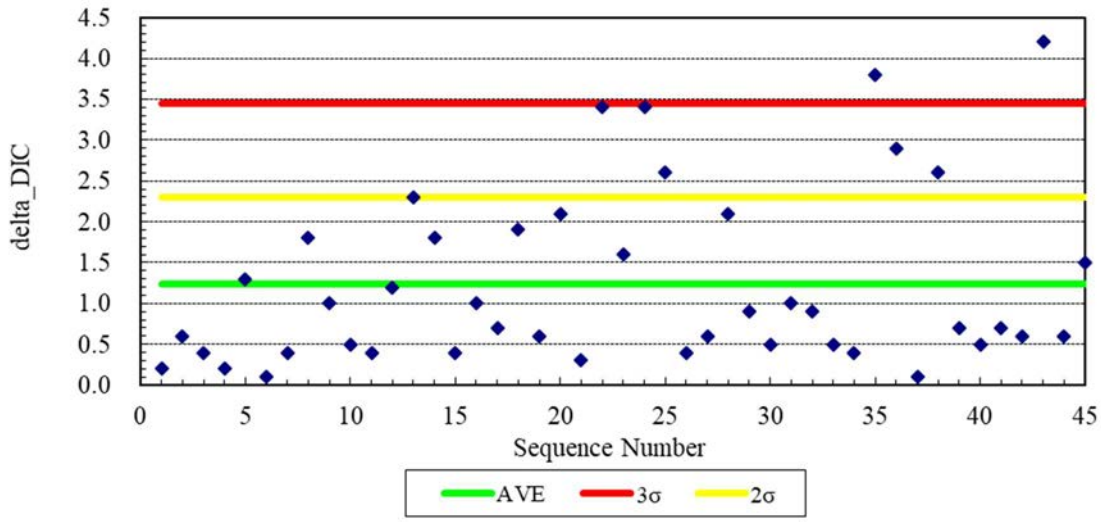

Figure 2.3.3-1 Range control chart of the absolute differences of replicate measurements of DIC carried out during this cruise. AVE represents the average of absolute difference, 3σ the upper control limit (standard deviation of AVE × 3), and 2σ upper warning limit (standard deviation of AVE × 2).

2.3.4 Total alkalinity

Masahide WAKITA	**JAMSTEC**	**PI**
Nagisa FUJIKI	**MWJ**	**Operation Leader**
Masahiro ORUI	**MWJ**	

(1) Objective

Concentration of CO_2, one of the greenhouse gasses, in the atmosphere is now increasing owing to human activities such as burning of fossil fuels. Because the ocean is thought to be a key player to absorb the increased atmospheric CO_2, to clarify the mechanism of CO_2 absorption and to estimate absorption capacity are important and urgent tasks. Increasing of the CO_2 absorption also causes ocean acidification. When CO_2 dissolves into seawater, chemical reaction takes place and CO_2 alters its appearance into several species. Unfortunately, the concentrations of the individual species of the CO_2 system in seawater cannot be measured directly. There are, however, four parameters that can be measured (i.e. total dissolved inorganic carbon, total alkalinity, pH, and pCO_2), these are used to obtain description of the CO_2 system in sea water (Dickson et al., 2007). In the MR22-03 cruise, total dissolved inorganic carbon and total alkalinity were measured on board. We here report the latter parameter in this section.

(2) Methods, Apparatus and Performance

(2-1) Seawater sampling

Seawater samples were collected by 12 L sampling bottles mounted on the CTD/Carousel Water Sampling System and a bucket at 15 stations. The seawater from the sampling bottle was filled into the 250 mL borosilicate glass bottles (SCHOTT DURAN) using a sampling silicone rubber tube with PFA tip. The water was filled into the bottle from the bottom smoothly, without rinsing, and overflowed for 2 times bottle volume (20 seconds). These bottles were pre-washed in advance by soaking in 5 % alkaline detergent (decon90, Decon Laboratories Limited) for more than 3 hours, and then rinsed 5 times with tap water and 3 times with Milli-Q deionized water. The samples were stored in a refrigerator at approximately 5 °C before the analysis, and were put in the water bath with its temperature of about 25 °C for one hour just before analysis.

(2-2) Seawater analyses

The total alkalinity was measured using a spectrophotometric system (Nihon ANS, Inc.) using a scheme of Yao and Byrne (1998). The calibrated volume of sample seawater (ca. 42 mL) was transferred from a sample bottle into the titration cell with its light path length of 4 cm long via dispensing unit. The TA is calculated by measuring two sets of absorbance at three wavelengths (730, 616, and 444) nm applied by the spectrometer (TM-UV/VIS C10082CAH, Hamamatsu Photonics). One is the absorbance of seawater sample before injecting an acid with indicator solution (bromocresol green sodium salt) and another the one after the injection. For mixing the acid with indicator solution and the seawater sufficiently, they are circulated through the line by a peristaltic pump equipped with periodically renewed TYGON tube 5 minutes before the measurement. Nitrogen bubble were introduced into the titration cell for degassing CO_2 from the mixed solution sufficiently.

The TA is calculated based on the following equation:

$$pH_T = 4.2699 + 0.002578 \times (35 - S) + \log((R(25) - 0.00131) / (2.3148 - 0.1299 \times R(25))) - \log(1 - 0.001005 \times S) \quad (1)$$

$$A_T = (N_A \times V_A - 10^{pHT} \times DensSW(T, S) \times (V_S + V_A)) \times (DensSW(T, S) \times V_S)^{-1} \quad (2)$$

where R(25) represents the difference of absorbance at 616 nm and 444 nm between before and after the injection. The absorbance of wavelength at 730 nm is used to subtract the variation of absorbance caused by the system. DensSW (T, S) is the density of seawater at temperature (T) and salinity (S), N_A the concentration of

the added acid, V_A and V_S the volume of added acid and seawater, respectively.

(3) Preliminary result

The repeatability of this system was 2.1 μmol kg^{-1} (n = 40) which was estimated from standard deviation of measured KRM value during this cruise. A few replicate samples were taken at most of stations and the difference between each pair of analyses was plotted on a range control chart (see fig. 2.3.4-1). The average of the difference was provisionally 1.5 μmol kg^{-1} (n = 44) with its standard deviation of 1.2 μmol kg^{-1}.

(4) Data archive

Obtained data will be submitted to the Data Management Group (DMG) of JAMSTEC.

(5) References

Dickson, A. G., Sabine, C. L. & Christian, J. R. (Eds.). (2007). Guide to best practices for ocean CO_2 measurements, PICES Special Publication 3: North Pacific Marine Science Organization.

Yao, W. and Byrne, R. H. (1998). Simplified seawater alkalinity analysis: Use of linear array spectrometers. Deep-Sea Research I, 45, 1383-1392.

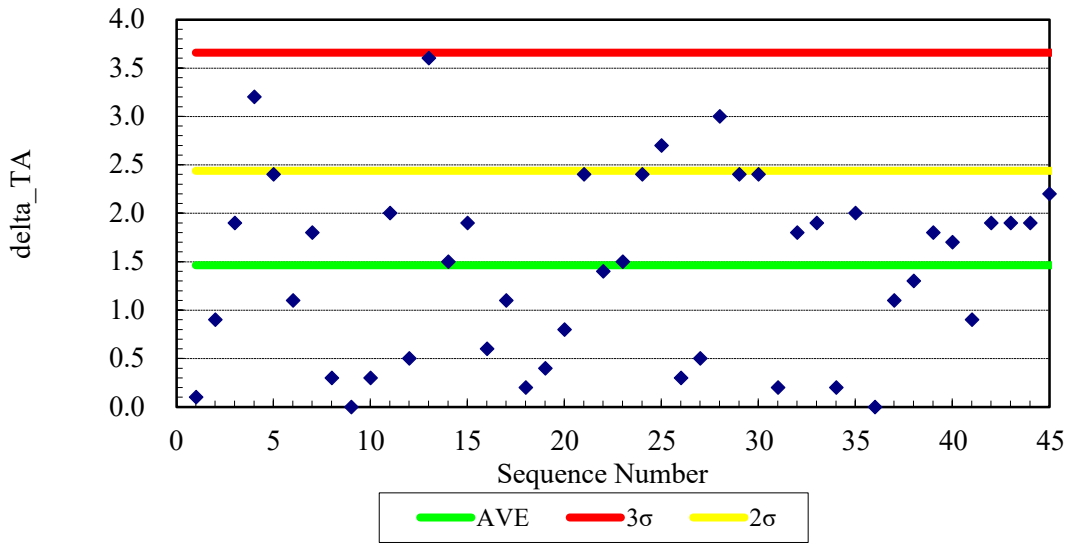

Figure 2.3.4-1 Range control chart of the absolute differences of replicate measurements of TA carried out during this cruise. AVE represents the average of absolute difference, 3σ the upper control limit (standard deviation of AVE × 3), and 2σ upper warning limit (standard deviation of AVE × 2).

2.3.5 DIC, TA, Nutrients-UV

Yoshiyuki NAKANO JAMSTEC

(1) Objective

When measuring DIC in seawater, mercury (II) chloride is usually added to the sample to kill organisms in the seawater. However, mercury (II) chloride is a highly poisonous chemical that requires careful handling, and liquid waste disposal must be entrusted to a waste disposal company. Furthermore, it is highly likely that the use of mercury (II) chloride will be discontinued in a few years due to international mercury control treaties, so alternative sterilization methods are needed. Therefore, we have been developing a water sampling sterilization device that utilizes a new ultraviolet (UV) light source. Our objective in this cruise is to test the water sampling sterilization device using each layer water sampling of Niskin bottles.

(2) Method

We utilize a UV Luminous Array Film (UV-LAFi) for the water sampling sterilization device. UV-LAFi is a new deep-UV light source featuring surface emission and broad wavelength, and it can be expected to have higher bactericidal effect than UV-LED at the same output. UV-LAFi technologies were developed by Shikoh Tech Co., Ltd. The Basic structure for UV-C light source is based on mercury-free plasma emission technology. We wound the UV-LAFi onto a 150 mm long, Φ30 mm quartz tube. The mechanism of the water sampling sterilization device is that while seawater passes through the quartz tube (3-4 seconds), it is irradiated with UV-C from all directions, killing organisms in the seawater.

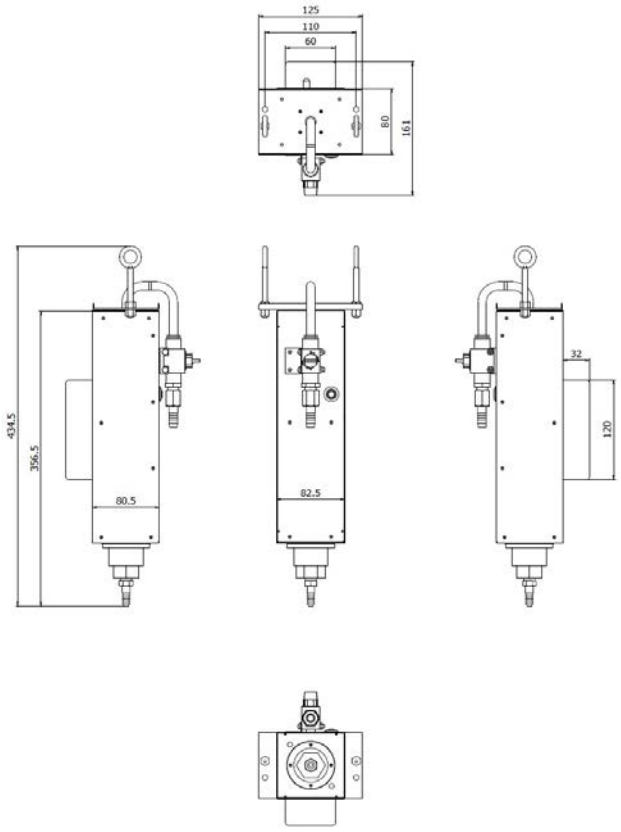

Fig. 2.3.5-1. Dimensions of the water sampling sterilization device.

(3) Preliminary results

We sampled DIC, TA, and Nutrients at St. 1, St. 4, and St. 6 in this cruise. We present here only the DIC data at St. 1 as a preliminarily result. We took three types of samples: mercury (II) chloride added (Hg), UV irradiated (UV), and control (none), and performed a preservation test at room temperature for about one month. The DIC samples were measured seven times at approximately 5-day intervals during the cruise. We used Hg as the reference and defined measurements with a difference from Hg greater than 5 µmol/kg as outside the error range. For the none sample, the difference from Hg was outside the error range for all after the third measurement. The UV samples differed from Hg only twice outside the error range, and the differences were small. The average difference between Hg and UV over the entire preservation test period was 2.7 µmol/kg, and we successfully tested the preservation of DIC samples without the addition of ferric mercury chloride using a water sampling sterilization device.

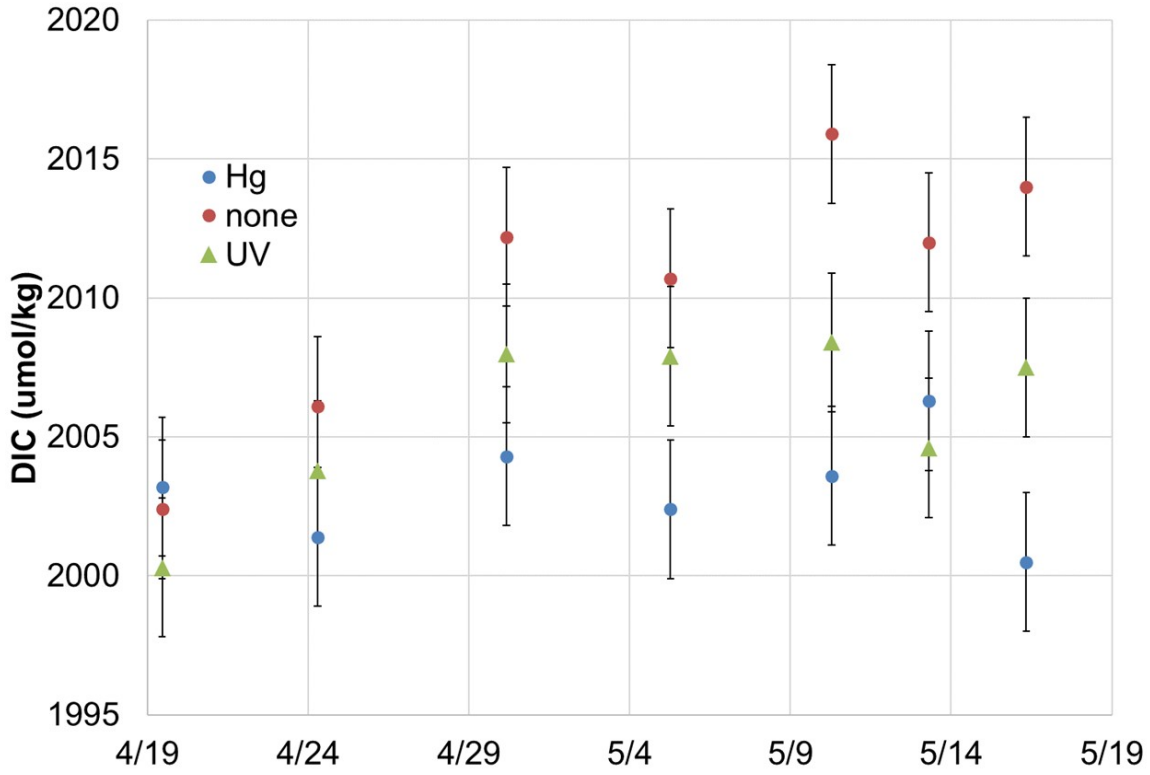

Fig. 2.3.5-2. DIC preservation test result (Hg ●, non ● and UV ▲) at St.1 from April 19 to May 16.

(4) Data Archive

All data will be submitted to JAMSTEC Data Management Office (DMO) and is currently under its control.

Reference

Kosako, T., Guo, B., Tanaka, H., Hirakawa, H., Awamoto, K., Shinoda, T. (2013) Progress in Luminous Array Film (LAFi) with Plasma Tube Technology for Seamless Tilling Super-large-area Display. SID Dig., 44(1), pp. 49-52.

Awamoto. K., Hirakawa, H., Takahashi, J., Hidaka, T. and Shinoda, T. (2016) Development of the Flexible Surface Light Source Using Luminous Array Film Technology. Proceeding of IDW '16, pp. 504-507.

Awamoto. K., Hirakawa, H., Hidaka, T. Takahashi, J., Makino, T. and Shinoda, T. (2018) Development of the Mercury Free Deep UV Surface Light Source with Plasma Technologies. Proceeding of the 2018 IEICE Society Conference, pp. 158.

2.3.6 pH/pCO_2-vertical (pH/pCO_2 sensor)

Kiminori SHITASHIMA **Tokyo University of Marine Science and Technology** **PI**
Miaka YAMAGUCHI **Tokyo University of Marine Science and Technology**

(1) Objective

The measurement of pH in the marine system is important because the pH of seawater reflects the oceanic carbon cycles and the exchange of CO_2 between the atmosphere and the ocean. Furthermore, pH relates to and the biological and chemical processes occurring in the ocean. Concerning the global warming, change of pH and pCO_2 in seawater should preferably be observed continually in a long term and a wide area (vertically and horizontally) to monitor air-sea CO_2 exchange and oceanic carbon cycle. In-situ measurement with a sensor is the most suitable for such observations.

The objective of this study is to develop high performance pH/pCO_2 sensor for in situ measurement in the deep sea and apply it for chemical oceanography

(2) Instruments and methods

The in-situ pH sensor employs an Ion Sensitive Field Effect Transistor (ISFET) as a pH electrode, and the Chloride ion selective electrode (Cl-ISE) as a reference electrode. The ISFET is a semiconductor made of p-type Si coated with SiO_2 and Si_3N_4 that can measure H^+ ion concentration in aqueous phase. New ISFET-pH electrode specialized for oceanographic use was developed. The Cl-ISE is a pellet made of several chlorides having a response to the chloride ion, a major element in seawater. The electric potential of the Cl-ISE is stable in the seawater, since it has no inner electrolyte solution. The in-situ pH sensor has a quick response (less than a second), high accuracy (±0.003pH) and pressure-resistant performance. The pCO_2 sensor was devised to incorporate the above-mentioned newly developed in-situ pH sensor to measure the in-situ pCO_2 in seawater. The principle of pCO_2 measurement by the pCO_2 sensor is as follows. Both the ISFET-pH electrode and the Cl-ISE of the pH sensor are sealed in a unit with a gas permeable membrane whose inside is filled with inner electrolyte solution with 1.5 % of NaCl. The pH sensor can detect pCO_2 change as pH change of inner solution caused by permeation of carbon dioxide gas species through the membrane. An amorphous Teflon membrane (Teflon AF™) manufactured by DuPont was used as the gas permeable membrane. The in-situ (3,000m, 1.8ºC) response time of the pCO_2 sensor was less than 60 seconds. The diode on ISFET can measure the temperature of seawater simultaneously. ISFET and Cl-ISE are connected to pH converter circuit in the pressure housing through the underwater cable connector. The pressure housing includes pH converter circuit, A/D converter, data logger RS-232C interface and Li ion battery.

Two pH/pCO_2 sensors were installed to the CTD-CMS, and in-situ data of pH and pCO_2 ware measured every 1 second during descent and ascent of the CTD-CMS. Before and after the observation, the pH sensor was calibrated using two different standard buffer solutions, 2-aminopyridine (AMP; pH 6.7866) and 2-amino-2-hydroxymethil-1,3-propanediol (TRIS; pH 8.0893) described by Dickson and Goyet, for the correction of electrical drift of pH data. In this cruise, the calibration of the pCO_2 sensor was conducted using two different seawaters, surface and deep seawaters which measured pCO_2 concentration, before and after the observation. The recorded data (pH, pCO_2, temperature) is stored in the data logger. After recovery of the sensor, the data is transferred from the data logger into a personal computer (PC) connected with RS-232C cable, and the in-situ pH and pCO_2 are calculated using calibration data of each standards in a PC.

(3) Parameters

In-situ pH and pCO_2

(4) Observation log

Station	Date (m/d/y)	Cast
St. 1	4/17/2022	Cast 2
St. 2	4/18/2022	Cast 1
St. 3	4/19/2022	Cast 1
St. 4	4/21/2022	Cast 2
St. 5	4/23/2022	Cast 1
St. 6	4/26/2022	Cast 1
St. 7	4/25/2022	Cast 1
St. 8	4/26/2022	Cast 1
St. 9	4/28/2022	Cast 1
St. 10	4/30/2022	Cast 1
St. 11	5/2/2022	Cast 1, Cast 2
St. 12	5/8/2022	Cast 1
St. 13	5/10/2022	Cast 1
St. 14	5/15/2022	Cast 1

(5) Data archives

All data will be archived at Tokyo University of Marine Science and Technology after checking of data quality and submitted to Data Management Group (DMG) of JAMSTEC.

Fig. 2.3.6-1 Photo of pH/pCO_2 sensors on the frames of CTD-CMS.

2.3.7 Dissolved organic carbon and total dissolved nitrogen

Masahide WAKITA JAMSTEC

(1) Objectives

Variabilities in the concentration of dissolved organic carbon (DOC) in seawater have a potentially great impact on the carbon cycle in the marine system, because DOC is a major global carbon reservoir. A change by < 10% in the size of the oceanic DOC pool, estimated to be ~ 700 GtC (IPCC, 2013), would be comparable to the annual primary productivity in the whole ocean. In fact, it was generally concluded that the bulk DOC in oceanic water, especially in the deep ocean, is quite inert based upon ^{14}C-age measurements. Nevertheless, it is widely observed that in the ocean DOC accumulates in surface waters at levels above the more constant concentration in deep water, suggesting the presence of DOC associated with biological production in the surface ocean. This study presents the distribution of DOC in the western subarctic North Pacific.

(2) Sampling

Seawater samples of DOC and TDN were collected by surface bucket sampling and 10 liter Niskin bottles mounted on the CTD/Carousel Water Sampling System and brought the total to ~360. Seawater from the Niskin bottle or surface water monitoring was transferred into 60 ml High Density Polyethylene bottle (HDPE) for DOC/TDN and rinsed with same water three times. Water taken from the surface to bottom is filtered using precombusted (450°C) GF/F inline filters as they are being collected from the Niskin bottle or surface bucket sampling. After collection, samples are frozen upright and preserved at ~ -20 °C cold until analysis in our land laboratory. Before use, all glassware was muffled at 550 °C for 5 hrs.

(3) Analysis

Prior to analysis, samples are returned to room temperature and acidified to pH < 2 with concentrated hydrochloric acid. DOC/TDN analysis was basically made with a high-temperature catalytic oxidation (HTCO) system improved a commercial unit, the Shimadzu TOC-L with a TNM-L units (Shimadzu Co.). In this system, the non-dispersive infrared was used for carbon dioxide produced from DOC during the HTCO process (temperature: 720 °C, catalyst: 0.5% Pt-Al_2O_3). Non-purgeable dissolved nitrogen compounds are combusted and converted to NO which, when mixed with ozone, chemiluminesces for detection by a photomultiplier. The consensus reference material for DOC and TDN (Hansell 2005) was analyzed during the sample measurements.

(3) Preliminary result

The distributions of DOC and TDN will be determined as soon as possible after this cruise.

(4) Data archive

These obtained data will be submitted to JAMSTEC Data Management Group (DMG).

2.3.8 Trace elements

Koji SUGIE **JAMSTEC PI**
Nanako TONEDACHI **Tokyo University of Marine Science and Technology**
Kiminori SHITASHIMA **Tokyo University of Marine Science and Technology**
Minako KURISU **JAMSTEC**
Yuta ISAJI **JAMSTEC**

(1) Objectives

Some trace metals such as iron, manganese and zinc are essential for phytoplankton growth because they are co-factors of many essential enzymes. However, trace metal distribution in the western Pacific was rarely investigated before. In addition, iron availability is one of the most important factors for regulating phytoplankton productivity during summer. However, the data of trace metals including iron is scarce and data availability is mostly limited during summer (August and September). In this cruise, we collected seawater samples for multiple trace metals using R/V Mirai in the western North Pacific region during early spring. Furthermore, we collected samples for analyses on δ^{56}Fe of dissolved Fe and concentration of iron-containing heme protein (Hem-Fe) to estimate the origin of Fe and functioning Fe in organisms in the western Pacific region, which significantly improve our understanding of the biogeochemical cycling of Fe and productivity of lower trophic levels. Another target is developing the method of on-board analysis of toxic elements such as Cd, Pb, Hg and As. In this cruise, we collected seawater samples for toxic elements to test the sensitivity of newly developing method for lower concentration samples.

(2) Instruments and methods

Water sampling with Teflon-coated Niskin-X sampling bottles. Niskin-X sampling bottles were directly attached to CTD-CWS and sampling bottles were fired with depth trigger using Auto Fire Module (Seabird). Sampling depth will also be checked with salinity or macronutrient concentrations and their ratios (NO_3, NO_2, PO_4, $Si(OH)_4$) by comparing our sampling bottles and routine samplings conducted at the same station. The samples for dissolved trace metals were obtained the filtrate of 0.2 μm Acropac capsule cartridge filter (Pall Co. Ltd.) under gravity pressure which was connected to the spigot of Niskin-X sampling bottles. For total dissolvable sample, unfiltered seawater was directly collected into the sampling bottles. Sampling bottles (Teflon® PFA for dissolved and total dissolvable trace metals and LDPE for δ^{56}Fe of dissolved Fe) were rigorously acid-washed and rinsed with pure-water (>18.2 MΩ, Millipore). Samples were acidified using pure-HCl (TAMAPURE AA10, Tama Chemicals) to pH ~1.8 aboard in clean booth. Seawater samples will be measured using ICP-MS in on-land laboratory according to the method of Sohrin et al. (2008, Anal. Chem.) and Conway et al. (2013, Anal. Chim. Acta). Hem-Fe and particulate Fe were filtered pre-combusted GF-75 (nominal pore size, 0.3 μm) and acid-washed omnipore (nominal pore size, 0.45 μm) filters, respectively. To remove extracellularly absorbed Fe, filter samples for particulate Fe were treated with oxalate-EDTA solution (Tovar-Sanchez et al., 2003). Filter samples were stored at -20°C until on-land analysis.

(3) Parameters

Dissolved and total dissolvable Al, As, Hg, Mn, Fe, Co, Ni, Cu, Zn and Cd, δ^{56}Fe of dissolved Fe, particulate Fe, Hem-Fe and macronutrients (NO_3, NO_2, NH_4, PO_4, $Si(OH)_4$) and/or salinity.

(4) Observation log

Station	Date (m/d/y)	Position	Sampling depth (dbar)
St. 4	4/21/2022	25°03.38'N, 144°55.90'E	10, 20, 50, 75, 107, 200
St. 6	4/24/2022	34°47.43'N, 141°17.81'E	10, 20, 50, 75, 100, 200
St. 7	4/25/2022	34°58.96'N, 145°00.05'E	10, 20, 40, 75, 100, 200
St. 9	4/28/2022	35°03.41'N, 157°36.57'E	10, 20, 45, 75, 100, 200
St. 11	5/2/2022	46°59.87'N, 160°01.72'E	400, 600, 800, 1000, 1200, 1500
St. 11	5/4/2022	46°59.57'N, 160°00.69'E	10, 20, 54, 100, 125, 200
St. 13	5/12/2022	43°58.19'N, 155°02.35'E	10, 20, 53, 100, 125, 200

Obtained parameters at each station

	Trace metals	δ^{56}Fe	Hem-Fe & P-Fe	Toxic metals	Salinity	Nutrients
St. 4	○	○	○		○	
St. 6	○		○	○	○	
St. 7	○		○		○	
St. 9	○		○		○	
St. 11	○	○	○	○		○
St. 13	○	○	○		○	○

(5) Data archives

All data obtained during MR22-03 cruise will be submitted to Data Management Group (DMG) of JAMSTEC after the sample analysis and validation. The data will be opened to the public via "Data Research System for Whole Cruise Information (DARWIN)" in JAMSTEC web site or elsewhere.

(6) Preliminary data

Vertical profiles of temperature and salinity of each station that obtained trace metal samplings with CTD-CWS system during MR22-03 cruise.

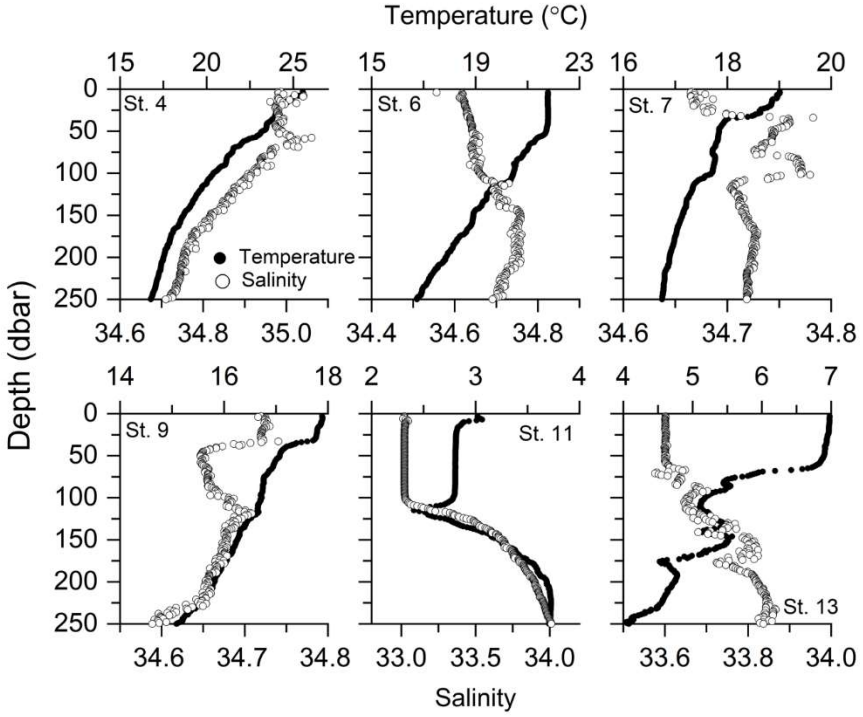

Fig. 2.8.3-1. Vertical profiles of temperature and salinity at the Sts. 4, 6, 7, 9, 11 and 13. Open and filled circles represent temperature and salinity, respectively.

2.3.9 Iodine

Satoko OWARI	**Tokyo University of Marine Science and Technology**	**PI**
Mayu OHI	**Tokyo University of Marine Science and Technology**	
Kiminori SHITASHIMA	**Tokyo University of Marine Science and Technology**	

(1) Objective
Development of on-board analysis method of iodine in the ocean.

(2) Instruments and methods
After seawater sampling from Niskin-X bottles, the samples were filtered by using 0.2 μm capsule cartridge filter and stored in refrigerator. The samples will be analyzed on-land after the cruise, but we tried to analyze on-board for some samples. The spectrophotometry that was developed for interstitial water analysis at IODP was applied for on-board analysis in this cruise.

(3) Parameters
Dissolved I^-, IO_3^- and total I.

(4) Observation log

Station	Date (m/d/y)	Sampling depth (dbar)
St. 4	4/21/2022	0, 10, 20, 30, 40, 60, 76, 100, 125, 150, 175, 200, 250, 300, 500, 700, 1000, 2000, 3000
St. 5	4/23/2022	0, 10, 20, 30, 40, 60, 75, 100, 125, 150, 175, 200, 250, 300, 500, 600, 1000, 2000, 3000, 5000
St. 6	4/26/2022	0, 10, 20, 30, 40, 60, 76, 100, 126, 160, 176, 200, 260, 300, 600, 800, 1000, 2000, 3000
St. 8	4/26/2022	0, 10, 20, 30, 40, 60, 76, 100, 126, 150, 176, 200, 250, 300, 600, 800, 1000, 2000, 3000
St. 9	4/28/2022	0, 10, 20, 30, 40, 50, 75, 100, 125, 150, 176, 200, 260, 300, 600, 800, 1000, 2000, 3000, 4000, 5000
St. 10	4/30/2022	0, 10, 20, 30, 40, 50, 76, 100, 126, 150, 176, 200, 250, 300, 500, 800, 1000, 2000, 3000
St. 11	5/2/2022	0, 10, 20, 30, 40, 50, 75, 100, 125, 150, 175, 200, 250, 300, 500, 600, 1000, 2000, 3000, 4000, 5000
St. 14	5/15/2022	0, 12, 20, 28, 40, 46, 76, 91, 135, 150, 175, 200, 250, B-10,

(5) Data archives
All data will be archived at Tokyo University of Marine Science and Technology after checking of data quality and submitted to Data Management Group (DMG) of JAMSTEC.

2.3.10 Nitrification

Takuhei SHIOZAKI **Atmosphere and Ocean Research Institute, The University of Tokyo** **PI**

(2) Objectives
Water samples were collected using a bucket and Niskin bottles to examine nitrification rate.

(3) Parameters
Nitrification rate
Chlorophyll *a*
DNA

(4) Instruments and methods
Experiments were performed at station 5, 9, and 11. Water samples for the nitrification rate and DNA analysis were collected in a bucket and Niskin-X bottles from those layers having surface light intensities of 100, 1, and 0.1% and depths of 500 m, 1000 m, 3000 m, and bottom depth minus 10 m. Samples for chlorophyll a were collected from the light depths.

Nitrification rates were evaluated by a ^{15}N tracer method. ^{15}N-labeled ammonium was added to the bottles to reach final concentrations of 99 nmol N L^{-1}. After addition of the tracers, the incubation bottles were placed into on-deck incubators cooled by flowing surface seawater or in a thermostatic incubator. Light levels were adjusted using neutral-density screens or aluminum foil. Initial and incubated samples were filtered through a 0.2-μm pore size cellulose acetate filter (DISMIC, Advantec MFS) and the filtrates were collected in 50-mL polypropylene bottles for isotope measurement and in 10-mL acrylic tubes to measure the nitrate + nitrite concentration. Nitrate + nitrite concentration was immediately determined on board. The samples for isotope measurement were kept frozen until analyses on land.

Samples for DNA analysis were filtered onto Sterivex-GP pressure filter units with a 0.22 μm pore size (Millipore). Samples for chlorophyll *a* of 290 ml were filtered onto 25-mm Whatman GF/F filters, and the chlorophyll *a* concentrations were measured fluorometrically using a Turner Design 10-AU fluorometer after extraction with N', N'-dimethylformamide on board.

(5) Data archives
These data obtained in this cruise will be submitted to the Data Management Group of JAMSTEC when ready.

2.3.11 Radioactivity (Gamma-ray sensor)

Kiminori SHITASHIMA Tokyo University of Marine Science and Technology PI

(1) Objective

Underwater in-situ gamma-ray measurement is important scientific priority for oceanography, especially for survey and monitoring of the concentration distributions of natural and anthropogenic gamma-ray. The sensor was applied to observe and monitor natural gamma-ray in the deep open ocean.

(2) Instruments and methods

A plastic scintillator is made from polystyrene that doped NaI(Tl) and it absorbs gamma-ray like as liquid or crystal scintillator. The plastic scintillator was coated by light-resistant paint and used as a part of pressure housing. Therefore, the sensor can expect high sensitivity in comparison with NaI(Tl) crystal sealed in a container because the plastic scintillator contacts seawater directly. This sensor consists of plastic scintillator, photomultiplier tube, preamplifier unit, high-voltage power supply, data logger and lithium-ion battery, and all parts are stored in a pressure housing. The sensor was installed to the CTD-CMS frame and in-situ data of radon was measured every 1 second during descent and ascent of the CTD-CMS system.

(3) Parameters

In-situ gamma-ray

(4) Observation log

Station	Date (m/d/y)	Cast
St. 1	4/17/2022	Cast 2
St. 2	4/18/2022	Cast 1
St. 3	4/19/2022	Cast 1
St. 4	4/21/2022	Cast 2
St. 5	4/23/2022	Cast 1
St. 6	4/26/2022	Cast 1
St. 7	4/25/2022	Cast 1
St. 8	4/26/2022	Cast 1
St. 10	4/30/2022	Cast 1
St. 11	5/6/2022	Cast 4, Cast 5
St. 12	5/9/2022	Cast 2, Cast 3

(5) Data archives

All data will be archived at Tokyo University of Marine Science and Technology after checking of data quality and submitted to Data Management Group (DMG) of JAMSTEC.

Fig. 2.3.6-1 Photo of gamma-ray sensors on the frames of CTD-CMS.

2.3.12 Environmental DNA

Masahide WAKITA **JAMSTEC**
Akihide KASAI **Hokkaido University**

(1) Objectives

To depict the aquatic biodiversity is essential to reveal the substantial impacts of climate change on the marine ecosystems. Fishes are one of the major components of the ecosystem and can be very susceptible to global warming. Because they are important for the economy, their ecological changes will also influence human activity.

Analyzing environmental DNA (eDNA) is an emerging method to assess aquatic community composition. eDNA originated from aquatic organisms in various forms (e.g., cells, feces, gametes) can be retrieved from seawater and used in quantitative PCR (qPCR) assay or metabarcoding to identify organisms present in the study site. Because the eDNA approach has successfully been applied to various environments (river, lake, coastal area), it can also be considered a promising tool for marine ecosystems. This cruise's primary aim is to collect eDNA samples to analyze the fish community in the western subarctic North Pacific.

(2) Sampling

Seawater samples of eDNA were collected by the surface bucket sampling (all stations) and 12 liter Niskin bottles mounted on the CTD/Carousel Water Sampling System at the depths of 10m, 50m, and 100m (Sta.11 (K2), Cast.3), and brought the total to 36. Seawater from bucket or Niskin bottle was transferred into 10 L polyethylene bag rinsed with same water three times. Seawater sample is vacuum-filtered using 0.45 μm Sterivex^{TM}-HV PVDF filters (Millipore) with a suction filtration pump (Merck, Ez-Stream) or an aspirator (As-one, GAS-1N). After filtrating, filters are filled with 1.6 ml of RNAlater and preserved at ~ -20 °C cold until analysis in our land laboratory. Before use, all equipment were washed using bleach solution. These samples will be the subject of metabarcoding analysis to clarify the species composition of fishes.

(3) Preliminary result

The vertical distributions of eDNA will be determined as soon as possible after this cruise.

(4) Data archive

These obtained data will be submitted to JAMSTEC Data Management Group (DMG).

2.3.13 Nitrogen isotope of nitrate

Akiko MAKABE **JAMSTEC**
Masahide WAKITA **JAMSTEC**
Chisato YOSHIKAWA **JAMSTEC**

(1) Objective

Nitrate is one of the major nutrients in the ocean. Both nitrogen and oxygen isotopic compositions of nitrate are known to be a powerful tool to trace nitrogen dynamics, such as nitrogen fixation, assimilation, nitrification, and denitrification in the ocean. The oxygen isotopic composition of nitrate is also useful to estimate contribution of atmospheric deposition to nitrogen source in the surface ocean. To understand the nitrogen cycle in the western North Pacific, we will determine the δ^{15}NNitrate and δ18ONitrate values there.

(2) Methods, Apparatus and Performance

(2-1) Seawater sampling

Seawater samples were collected by the rosette-mounted 12 liter of Niskin bottles and a bucket at K2 station. In addition, samples were collected from the surface layer of the underway 15 stations using a bucket or continuous sea surface monitoring system. Seawater was sampled in a 15 mL or 50 mL plastic bottle through an in-line filter cartridge with GF/F filter. Samples were preserved at -20℃ until isotopic analysis.

(2-2) Seawater analysis

Nitrogen and oxygen isotopic compositions of nitrate will be measured by the denitrifier method (Sigman et al. 2001, Casciotti et al. 2002) after removal of nitrite with sulfamic acid (Granger and Sigman, 2009). Briefly, nitrate is converted to N_2O by a denitrifying bacteria that lack N_2O-reductase activity. The produced N_2O is then analyzed using a ThermoFinnigan GasBench + PreCon trace gas concentration system interfaced to a ThermoScientific Delta V Plus isotope-ratio mass spectrometer at JAMSTEC.

(3) References

Granger J., and D. M. Sigman (2009), Removal of nitrite with sulfamic acid for nitrate N and O isotope analysis with the denitrifier method. Rapid Commun. Mass Spectrom., 23, 3753–3762.

Sigman, D. M., K. L. Casciotti, M. Andreani, C. Barford, M. Galanter, and J. K. Böhlke (2001), A bacterial method for the nitrogen isotopic analysis of nitrate in seawater and freshwater. Analytical Chemistry, 73(17), 4145–4153.

Casciotti, K. L., D. M. Sigman, M. G. Hastings, J. K. Böhlke, and A. Hilkert (2002), Measurement of the Oxygen Isotopic Composition of Nitrate in Seawater and Freshwater Using the Denitrifier Method, Analytical Chemistry, 74(19), 4905-4912.

2.3.14 Fluorescent dissolved organic matter

Masahito SHIGEMITSU **JAMSTEC**
Masahide WAKITA **JAMSTEC**

(1) Objective

In situ fluorometers (Seapoint UV fluorometer, Seapoint) for measuring chromophoric dissolved organic matter were attached on CTD, POPPS, and RAS systems in this cruise. In order to calibrate the fluorometers, seawater samples were collected for measurement of fluorescent dissolved organic matter (FDOM).

(2) Material and method

(2)-1 Seawater sampling

Seawater samples were filtered in the same way as DOC, and the filtrates were collected into acid-washed and pre-combusted glass vials with acid-washed Teflon®-lined caps after triple rinsing. Then, the samples were stored frozen in the dark until analysis on land.

(2)-2 Seawater analysis

Excitation-emission matrix (EEM) fluorescence spectra will be measured in a land laboratory using the Horiba Scientific Aqualog after the samples are acclimated to laboratory temperature in the dark. Emission scans from 248 to 829 nm will be obtained at 2.33 nm intervals for performing sequential excitation from 240 and 560 nm at 5 nm intervals by using an integration time of 12 s and employing the high charge-coupled device (CCD) gain mode. Blank subtraction and normalization of fluorescence intensities to Raman Units (RU) (Lawaetz and Stedmon, 2009) will also be carried out as post-measurement steps. The excitation and emission wavelengths of the fluorometers are 370 nm and 440 nm, respectively. Thus, the fluorescence intensities for EEMs corresponding to those obtained by the fluorometers will be interpolated between excitation/emission wavelength pairs of 370/439.281 nm and 370/441.590 nm, and be used to calibrate the data collected by the fluorometers as in Shigemitsu et al. (2020).

(3) Reference

Lawaetz, A.J., and C.A. Stedmon (2009). Fluorescence intensity calibration using the Raman scatter peak of water. Appl. Spectrosc. 63(8), 936-940.

Shigemitsu, M., H. Uchida, T. Yokokawa, K. Arulananthan, and A. Murata (2020). Determining the distribution of fluorescent organic matter in the Indian Ocean using in situ fluorometry. Front. Microbiol. 11:589262, doi: 10.3389/fmicb.2020.589262.

2.4 Biological oceanography

2.4.1 Phytoplankton pigments

Tetsuichi FUJIKI	**JAMSTEC**	**PI**
Kazuhiko MATSUMOTO	**JAMSTEC**	
Hiroaki SAKOH	**MWJ**	**Operation leader**
Riho FUJIOKA	**MWJ**	

(1) Objective

Phytoplankton biomass can estimate as the concentration of chlorophyll *a*, because all oxygenic photosynthetic plankton contain chlorophyll *a*. The objective of this study is to investigate the vertical distribution of phytoplankton biomass and size as chlorophyll *a* by using the fluorometric determination.

Furthermore, the chemotaxonomic assessment of phytoplankton populations present in natural seawater requires taxon-specific algal pigments as good biochemical markers. In this cruise, we collect samples to investigate the marine phytoplankton community structure by the marine phytoplankton pigments measured by using the high-performance liquid chromatography (HPLC).

(2) Parameters

Total chlorophyll *a*, Size-fractionated chlorophyll *a*, Phytoplankton pigments

(3) Instruments and Methods

We collected 500ml seawater samples for total chlorophyll *a* from 3 to 18 depths and 1000ml seawater samples for size-fractionated chlorophyll *a* from 12 to 13 depths between the surface (bucket) and 300 dbar depth (Niskin-X) including a subsurface chlorophyll *a* maximum (SCM). The SCM was determined by a Chlorophyll Fluorometer (Seapoint Sensors, Inc.) attached to the CTD system. 500ml seawater samples for total chlorophyll *a* were vacuum-filtrated (< 0.02 MPa) through the 25mm-diameter glass microfiber filter (Whatman GF/F) and 1000ml seawater samples for size-fractionated chlorophll *a* were passed through 10 μm, 3 μm and 1 μm pore-size 47mm-diameter polyester track etched membrane filters, and the 25mm-diameter glass microfiber filter (Whatman GF/F). Phytoplankton pigments retained on the filters were extracted in a polypropylene tube with 7 ml of N,N-dimethylformamide (FUJIFILM Wako Pure Chemical Corporation Ltd.) (Suzuki and Ishimaru, 1990). The tubes were stored at -20 °C under the dark condition to extract chlorophyll *a* at least for 24 hours. Some tubes were kept at -80°C under the dark condition until the extraction. Chlorophyll *a* concentrations were measured by the fluorometer (10-AU, TURNER DESIGNS). Before the chlorophyll *a* measurement of seawater samples, a fluorometer was calibrated on board against a pure chlorophyll *a* (Sigma-Aldrich Co., LLC). To estimate the chlorophyll *a* concentrations, we applied the fluorometric "Non-acidification method" (Welschmeyer, 1994). For HPLC measurements of marine phytoplankton pigments, we collected 2000ml seawater samples from 3 to 13 depths between the surface (bucket) and 200 dbar depth (Niskin-X) including a subsurface chlorophyll *a* maximum (SCM). 2000ml seawater samples were vacuum-filtrated (< 0.02 MPa) through the 47mm-diameter glass microfiber filter (Whatman GF/F). The sample filters were vacuum-dried in a freezer (0 °C) for at least 2 hours. For measurement, these samples were kept at -80°C under the dark condition.

(4) Station list

The number of samples, stations and the sampling positions were shown in fig. 2.4.1 and Table 2.4.2.

(5) Preliminary Results

At each station, water samples were taken in replicate for random layer. Results of replicate sample measurements were shown in table 2.4.1. As the typical example, vertical distributions of chlorophyll *a* concentrations at all stations except PE cast are shown from Fig.2.4.2 to Fig.2.4.4. The compositions of

size-fractionated chlorophyll *a* concentration in each depths at St.5 (KEO) and St.11 (K2) are shown in Fig.2.4.5 and Fig2.4.6, respectively.

(6) Data archives

These data obtained in this cruise will be submitted to the Data Management Group of JAMSTEC, and will be opened to the public via "Data Research System for Whole Cruise Information in JAMSTEC (DARWIN)" in JAMSTEC web site.

http://www.godac.jamstec.go.jp/darwin/e

(7) Reference

Suzuki, R., and T. Ishimaru (1990), An improved method for the determination of phytoplankton chlorophyll using N, N-dimethylformamide, *J. Oceanogr. Soc. Japan*, 46, 190-194.

Welschmeyer, N. A. (1994), Fluorometric analysis of chlrophyll *a* in the presence of chlorophyll *b* and pheopigments. *Limnol. Oceanogr.* 39, 1985-1992.

Table 2.4.1. Results of the chlorophyll *a* replicate sample measurement with fluorometry.

	All samples
Number of replicate sample pairs	50
Standard deviation (μg L^{-1})	0.022

Table 2.4.2. The number of samples at each station (St.)

Date	St.	Cast	Number of samples		
			Total chlorophyll *a*	Size-fractionated chlorophyll *a*	HPLC
2022/4/17	001	002	16	-	6
2022/4/18	002	001	16	-	6
2022/4/18	PE1	001	9	-	3
2022/4/19	003	001	16	-	6
2022/4/19	PE2	001	9	-	3
2022/4/20	004	001	9	-	3
2022/4/21	004	002	16	-	9
2022/4/21	PE4	001	9	-	3
2022/4/23	005	001	9	-	3
2022/4/23	005	003	16	12	12
2022/4/24	006	001	16	-	2
2022/4/25	007	001	16	-	2
2022/4/26	008	001	16	-	-
2022/4/28	009	001	18	-	3
2022/4/29	010	001	16	-	-
2022/5/2	011	002	16	-	-
2022/5/3	011	003	24	13	13
2022/5/8	012	001	16	-	1
2022/5/12	013	001	20	-	9
2022/5/15	014	001	16	-	-
2022/5/15	015	001	12	-	-

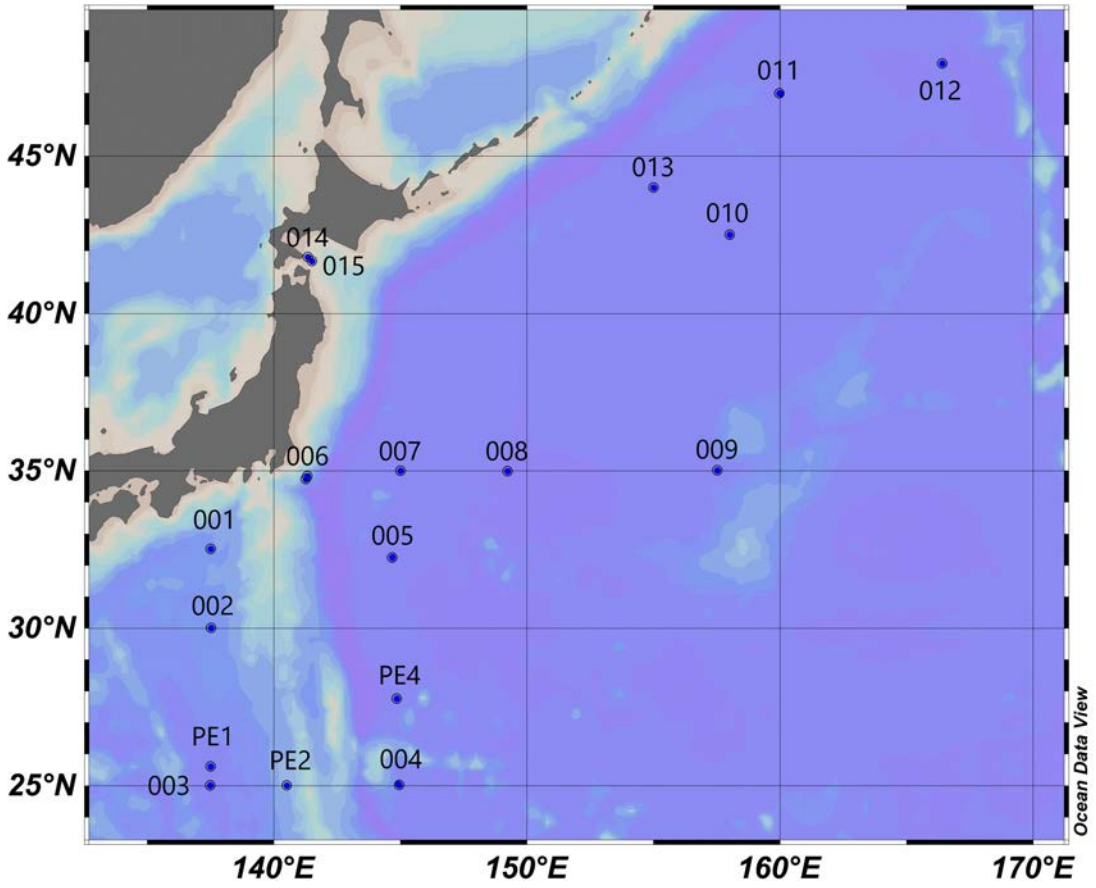

Figure 2.4.1. Sampling position of phytoplankton pigments samples in MR22-03.

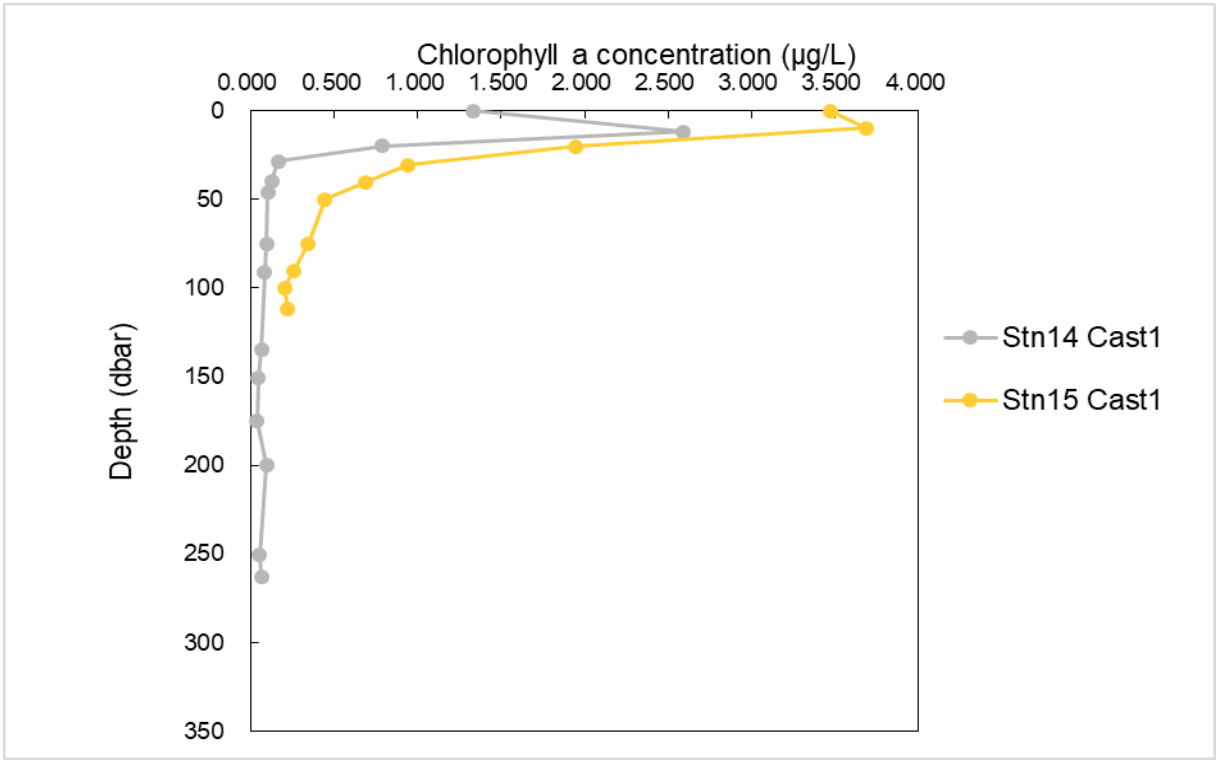

Figure 2.4.2. Vertical distribution of chlorophyll *a* from station 1 to13 except PE and size-fractionation sampling (St.5 cast3 and St.11 cast3) cast.

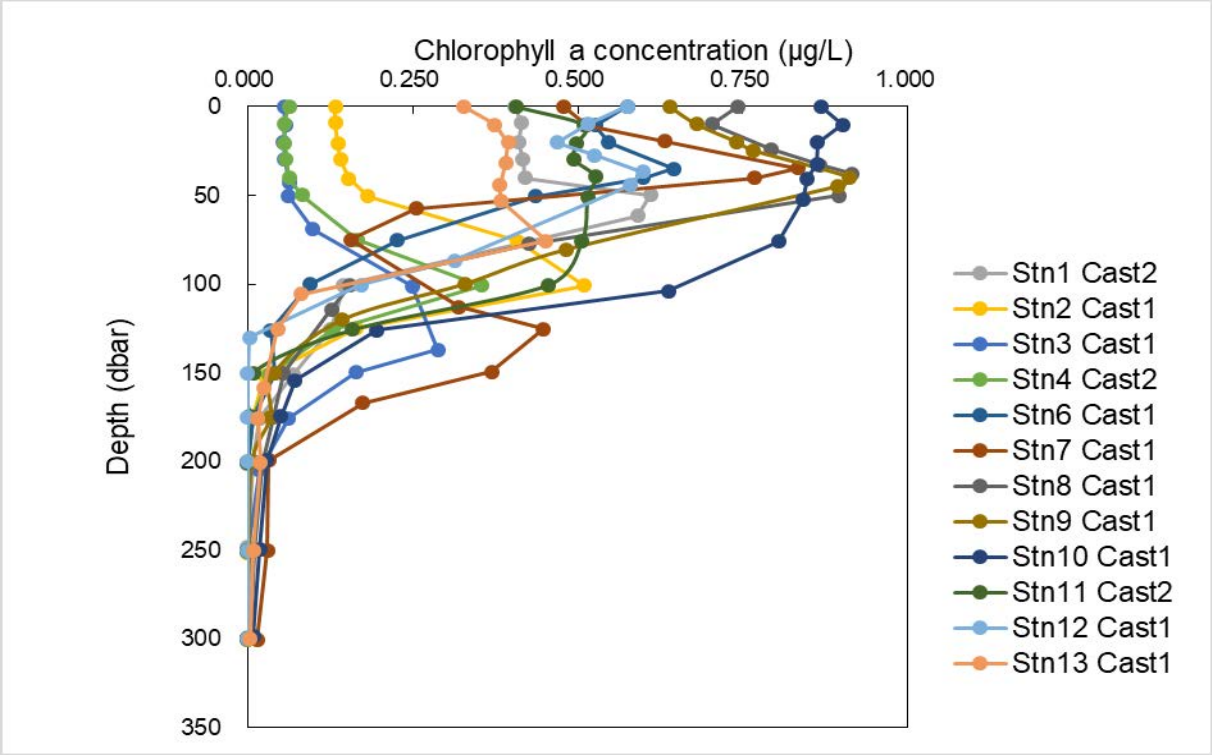

Figure 2.4.3. Vertical distribution of chlorophyll *a* at St.14 and St.15.

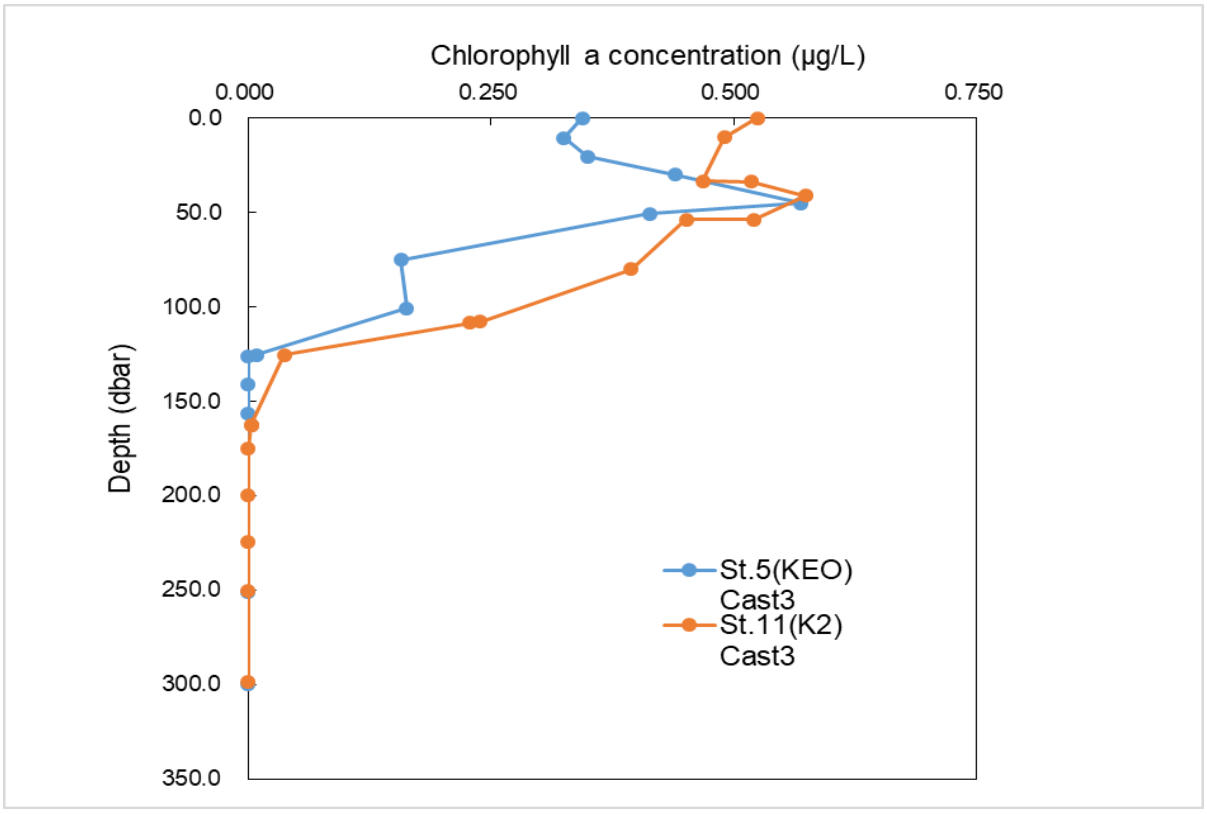

Figure 2.4.4. Vertical distribution of chlorophyll *a* at St.5 (KEO), and St.11 (K2).

Figure 2.4.5. Compositions of size-fractionated chlorophyll *a* concentration at St.5 (KEO).

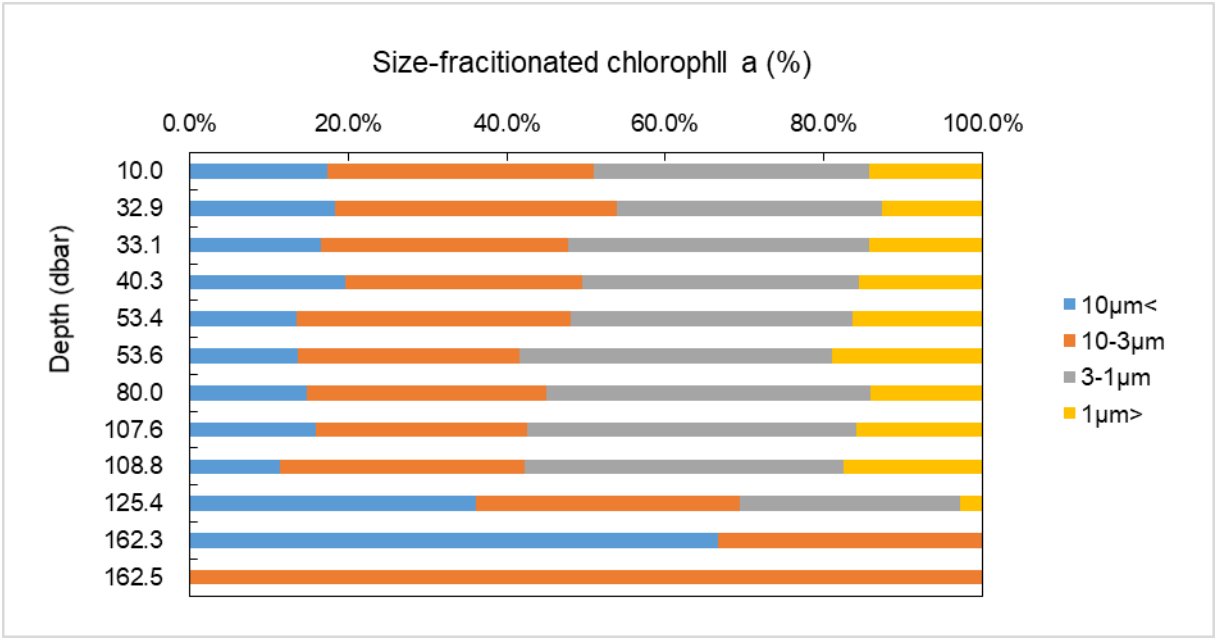

Figure 2.4.6. Compositions of size-fractionated chlorophyll *a* concentration at St.11 (K2).

2.4.2 Primary productivity

Takuhei SHIOZAKI **Atmosphere and Ocean Research Institute, The University of Tokyo** **PI**
Qin HONG-WEI **Atmosphere and Ocean Research Institute, The University of Tokyo**

(1) Objectives
Water samples were collected by a bucket and Niskin bottles to examine the primary production.

(2) Parameters
Primary production
Particulate organic carbon / nitrogen (POC/N)
Size fractionated chlorophyll *a* (>3 μm and 0.2–3 μm)
Size fractionated DNA (>3 μm and 0.2–3 μm)

(3) Instruments and methods
Water samples have been collected in five different depths based on 100, 25,10,1, and 0.1% of surface light intensity at all station except station 3 and 15. The light profile was determined by a CTD-attached PAR sensor just before the CTD water sampling. The water samples of 100% light intensity were collected in the sea surface by a bucket.

Samples for primary production were collected duplicate by using 1.2L polycarbonate bottles. They were then added ^{13}C-labeled sodium bicarbonate at a final concentration of 200 μmol L^{-1}. The bottles would be covered with different neutral-density screens to adjust the light intensity and incubated for 24 h in an on-deck incubator which filled with flowing surface seawater. Incubations were terminated by filtration onto pre-combusted (450°C, 6h) GF/F filters. Samples for POC/N (2 L) were also filtered onto pre-combusted GF/F filters. Samples for size fractionated DNA (2.3 L) and chlorophyll *a* (0.5L) were sequentially filtered onto 3- and 0.2-μm filters. The filters for DNA were stored at a freezer until onshore analysis. The chlorophyll a concentrations were measured fluorometrically using a Turner Design 10-AU fluorometer after extraction with N', N'-dimethylformamide on board.

(4) Data archives
These data obtained in this cruise will be submitted to the Data Management Group of JAMSTEC when ready.

2.4.3 Photosynthesis–irradiance parameters of phytoplankton

Kazuhiko MATSUMOTO **JAMSTEC**
Fumikazu TAKETANI **JAMSTEC**
Yoshihisa MINO **Nagoya university**
Misato KUWAHARA **MWJ**

(1) Objectives
Atmospheric deposition is expected to be an important source of limiting nutrients to the ocean, potentially stimulating marine primary productivity. To investigate the impact of atmospheric deposition, photosynthetic characteristics of marine phytoplankton are estimated by the photosynthesis–irradiance (P–E) experiment.

(2) Methods and Instruments
(2-1) Sampling
Seawater samples were collected at three depths using Niskin-X bottles installed acid-cleaned O-ring and a bucket. Sampling logs are listed in Table 2.4.3.

(2-2) Incubation
Seawater samples were transferred into eight acid-cleaned, transparent bottles. Rainwater addition experiments were conducted at some stations. Just before the incubation, $NaH^{13}CO_3$ was added to each bottle at a final concentration of 0.2 mM, sufficient to enrich the bicarbonate concentration by about 10%. The time-zero samples were filtered immediately after the addition of ^{13}C solution. Photosynthesis–irradiance (P–E) parameters were estimated by the carbon uptake experiments in laboratory. Three incubators were filled with water, and their water temperature were controlled appropriately by water chillers. Each incubator was illuminated at one end by a 500W halogen lamp attached infrared cut-off filter, and bottles were arranged linearly against the lamp and controlled light intensity by shielding with a neutral density filter on lamp side. Incubations were conducted for 3 h during daytime.

(2-3) Measurement
After the incubation, water samples were immediately filtered through a pre-combusted GF/F filter, then the filters were dehydrated in a dry oven (40 ºC), and the remained inorganic carbon in the filter was removed by fuming HCl. The incorporation of inorganic ^{13}C content of the particulate fraction will be measured with an automatic nitrogen and carbon analyzer mass spectrometer (SerCon, Ltd., UK) based on the method of Hama et al. (1983) on land. The analytical function and parameter values used to describe the relationship between the photosynthetic rate (P) and scalar irradiance (E) are best determined using a least-squares procedure from the following equation (Platt et al., 1980).

$$P = P_{max}(1-e^{-\alpha E/Pmax})e^{-b\alpha E/Pmax}$$

where, P_{max} is the light-saturated maximum photosynthetic rate, α is the initial slope of the P vs. E curve, b is a dimensionless photoinhibition parameter. The chl *a*-specific, light absorption coefficient spectrum of phytoplankton were measured using a quantitative filter technique (QFT) method (Kishino et al., 1985), then the P–E data have been corrected for the spectrum of the lamp source following the method of Kyewalyanga et al. (1997).

As for the surface sample, the maximum photochemical quantum efficiency of photosystem II of phytoplankton was measured by using a fast repetition rate (FRR) fluorometer to examine a change in their photo-physiological state during incubation.

(3) Data archive

The data obtained during this cruise will be submitted to JAMSTEC Data Management Group (DMG).

(4) References

Hama T, Miyazaki T, Ogawa Y, Iwakuma T, Takahashi M, Otsuki A, Ichimura S (1983), Measurement of photosynthetic production of a marine phytoplankton population using a stable 13C isotope. Marine Biology 73: 31-36.

Platt T, Gallegos CL, Harrison WG (1980), Photoinhibition of photosynthesis in natural assemblages of marine phytoplankton. Journal of Marine Research 38: 687-701.

Kishino, M., M. Takahashi, N. Okami, and S. Ichimura (1985), Estimation of the spectral absorption coefficients of phytoplankton in the sea, Bulletin of Marine Science, 37, 634-642.

Kyewalyanga, M. N., T. Platt, and S. Sathyendranath (1997), Estimation of the photosynthetic action spectrum: implication for primary production models, Marine Ecology Progress Series, 146: 207-223.

Table 2.4.3 Sampling locations for P–E experiment

Station	Date Collected (UTC)		Latitude		Longitude	
	Date	Time	Deg.	N/S	Deg.	E/W
PE1*	2022/4/18	21:35	25.6094	N	137.499	E
PE2*	2022/4/19	21:37	25.0004	N	140.4991	E
PE3 (004)*	2022/4/20	20:42	25.0176	N	144.9463	E
RC1*	2022/4/21	10:00	25.7407	N	145.1404	E
PE4*	2022/4/21	20:38	27.7621	N	144.8561	E
PE5 (005)*	2022/4/22	20:40	32.2579	N	144.6726	E
PE6 (009)	2022/4/28	0:22	35.0145	N	157.5129	E
PE7 (011)	2022/5/3	19:41	46.9998	N	160.0002	E
PE8 (012)	2022/5/8	3:01	47.9519	N	166.4092	E
PE9 (013)	2022/5/11	22:42	43.9979	N	155.0042	E

*FRRF measurements were also conducted.

2.4.4 Assessment of algal photosynthesis in planktic foraminifera

Tetsuichi FUJIKI **JAMSTEC**
Katsunori KIMOTO **JAMSTEC**

(1) Objective

Symbiont-bearing planktic foraminifers are widely distributed in the euphotic zone of the tropical and subtropical ocean. The paradigm for the symbiosis is that the algae supply photosynthates to the host foraminifer, and in return the host provides the symbionts with nutrients and carbon dioxide generated through its catabolic pathways (Anderson and Bé 1976). The host–symbiont relationship is probably a strategy for survival of these organisms in oligotrophic environments. However, despite the fact that the relationship between host foraminifers and symbiotic algae has been studied for more than 40 years, it has not been well understood because of the small size of the host foraminifers and the difficulty of measuring the biomass and photosynthetic activity of the symbiotic algae within the host.

Since the late 1990s, fast repetition rate (FRR) fluorometry has been used widely as a convenient technique to assess phytoplankton productivity (Kolber et al.1998; Suggett et al. 2001). FRR fluorometry involves optical measurement of a single-turnover fluorescence induction curve in photosystem II (PSII) and can provide information about the biomass and photosynthetic activity of an organism. An advantage of FRR fluorometry is that measurements can be carried out rapidly and non-destructively without the use of chemicals. The method can therefore be used to make continuous measurements of the biomass and photosynthetic activity of an organism.

In this study, we used FRR fluorometry to measure the biomass and photosynthetic activity of symbiotic algae within foraminifers and examined the host–symbiont relationship between foraminifers and algae.

(2) Sampling and measurements

Sampling was conducted by the NORPAC net vertically from a depth of 150 m to the surface at stations 1- 6 in the subtropical region of the western North Pacific. A stereomicroscope was used to isolate symbiont-bearing foraminifers from the particles collected by the NORPAC net, and the foraminifers were transferred to 12-well plates filled with seawater that had been passed through a membrane filter (0.45 mm pore size).

To make FRR fluorometric measurements on the symbiotic algae within an individual foraminifer, we transferred a host cell into a custom-built quartz glass cuvette and placed the cuvette in the measurement position of an FRR fluorometer (DF-14; Kimoto Electric). To generate a PSII fluorescence induction curve for the symbiotic algae, the foraminifer in the cuvette was exposed to a series of blue light excitation flashes. The fluorescence signal from the symbiotic algae was detected by a photomultiplier tube. The PSII parameters were calculated by fitting the PSII induction curve to the numerical model described by Kolber et al. (1998). Details about the instrument and measurement protocol were described by Fujiki et al. (2014).

(3) References

Anderson OR, Bé AWH (1976) The ultrastructure of a planktonic foraminifer, *Globigerinoides sacculifer* (Brady), and its symbiotic dinoflagellates. J Foram Res 6:1–21.

Fujiki T, Takagi H, Kimoto K, Kurasawa A., Yuasa T, Mino Y (2014) Assessment of algal photosynthesis in planktic foraminifers by fast repetition rate fluorometry. J Plankton Res 36:1403–1407.

Kolber ZS, Prášil O, Falkowski PG (1998) Measurements of variable chlorophyll fluorescence using fast repetition rate techniques: defining methodology and experimental protocols. Biochim Biophys Acta 1367:88–106.

Suggett D, Kraay G, Holligan P, Davey M, Aiken J, Geider R (2001) Assessment of photosynthesis in a spring cyanobacterial bloom by use of a fast repetition rate fluorometer. Limnol Oceanogr 46:802–810.

2.4.5 Effect of ammonia on phytoplankton

Masatoshi KISHI JAMSTEC

(1) Objectives

Ammonia is one of the primary sources of nitrogen for phytoplankton production and can be provided to the marine environment through regeneration, precipitation, and anthropogenic activities. While low concentrations of ammonia can enhance the photosynthesis especially at nutrient-depleted areas, a high concentration can negatively affect the growth of phytoplankton owing to the strong toxicity of free ammonia (NH_3). Since the ammonia tolerance differs depending on the types of phytoplankton, the responses towards ammonia provision may differ across various regions. Therefore, this study evaluated the effect of ammonia on algal photosynthetic activities in various areas in the north Pacific.

(2) Parameters

FRRf
Chlorophyll fluorescence
pH
Phytoplankton community (Sta. 3 and the latter)
Nutrients (Sta. 6 and the latter)
Chlorophyll *a* (Sta. 11, 13, and 14)

(3) Instruments and methods

Seawater samples were collected at 25% optical depth using Niskin bottles with cleaned Viton O-ring at 9 stations (Table 2.4.5.1). The water samples taken before noon were immediately used for the incubation experiments, while those taken after noon were stored under dark at *in-situ* temperatures until the next morning.

Incubation experiments were conducted using semi-transparent 125-mL LDPE Nalgene bottles with 80 mL of seawater samples. The incubation temperatures were decided based upon the sea surface temperature at each water collection. For Sta. 1 and 3, copper feeding test (3 to 5000 nM) was also conducted in addition to the ammonia feeding test without replicate (E1 in Table 2.4.5.1). For other stations, the ammonia feeding test was conducted with 6 concentrations (0, 0.5, 5, 50, 500, and 2500 μM) in triplicates (E2 in Table 2.4.5.1). Samples were taken at 0, 4-6, 10-12, and 24 hours for the measurements indicated above (cf. 2. Parameters).

Table 2.4.5.1. Sample collection areas and experimental conditions.

Area	Latitude	Longitude	Depth (m)	Date and Time of collection (UTC)	Incubation Temp. (°C)	Experimental category*
Sta. 01	32.31.26 N	137.29.90 E	37.3	2022 4 16 22:15	20	E1
Sta. 03	25.00.30 N	137.29.04 E	42.0	2022 4 19 07:30	25	E1
Sta. 04	25.00.93 N	144.57.13 E	48.4	2022 4 20 21:15	25	E2
Sta. 05	32.15.56 N	144.40.56 E	31.6	2022 4 22 21:40	20	E2
Sta. 06	34.49.09 N	141.19.20 E	29.8	2022 4 24 12:00	22	E2
Sta. 09	35.00.17 N	157.30.15 E	24.7	2022 4 28 03:50	18	E2
Sta. 11	47.00.01 N	159.59.97 E	32.8	2022 5 3 21:50	4.0	E2
Sta. 13	43.59.90 N	155.00.17 E	31.8	2022 5 12 01:52	7.0	E2
Sta. 14	41.48.01 N	141.20.48 E	27.6	2022 5 15 03:44	8.5	E2

*E1 constituted of both ammonia and copper feeding tests without replicate, while E2 comprised only of ammonia feeding tests with triplicates.

(4) Preliminary results

In most areas tested, varying ammonia concentration induced differential effect on phytoplankton community, resulting in higher growth than the control at low concentrations and reduced growth at high concentrations (e.g., Fig. 2.4.5.1).

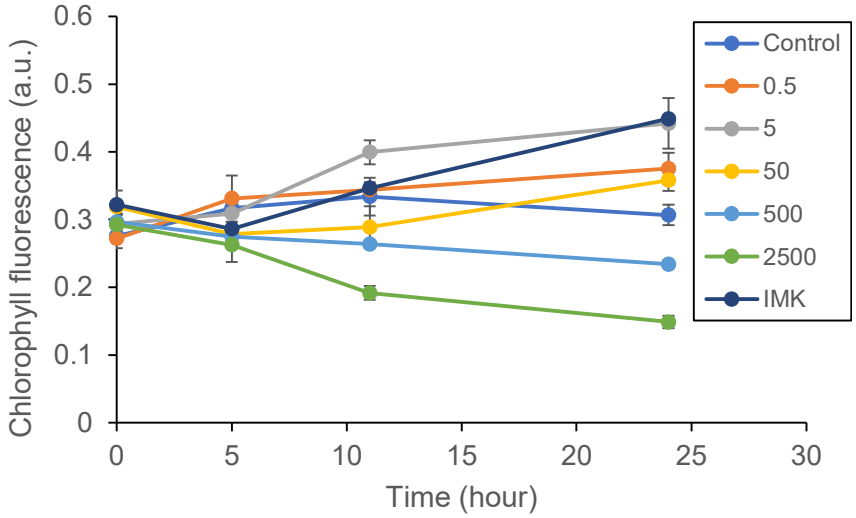

Fig. 2.4.5.1 Representative growth curves with the samples at Sta. 6. Numbers in the legend indicate the total ammonia concentration in micromolar. IMK indicates synthetic medium as a positive control.

Enhanced growth by ammonia feeding was apparent in southern regions such as Stas. 3, 4, 5, 6, and 9, where addition of 0.5 to 50 µM induced higher chlorophyll fluorescence than the control after a short cultivation (Fig. 2.4.5.2 a-e). On the other hand, not an apparent growth enhancement by ammonia feeding was observed in northern regions (i.e. Stas. 11, 13 and 14; Fig. 2.4.5.2 f-h), at which incubation temperature was as low as less than 10°C (Table 2.4.5.1).

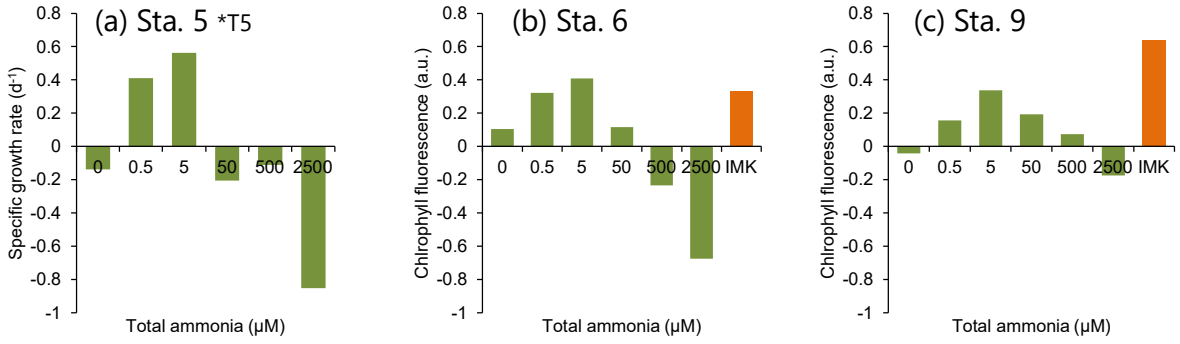

Fig. 2.4.5.2 Chlorophyll fluorescence after incubation with ammonia addition. The values were obtained after 24 hours of incubation (T24) except when otherwise noted.

For Stas. 5, 6, and 9, the final chlorophyll fluorescence was higher than the initial values at adequate ammonia concentrations. The maximum specific growth rates ranged between 0.33 and 0.56 d^{-1} in these areas (Fig. 2.4.5.3). While 50 µM inhibited the growth in Sta 5, phytoplankton community in Sta. 6 tolerated 50 µM, and that in Sta. 9 even tolerated 500 µM.

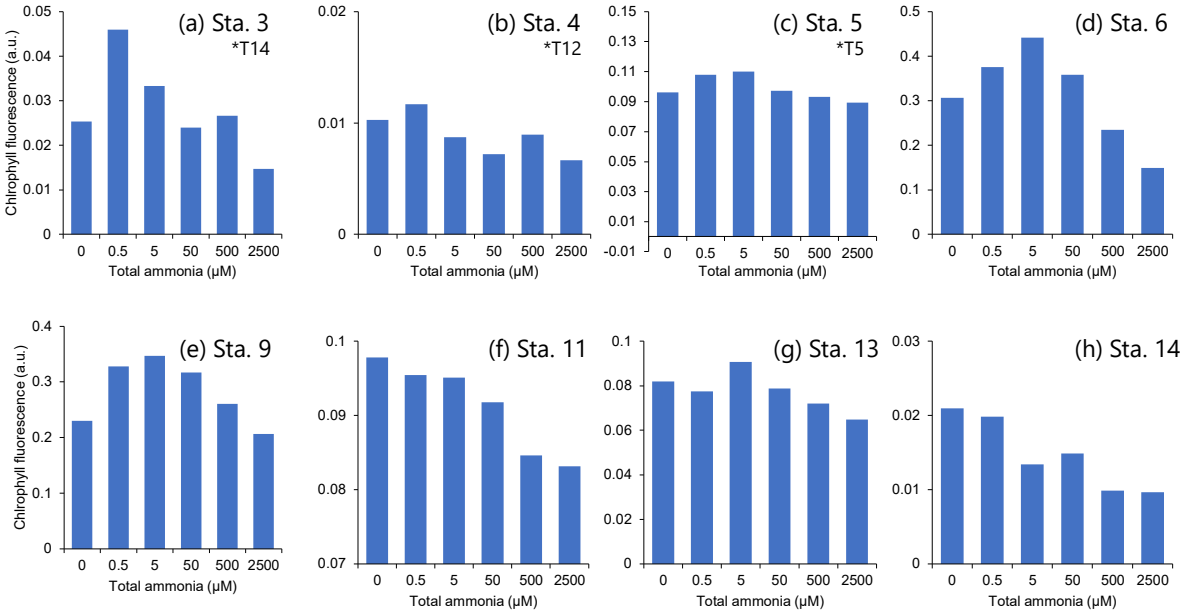

Fig. 2.4.5.3 Specific growth rates over the incubation with ammonia addition. The growth rate was calculated between the initial chlorophyll fluorescence and the last (T24) unless otherwise noted. IMK indicates addition of synthetic medium as a positive control.

Fluorescence response with FRRf and phytoplankton community analyses will be conducted to elucidate the mechanisms of the differential responses towards ammonia feeding in different regions.

(5) Data archives

Data obtained in this cruise will be submitted to the Data Management Group of JAMSTEC when ready.

2.4.6 Marine snow

Takuhei SHIOZAKI **Atmosphere and Ocean Research Institute, The University of Tokyo** **PI**
Qin HONG-WEI **Atmosphere and Ocean Research Institute, The University of Tokyo**

(1) Objectives
Sinking suspended particles were collected by Marine Snow Catcher (MSC) to examine the microbial community structures.

(2) Parameters
DNA
Particulate organic carbon / nitrogen (POC/N)
Size fractionated chlorophyll *a* (>3 μm and 0.2–3 μm)
Salinity
Nutrients

(3) Instruments and methods
During this cruise, two kinds of MSC were used (Normal and Giant) to collect sinking and suspended particles. Normal and giant MSC can collect 120 and 370 L seawater, respectively. Samples were collected from subsurface chlorophyll maximum (SCM) and 1000 m depth (except at St.14 where the sample was collected at 250 m) using Normal and Giant MSC, respectively at all stations except station 3 and 15. The MSC deployment was performed using the ship's A-frame. The speed of wire out is set to be 1.0 m s^{-1}. After reaching the desired depth, the MSC was closed using a messenger. After collecting the water sample, winch wire was wound up at 1.0 m s^{-1}. Both Normal and Giant MSC were kept on the deck for 2 hours to make the suspended and sinking particles separated, after 2 hours, samples would be collected.

Samples for DNA and POC/N were collected from the sinking fraction. From the suspended fraction, samples for size-fractionated DNA and chlorophyll *a*, POC/N, salinity, and nutrients were collected. The DNA in the sinking fraction were filtered onto 3-μm polycarbonate filters. The DNA and chlorophyll a in the suspended fraction were sequentially filtered onto 3- and 0.2-μm filters. Seawater samples for salinity and nutrients analysis were collected in 250 ml brown grass bottles and 10 mL acrylic tubes, respectively, and were immediately measured on board.

(4) Data archives
These data obtained in this cruise will be submitted to the Data Management Group of JAMSTEC when ready.

2.4.7 Particulate organic carbon

Yoshihisa MINO **Nagoya University**
Tetsuichi FUJIKI **JAMSTEC**

(1) Objective
A profile of the particulate organic carbon (POC) concentrations is determined in station K2 where BGC Argo float is deployed, in order to calibrate data from optical backscattering sensor attached to the float against POC measurements.

(2) Sampling
Approximately 2 to 4 liters of seawater were collected by CTD-CWS at the depths from surface to 2,000 m in station K2 and filtered through pre-combusted 25-mm diameter Whatman GF/F filters and the filters were kept frozen until POC analysis on shore.

(3) Analysis
The filter samples are exposed to HCl fumes overnight to remove carbonates, dried in vacuum, and then pelletized with a tin disk. The POC in the pellets is measured with an elemental analyzer (EA1110, Thermo Fisher Scientific) at Nagoya University.

(4) Data archive
Data will be submitted to JAMSTEC Data Management Group (DMG) within 2 years.

2.4.8 Zooplankton (planktic foraminifers, radiolarians, and thecosomatous pteropods)

Katsunori KIMOTO **JAMSTEC**
Tetsuichi FUJIKI **JAMSTEC**
Haruka TAKAGI **Chiba University**

(1) Objectives

The ocean has already absorbed about 30% of the total anthropogenic CO_2 (approximately 155 GtC) since the industrial revolution (IPCC AR5, 2013). This reduces ocean pH (Ocean acidification, OA) and causes wholescale shift in seawater carbonate chemistry. OA also give several impacts to the biological processes; one well-known effect is the lowering of calcium carbonate saturation state, which give negative impact to shell-forming marine organisms such as pteropods and planktic foraminifers etc. OA also affect zooplankton other than the shell-forming organisms, and characteristics of the zooplankton community will be changed. Therefore, we are observing long-term change of zooplankton biomass at K2 and adjacent areas in the North Pacific by using the plankton collecting apparatus and performing some biological/geochemical analysis to evaluate the biological impact to OA.

In this cruise, for better understanding of biological responses to carbonate saturation status, we aimed for following themes,

a) understanding vertical distributions of pteropods and planktonic foraminifer communities, and change of their shell densities with water depths,
b) clarifying population dynamics of planktic foraminifers with water depth in the North Pacific,
c) understanding phenotypic and genetic variabilities in the mixed layer for pteropods, and their population structure,
d) and investigate the photochemical systems and its relationship between photosymbiotic algae and host Rizalians (foraminifera and radiolarians) in the North Pacific.

(2) Methods

Zooplankton sampling was conducted at all stations (See Table 2.10.1). For the purpose (a), we collected specimens by using the Vertical Multi-depth Plankton Sampler (VMPS-3K, Tsurumi Seiki co., Ltd, Fig. 2.10.1). VMPS-3K equipped 2 or 3 plankton nets (63 μm mesh, NXX25), magnetic flow-meter, fluorometer (Wet Lab Inc.) and CTD sensors (Sea-bird Electrics), and was hauled vertically at a speed of 0.5 m/sec. Opening/closing of each net is electrically controlled from the lab on the ship, we can collect vertically stratified sample sets together with the environmental sensing data. Collected samples were immediately fixed by the ethanol (99.5 %) and stored in the refrigerator (~4 °C). For (b), planktic foraminifers were picked under the stereomicroscope and transported to the microslides with ethanol (99.5 %) and stored in the refrigerator (~ 4 °C). In those samples, some individuals of planktic foraminifer were fixed by 2.5 % glutarardehyde solution and stored in the refrigerator (~4°C) in order to observe the cell structures by TEM. For (c), a single NORPAC net (63 μm mesh, NXX25, 2m length) was vertically hauled. Living pteropods and foraminifers were immediately sorted under the stereomicroscope in the lab and fixed by 99.5 % EtOH, and then stored in the refrigerator at the 4°C temperature. Finally, for (d), some individuals of foraminifers and radiolarians were picked under the stereomicroscope and cleaned in the filtered seawater. They were stored in the RNA storage solution and kept in the deep freezer (-80°C).

(3) Onshore study in the future

Pteropod and planktonic foraminiferal shells will be analyzed by the Micro-focus X-ray CT (MXCT) equipped in JAMSTEC HQ in order to elucidate relationships between the multiple stressors (e.g. oceanic carbonate chemistry etc.) and individual shell morphology/density. For the population analysis of pteropods, DNA extraction from the preserved specimens and amplifying of gene sequences for the COI region of mtDNA will be performed. After the sequence alignments, population genetic analysis will be performed.

(4) Data Archive
All data will be submitted to JAMSTEC Data Management Office (DMO).

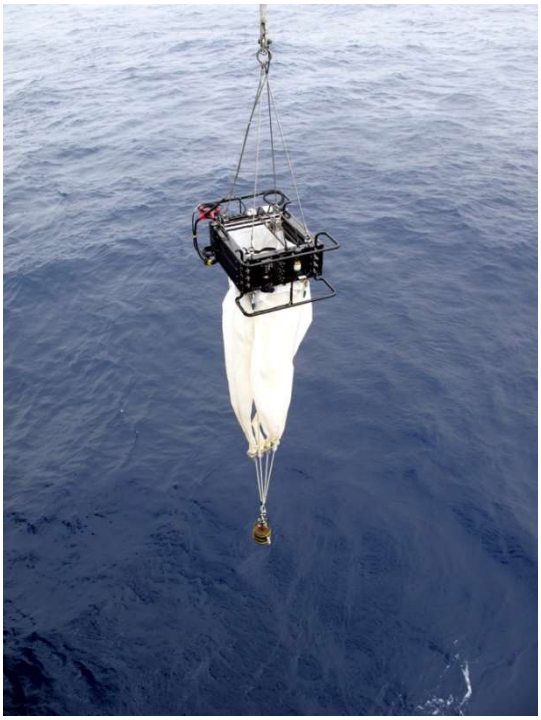

Fig. 2.4.8.1 The overview of VMPS (Vertical Multi-layer Plankton Sampler).

Table 2.4.8.1 Sampled locations and its detail during the MR22-03.

Station	Apparatus	Latitude			Longitude			Depth	Date		
Sta.1	NORPAC	32	31	N	137	30	E	0–150	2022	4	17
Sta.1	NORPAC	32	31	N	137	30	E	0–150	2022	4	17
Sta.1	NORPAC	32	31	N	137	30	E	0–150	2022	4	17
Sta.1	NORPAC	32	31	N	137	30	E	0–150	2022	4	17
Sta.2	NORPAC	30	00	N	137	31	E	0–150	2022	4	18
Sta.2	NORPAC	30	00	N	137	31	E	0–150	2022	4	18
Sta.2	NORPAC	30	00	N	137	31	E	0–150	2022	4	18
Sta.2	NORPAC	30	00	N	137	31	E	0–150	2022	4	18
Sta.3	NORPAC	25	00	N	137	30	E	0–150	2022	4	19
Sta.3	NORPAC	25	00	N	137	30	E	0–150	2022	4	19
Sta.3	NORPAC	25	00	N	137	30	E	0–150	2022	4	19
Sta.3	NORPAC	25	00	N	137	30	E	0–150	2022	4	19
Sta.4	NORPAC	25	02	N	144	56	E	0–150	2022	4	21
Sta.4	NORPAC	25	02	N	144	56	E	0–150	2022	4	21
Sta.4	NORPAC	25	02	N	144	56	E	0–150	2022	4	21
Sta.4	NORPAC	25	02	N	144	56	E	0–150	2022	4	21
Sta.5	NORPAC	32	15	N	144	41	E	0–150	2022	4	23
Sta.5	NORPAC	32	15	N	144	41	E	0–150	2022	4	23
Sta.5	NORPAC	32	15	N	144	41	E	0–150	2022	4	23
Sta.5	NORPAC	32	15	N	144	41	E	0–150	2022	4	23
Sta.6	NORPAC	35	00	N	141	00	E	0–150	2022	4	24
Sta.6	NORPAC	35	00	N	141	00	E	0–150	2022	4	24
Sta.6	NORPAC	35	00	N	141	00	E	0–150	2022	4	24
Sta.6	NORPAC	35	00	N	141	00	E	0–150	2022	4	24
Sta.7	NORPAC	35	00	N	145	00	E	0–150	2022	4	25
Sta.7	NORPAC	35	00	N	145	00	E	0–150	2022	4	25
Sta.7	NORPAC	35	00	N	145	00	E	0–150	2022	4	25
Sta.7	NORPAC	35	00	N	145	00	E	0–150	2022	4	25
Sta.8	NORPAC	34	59	N	149	10	E	0–150	2022	4	26
Sta.8	NORPAC	34	59	N	149	10	E	0–150	2022	4	26
Sta.8	NORPAC	34	59	N	149	10	E	0–150	2022	4	26
Sta.8	NORPAC	34	59	N	149	10	E	0–150	2022	4	26
Sta.9	VMPS	35	00	N	157	30	E	700–1000	2022	4	28
Sta.9	VMPS	35	00	N	157	30	E	500–700	2022	4	28
Sta.9	VMPS	35	00	N	157	30	E	300–500	2022	4	28
Sta.9	VMPS	35	00	N	157	30	E	150–300	2022	4	28
Sta.9	VMPS	35	00	N	157	30	E	30–150	2022	4	28
Sta.9	VMPS	35	00	N	157	30	E	0–30	2022	4	28

Table 2.4.8.1(continued) Sampled locations and its detail during the MR22-03.

Station	Apparatus	Latitude			Longitude			Depth	Date		
Sta.11(K2)	VMPS	47	00	N	160	00	E	700-1000	2022	5	4
Sta.11(K2)	VMPS	47	00	N	160	00	E	500-700	2022	5	4
Sta.11(K2)	VMPS	47	00	N	160	00	E	300-700	2022	5	4
Sta.11(K2)	VMPS	47	00	N	160	00	E	150-300	2022	5	4
Sta.11(K2)	VMPS	47	00	N	160	00	E	50-150	2022	5	4
Sta.11(K2)	VMPS	47	00	N	160	00	E	0-50	2022	5	5
Sta.11(K2)	NORPAC	47	00	N	160	00	E	0-150	2022	5	5
Sta.11(K2)	NORPAC	47	00	N	160	00	E	0-150	2022	5	5
Sta.11(K2)	NORPAC	47	00	N	160	00	E	0-150	2022	5	5
Sta.11(K2)	NORPAC	47	00	N	160	00	E	0-150	2022	5	8
Sta.12	VMPS	47	57	N	166	24	E	0-150	2022	5	8
Sta.12	VMPS	47	57	N	166	24	E	0-150	2022	5	8
Sta.12	VMPS	47	57	N	166	24	E	0-150	2022	5	8
Sta.12	VMPS	47	57	N	166	24	E	0-150	2022	5	12
Sta.13(KNOT)	VMPS	44	0	N	155	0	E	700-1000	2022	5	12
Sta.13(KNOT)	VMPS	44	0	N	155	0	E	500-700	2022	5	12
Sta.13(KNOT)	VMPS	44	0	N	155	0	E	300-500	2022	5	12
Sta.13(KNOT)	VMPS	44	0	N	155	0	E	150-300	2022	5	12
Sta.13(KNOT)	VMPS	44	0	N	155	0	E	50-150	2022	5	12
Sta.13(KNOT)	VMPS	44	0	N	155	0	E	0-50	2022	5	15
Sta.14	NORPAC	41	48	N	141	19	E	0-200	2022	5	15
Sta.14	NORPAC	41	48	N	141	19	E	0-200	2022	5	15
Sta.15	NORPAC	41	40	N	141	30	E	0-150	2022	5	16
Sta.15	NORPAC	41	40	N	141	30	E	0-150	2022	5	16

2.4.9 Bacteria

Masami ISHIDA **Tokyo University of Marine Science and Technology PI**
Kiminori SHITASHIMA **Tokyo University of Marine Science and Technology**
Mayu OHI **Tokyo University of Marine Science and Technology**

(1) Objective
The deep sea is a low-temperature, high-pressure environment, and many kinds of psychrophiles and piezophiles are inhabited in the deep sea. The final purpose of this study is to search for novel enzymes that degrade various ester compounds from psychrophiles and piezophiles, and to apply them to environmental conservation and industry.
In this voyage, the purpose is to isolate the psychrophiles and piezophiles inhabit in seawater collected from various depths of the survey area, and to search for novel ester-degrading enzymes.

(2) Methods
Seawater collected at each depth was kept at a low temperature and transferred to our laboratory. In order to concentrate bacteria in each seawater sample, the seawater samples were filtered with a membrane filter of 0.2 μm-pore size under decompression. A part of the concentrated liquid was smeared on nutrient marine agar MA media and cultured at a low temperature of 4°C to 10°C. For the rest of the concentrated liquid, glycerin was added and the mixture was cryopreserved at -80°C. Prepare a marine agar medium containing an ester-substrate EMA was prepared: the ester was used to examine the activity of degrading enzyme. Bacterial colonies obtained on the MA media was planted to the EMA media and cultured at low temperatures. Strains with clear zones around colonies were screened as candidates for strains with degradation activity of the objective ester.
The physiological properties of each candidate strain are analyzed. Each candidate strain is cultured in a liquid medium, and centrifuged to obtain supernatant containing the enzyme. The enzymatic properties such as temperature characteristics, pressure characteristics, and substrate specificity of the candidate enzymes are determined and compared each other. From these results, novel useful enzymes are selected.

(3) Parameters
Novel useful enzymes in seawater.

(4) Observation log
The seawater samples were collected form three layers (400m, 800m, 1000m) at twelve stations (St.1 ~ 11, St.13).

(5) Data archives
All data will be archived at Tokyo University of Marine Science and Technology after checking of data quality and submitted to Data Management Group (DMG) of JAMSTEC.

2.4.10. Marine gel particles derived from phytoplankton

Kazuhiko MATSUMOTO **JAMSTEC**
Kaori KAWANA **JAMSTEC**

(1) Objectives

Transparent exopolymer particles (TEP), i.e., polysaccharide-rich microgels that are produced primarily by the abiotic coagulation of phytoplankton exudates, are identifying as organic gels in the ocean interior. TEP is very sticky, and it aggregates with other suspended particles, resulting in the formation of sinking marine snow. In addition, TEP becomes enriched in the surface microlayer and expected to produce marine organic aerosol directly at the sea surface due to the interaction between wind and waves. To understand the processes of settling particles and organic aerosol formation, the concentrations of TEP are measured.

(2) Sampling and measurement procedure

Seawater samples were collected vertically with Niskin-X bottles and a bucket at the stations 005, 011 and 013. Samples were fixed with 1% (v/v) formalin and stored in refrigerator. The analyses will be conducted after the cruise on land as follows. The water samples of 200 mL are filtered onto 0.4-μm polycarbonate filters, and the filters are stained with 1 mL alcian blue solution which adjusted to pH 2.5 and rinsed thrice with 1 mL of Milli-Q water. Stained filter samples are stored in freezer until analysis. Filter samples are soaked for 2 - 5 h in 80% sulfuric acid (H_2SO_4) to elute the dye and then the absorbance of the solution is measured at 787 nm in a 1 cm cuvette. The calibration curve is produced by using a xanthan gum solution (XG, Sigma-Aldrich), and the TEP concentrations are represented as XG equivalent (Passow and Alldredge, 1995).

(3) Data archive

The data obtained during this cruise will be submitted to the JAMSTEC Data Management Group (DMG).

(4) Reference

Passow, U., and A. L. Alldredge (1995), A dye-binding assay for the spectrophotometric measurement of transparent exopolymer particles (TEP) in the ocean, Limnol. Oceanogr., 40(7): 1326-1335.

2.5 Hybrid profiling buoy system

2.5.1 Recovery and deployment

Tetsuichi FUJIKI **JAMSTEC**
Katsunori KIMOTO **JAMSTEC**
Minoru KITAMURA **JAMSTEC**
Masahide WAKITA **JAMSTEC**
Yoshiyuki NAKANO **JAMSTEC**
Kiminori SHITASHIMA **Tokyo University of Marine Science and Technology**
Yoshihisa MINO **Nagoya University**
Hiroki USHIROMURA **MWJ**
Masaki FURUHATA **MWJ**

Hybrid profiling buoy is combined two moorings, BGC mooring (biogeochemistry) and POPPS mooring (ocean productivity profiling system). We recovered Hybrid profiling buoy system at Station K-2 which were deployed at MR21-01 and deployed Hybrid profiling buoy system at Station K-2. Deployment operation took approximately 5 hours. After sinker was dropped, we positioned the mooring systems by measuring the slant ranges between research vessel and the acoustic releaser. The position of the mooring is finally determined as follow:

Table 2.5.1-1. Mooring positions of respective mooring systems.

	Recovery	Deployment
Mooring Number	K2H210223	K2H220507
Working Date	Feb. 23 2021	May. 07 2022
Latitude	47°00.19 N	47°00.33 N
Longitude	159°58.38 E	159°58.38 E
Sea Beam Depth	5,218 m	5,213 m

The deployment Hybrid profiling buoy consists of a top buoy with 24lbs (11kg) buoyancy, underwater winch, instruments, wire and ropes, recovery buoy with 496lbs (225kg) buoyancy, glass floats (Benthos 17" glass ball), dual releasers (Edgetech) and 4,911lbs (2,228kg) sinker. An ARGOS compact mooring locator was mounted on underwater winch, and a submersible recovery strobe was mounted on the top buoy. This mooring system was planned to keep the following time-series observational instruments are mounted approximately 130 m below sea surface. On the Hybrid profiling buoy, three Sediment Traps are installed on the 500 m, 1,000 m and 4,800 m. two Auto Sampling Systems (RAS) are installed on the 200 m and 300m. four Backscatter Meter are mounted on the SUS frame (175 m) and RAS(300m),, CTD (SBE-37) and Do Sensor (RINKO and Optode) are mounted on the dual acoustic releaser and inline SUS frame (175 m, 250 m and 780 m), Sediment Trap, RAS, underwater winch, top buoy. Details for each instrument are described below (section 2.5.3, 2.5.4, 2.5.5, 2.5.6, 2.5.7, 2.5.8, 2.5.9). Serial number of instruments are as follows:

Table 2.5.1-2. Serial numbers of instruments.

Recover			Deployment	
Station and type Mooring Number	K2 K2H210223		Station and type Mooring Number	K2 K2H220507
Top Buoy(130m) Iridium Transmiter Argos Transmitter Storobo FRRF (DF-14) PAR (QSP-2200) RINKO CTD (SBE19plusV2) Electorode pH sensor SUNA UV fluorometer	- ID:300025060204230 H12-009 (ID:197696) H12-010 780263013 20586 0277 19-7763 40145064001 NTR-1016 6238		Top Buoy(130m) Iridium Transmiter Argos Transmitter Storobo FRRF (DF-14) PAR (QSP-2200) RINKO CTD (SBE19plusV2) SUNA UV fluorometer ISFET pH/pCO2 sensor	Buoy03 ID:300025010934630 F01-38(ID:169773) E10-024 780265003 20623 0413 19-8008 NTR-1004 6223 -
Winch(150m) Argos Transmitter SBE37 OPTODE HpHS	- C01-081 2287 03 505063001		Winch(150m) Argos Transmitter SBE37 OPTODE	- C01-081 2287 03
SUS frame (175m) SBE37 OPTODE Backscatter Meter Underwater video system	SUS frame 1892 6 5167 1		SUS frame (175m) SBE37 OPTODE Backscatter Meter	SUS frame 1892 6 1741
RAS (200m) SBE37 OPTODE HpHS DEFI-D (Depth) UV fluorometer + RBR data logger	ML11241-10 2239 50 60100265002 0AGG026 6240 , 205142		RAS (200m) SBE37 OPTODE HpHS DEFI-D (Depth) UV fluorometer + RBR data logger	ML11241-09 2239 50 60100265001 0AGG026 6240,205142
SUS frame (225m) RINKO	SUS frame 0004		SUS frame (225m) SBE37 RINKO	SUS frame 2730 0004
SUS frame (250m) SBE37 RINKO	 2756 0092		SUS frame (250m) SBE37 RINKO	SUS frame 2756 0092
RAS (300m) SBE37 RINKO Backscatter Meter ISFET pH/pCO2	ML11241-11 2289, 051, 5168 pH:75-170 pH-F-1 pH:95-195 pH3’14T pCO2:100-199 pCO2 3’14		RAS (300m) SBE37 RINKO Backscatter Meter	ML11241-07 2289 051 1742

Table 2.5.1-2. continued

ADCP (370m) SBE37 OPTODE	1533 2288 9		ADCP (370m) SBE37 OPTODE	1434 2288 9
Sediment Trap, NGK (500m) SBE37 OPTODE	26S001 2748 10		Sediment Trap, NGK (500m) SBE37 OPTODE	26S029 2748 10
SUS frame (780m) SBE37 OPTODE	SUS frame 2738 5		SUS frame (780m) SBE37 OPTODE	SUS frame 2738 5
Sediment Trap, MARK7-21 (1000m) SBE37 RINKO ISFET pH/pCO2	ML10558-01 2285 7 pH:75-170 pH T-2 pH:98-200 pH 3-1 THR pCO2:90-200 pCO2 #3'T		Sediment Trap, MARK78H-21 (1000m) SBE37 RINKO	ML15362-02 2285 7
Sediment Trap, MARK7-21 (4800m)	ML11241-22		Sediment Trap, MARK78-H21 (4800m)	ML15362-01
Releaser Releaser SBE-37 CT sensor	27809 28533 2731 0744 , 0745		Releaser Releaser SBE-37	27824 34040 2731

Table 2.5.1-3. Recovery Hybrid profiling buoy system record.

Mooring Number	K2H210223				
Project	Time-Series		Depth	5,218.0	m
Area	North Pacific		Planned Depth	5,220.0	m
Station	K2		Length	5,089.8	m
Target Position	**47°00.35 N**		Depth of Buoy	130	m
	159°58.32 E		Period	1	year
ACOUCTIC RELEASERS					
Type	Edgetech		Edgetech		
Serial Number	28533		27809		
Receive F.	11.0	kHz	11.0	kHz	
Transmit F.	14.0	kHz	14.0	kHz	
RELEASE C.	**223307**		**344535**		
Enable C.	201054		360320		
Disable C.	201077		360366		
Battery	2 years		2 years		
Release Test	OK		OK		
RECOVERY					
Recorder	Masaki Furuhata		Work Distance	3	Nmile
Ship	R/V MIRAI		Send Enable C.	18:54	
Cruise No.	MR22-03		Releaser Depth	5168	m
Date	2022/5/2～5/3		Send Release C.	19:31	
Weather	O		Discovery Buoy	19:33	
Wave Hight	2.4	m	Pos. of Top Buoy	47-00.16	N
Seabeam Depth	-	m		159-57.87	E
Ship Heading	092	deg	Pos. of Start	47-00.39	N
Ship Ave.Speed	-	knot		159-57.61	E
Wind	< 097 deg > 7.9	m/s	Pos. of Finish	47-00.42	N
Current	< 001 deg > 0.1	cm/s		160-02.07	E

Table 2.5.1-4. Deployment Hybrid profiling buoy system record.

Mooring Number	K2H220507				
Project	Time-Series		Depth	5,213.0	m
Area	North Pacific		Planned Depth	5,220.0	m
Station	K2		Length	5,089.8	m
Target Position	**47°00.35 N**		Depth of Buoy	130	m
	159°58.32 E		Period	1	year
ACOUCTIC RELEASERS					
Type	Edgetech		Edgetech		
Serial Number	34040		27824		
Receive F.	11.0	kHz	11.0	kHz	
Transmit F.	14.0	kHz	14.0	kHz	
RELEASE C.	**233770**		**344674**		
Enable C.	221130		361121		
Disable C.	221155		361167		
Battery	4.5 years (lithiumBattery)		2 years		
Release Test	OK		OK		
DEPLOYMENT					
Recorder	Masaki Furuhata		Start	5.8	Nmile
Ship	R/V MIRAI		Overrun	500	m
Cruise No.	MR22-03		Let go Top Buoy	21:05	
Date	2022/5/6～5/7		Let go Anchor	00:56	
Weather	C		Sink Top Buoy	01:41	
Wave Hight	1.9	m	Pos. of Start	47-04.25	N
SeaBeam Depth	-	m		160-03.85	E
Ship Heading	225	deg	Pos. of Drop. Anc.	47-00.14	N
Ship Ave.Speed	-	knot		159-57.99	E
Wind	< 220 deg > 8.2	m/s	Pos. of Mooring	47-00.3280	N
Current	< 330 deg > 0.1	cm/s		159-58.3811	E

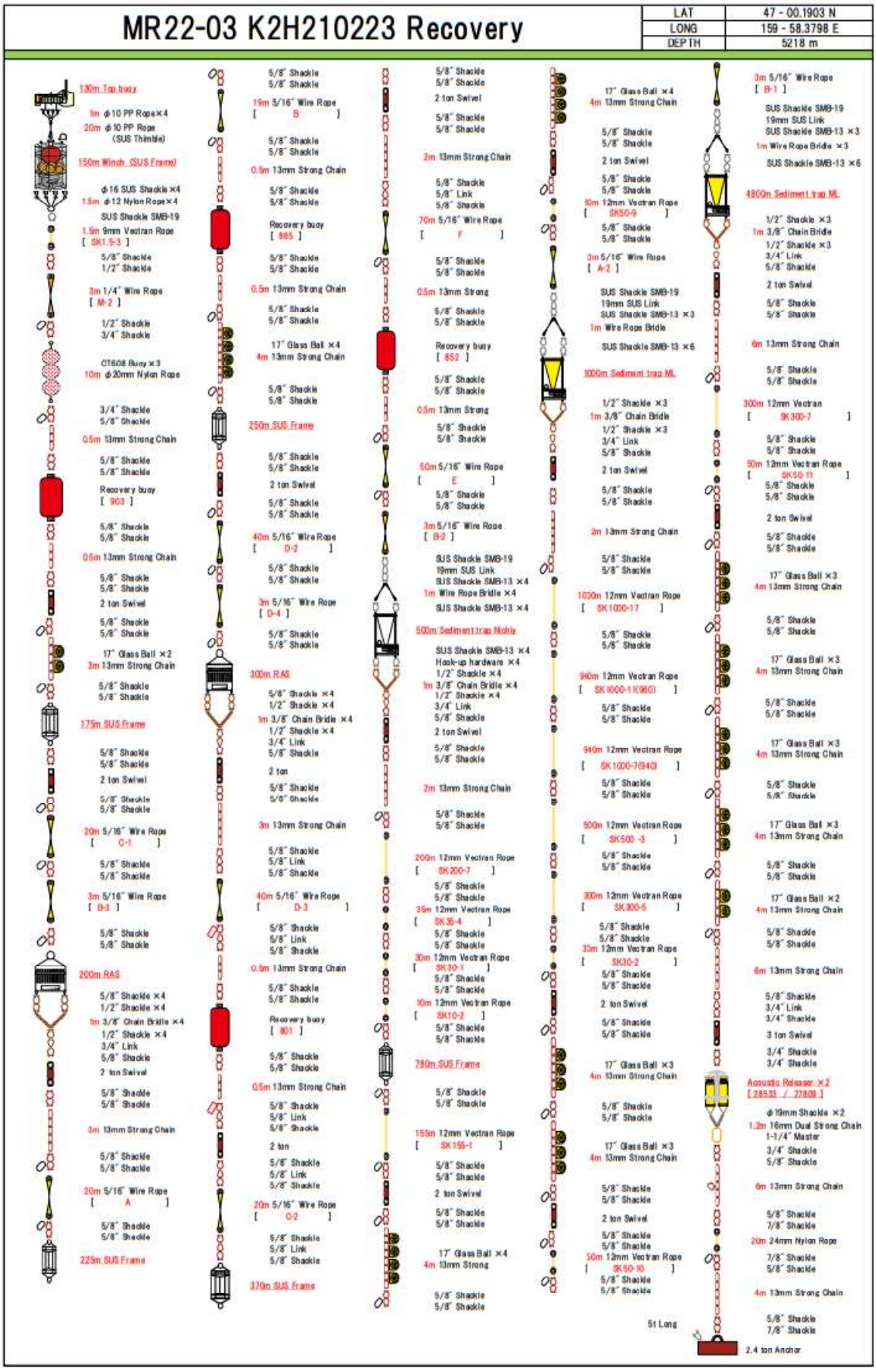

Figure 2.5.1-1. Hybrid profiling buoy system recovered.

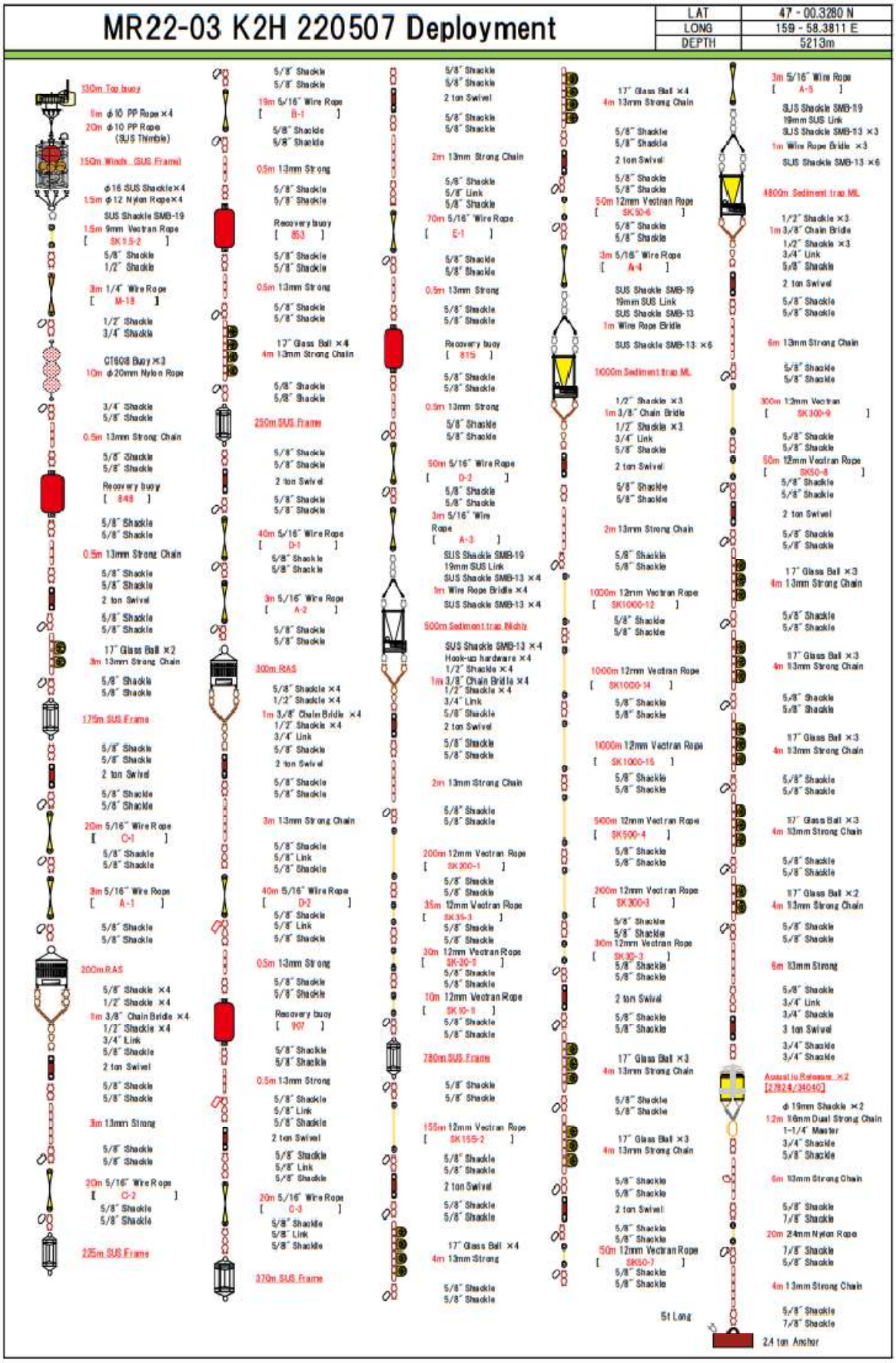

Figure 2.5.1-2. Hybrid profiling buoy system deployed.

2.5.2 Instruments and observation schedule

Tetsuichi FUJIKI	**JAMSTEC**
Katsunori KIMOTO	**JAMSTEC**
Minoru KITAMURA	**JAMSTEC**
Masahide WAKITA	**JAMSTEC**
Yoshiyuki NAKANO	**JAMSTEC**
Kiminori SHITASHIMA	**Tokyo University of Marine Science and Technology**
Yoshihisa MINO	**Nagoya University**
Hiroki USHIROMURA	**MWJ**
Masaki FURUHATA	**MWJ**

On mooring systems, instruments for details are as follows: *top buoy and underwater winch, RAS, Hybrid pH sensor, ADCP, Sediment trap, CTD, DO, Backscatter meter are described below (sections 2.5.3, 2.5.4, 2.5.5, 2.5.6, 2.5.7, 2.5.8, 2.5.9).

(1) ARGOS Beacon
The NOVATECH MMA-7500 ARGOS Beacon contains an ARGOS satellite transmitter designed as a ruggedized incident alerting system for oceanographic applications deployed anywhere in the world. It may be submerged for long periods in ocean depths to 7,500 m (24,000feet).

The device can be turned ON or OFF by triggering the internal reed switch with a magnet. The activation of the MMA-7500 is completely automatic and water sensor controlled. The water sensor is located in the antenna base – when submerged, the beacon goes into low-power hibernation mode.

The water sensor hysteresis is approx. 90 seconds. The beacon will continue to transmit for up to 90 seconds when submerged and will begin transmitting within 90 seconds of surfacing. At the surface the beacon transmits an ARGOS position data massage for 90 days.

(Specifications)

Transmitter Output:	1 watt	Harmonics:	-40 db minimum
Batteries:	8 CR123A Lithium cells	Battery Life:	90days at the surface
Operating Temp:	-40 ºC to +60ºC	Transmit Freq:	401.6300 MHz - 401.6800 MHz
Antenna:	Field replaceable 1/4 wave whip		
Max Depth:	7,500 m		
Weight:	in air 1.25lbs (0.56kg), In water 0.75lbs (0.34kg)		
Dimensions:	16.5"long (420mm),1.0"diameter (250mm)		

(2) Submersible Recovery Strobe
The NOVATECH MMF-7500 Mini-Flasher is intended to aid in the marking or recovery of oceanographic instruments, manned vehicles, remotely operated vehicles, buoys or structures. Due to the occulting (firing closely spaced bursts of light) nature of this design, it is much more visible than conventional marker strobes, particularly in poor sea conditions.

(Specifications)

Flash Rate:	Double burst 4 second delay.	Visible Range:	Up to 5 Nm
Battery Type:	7×CR123A Lithinm		
Life:	Approximately 6 days, standard configuration (double burst every 4s at 170 lm)		
Max. Depth:	7,500m	Switch:	Water conductivity
Weight:	air 1.44lbs(0.66kg) water 0.96lbs(0.44kg)		
Dimensions:	length 15.00” (381mm) Diameter 1.44” (29mm)		

2.5.3 Underwater profiling buoy system (POPPS)

Tetsuichi FUJIKI **JAMSTEC**
Masaki FURUHATA **MWJ**
Hiroki USHIROMURA **MWJ**

(1) Objective

An understanding of the variability in phytoplankton productivity provides a basic knowledge of how aquatic ecosystems are structured and functioning. The primary productivity of the world oceans has been measured mostly by the radiocarbon tracer method or the oxygen evolution method. As these traditional methods use the uptake of radiocarbon into particulate matter or changes in oxygen concentration in the bulk fluid, measurements require bottle incubations for periods ranging from hours to a day. This methodological limitation has hindered our understanding of the variability of oceanic primary productivity. To overcome these problems, algorithms for estimating primary productivity by using satellite ocean color imagery have been developed and improved. However, one of the major obstacles to the development and improvement of these algorithms is a lack of *in situ* primary productivity data to verify the satellite estimates.

During the past decade, the utilization of active fluorescence techniques in biological oceanography has brought marked progress in our understanding of phytoplankton photosynthesis in the oceans. Above all, fast repetition rate (FRR) fluorometry reduces the primary electron acceptor (Q_a) in photosystem (PS) II by a series of subsaturating flashlets and can measure a single turnover fluorescence induction curve in PSII. The PSII parameters derived from the fluorescence induction curve provide information on the physiological state related to photosynthesis and can be used to estimate gross primary productivity. FRR fluorometry has several advantages over the above-mentioned traditional methods. Most importantly, because measurements made by FRR fluorometry can be carried out without the need for time-consuming bottle incubations, this method enables real-time high-frequency measurements of primary productivity. In addition, the FRR fluorometer can be used in platform systems such as moorings, drifters, and floats.

The current study aimed to assess the vertical and temporal variations in PSII parameters and primary productivity in the western Pacific, by using an underwater profiling buoy system that uses the FRR fluorometer (system name: POPPS)

(2) Methods

(2-1) Description of the POPPS (for details, see Fujiki et al. 2008)

The POPPS consisted mainly of an observation buoy equipped with a submersible FRR fluorometer (DF-14, Kimoto Electric), a scalar irradiance sensor (QSP-2200, Biospherical Instruments), a CTD sensor (SBE19plusV2, Sea-Bird Scientific), a dissolved oxygen sensor (RINKO III, JFE Advantech), an electrode pH sensor (Kimoto Electric), a nitrate sensor (SUNA V2, Satlantic) and a CDOM sensor (Seapoint UV fluorometer, Seapoint) and an underwater winch (Fig. 2.5.1-1). The observation buoy moved between the winch depth and the surface at a rate of 0.2 m s^{-1} and measured the vertical profiles of phytoplankton fluorescence, irradiance, temperature, salinity, dissolved oxygen, pH, nitrate and CDOM. The profiling rate of the observation buoy was set to 0.2 m s^{-1} to detect small-scale variations (approx. 1 m) in the vertical profile. To minimize biofouling of instruments, the underwater winch was placed below the euphotic layer so that the observation buoy was exposed to light only during the measurement period. In addition, the vertical migration of observation buoy reduced biofouling of instruments.

(2-2) Measurement principle of FRR fluorometer

The FRR fluorometer measures the fluorescence induction curves of phytoplankton samples. To achieve cumulative saturation of PSII within 150 μs — i.e., a single photochemical turnover — the instrument generates a series of subsaturating blue flashes at a light intensity of 30 mmol quanta m^{-2} s^{-1} and a repetition rate of about 500 kHz. The PSII parameters are derived from the single-turnover-type fluorescence induction curve by using

the numerical fitting procedure described by Kolber et al. (1998). Analysis of fluorescence induction curves provides PSII parameters such as fluorescence yields, photochemical efficiency and effective absorption cross section of PSII, which are indicators of the physiological state related to photosynthesis. Using the PSII parameters, the rate of photosynthetic electron transport and the gross primary productivity can be estimated.

(2-3) Observations

At station K2, the POPPS deployed on 23 February 2021 during the MR21-01 cruise was recovered on 3 May 2022. The POPPS was newly-deployed on 7 May 2022, but the deployed POPPS did not work because of a problem with the underwater winch.

In addition, to gain a better understanding of observational data from the POPPS, separately from the POPPS, we moved up and down a submersible FRR fluorometer between surface and ~100 m at the station K2 using a ship winch, and measured the vertical and spatial variation in PSII parameters.

(3) References

Kolber ZS, Prášil O, Falkowski PG (1998) Measurements of variable chlorophyll fluorescence using fast repetition rate techniques: defining methodology and experimental protocols. Biochim Biophys Acta 1367:88–106.

Fujiki T, Hosaka T, Kimoto H, Ishimaru T, Saino T (2008) *In situ* observation of phytoplankton productivity by an underwater profiling buoy system: use of fast repetition rate fluorometry. Mar Ecol Prog Ser 353:81–88.

2.5.4 Remote Automatic Sampler (RAS)

Masahide WAKITA **JAMSTEC**
Hiroshi Uchida **JAMSTEC**
Yoshihisa Mino **Nagoya University**

In order to investigate the seasonal variation of pH in the intermediate layer, and the vertical gradients of biogeochemical properties which affects vertical diffusion flux across the boundary with the thermocline, RAS on 200m and 300m (Figure 1) will work following schedule (Table 1) and collect samples of dissolved inorganic carbon (DIC), total alkalinity (TA), nutrients (Phosphate, Nitrate + Nitrite, Silicate), $^{15}NO_3$ and salinity. We will compare these properties from 12 liter Niskin bottles mounted on the CTD/Carousel Water Sampling System for calibration on RAS samples at K2.

Salinity of RAS seawater samples were measured by salinometer (Model 8400B "AUTOSAL" Guildline Instruments). Salinity measured by salinometer were slightly lower than that observed by SBE-37 sensor (CTD). RAS samples (~500ml) were diluted with 2.5 ml of 20% saturated $HgCl_2$ solution for preservative. For chemical properties, the dilutions of RAS samples by $HgCl_2$ must be corrected by a ratio of salinity by SBE-37 to that by salinometer. We will correct measurements of DIC, TA and nutrients. We used coulometric technique and spectrophotometric system to measure DIC and TA, respectively. Nutrient (silicate, phosphate, and nitrate) concentrations were measured with a continuous flow analyzer. $^{15}NO_3$ will be measured by Tokai University.

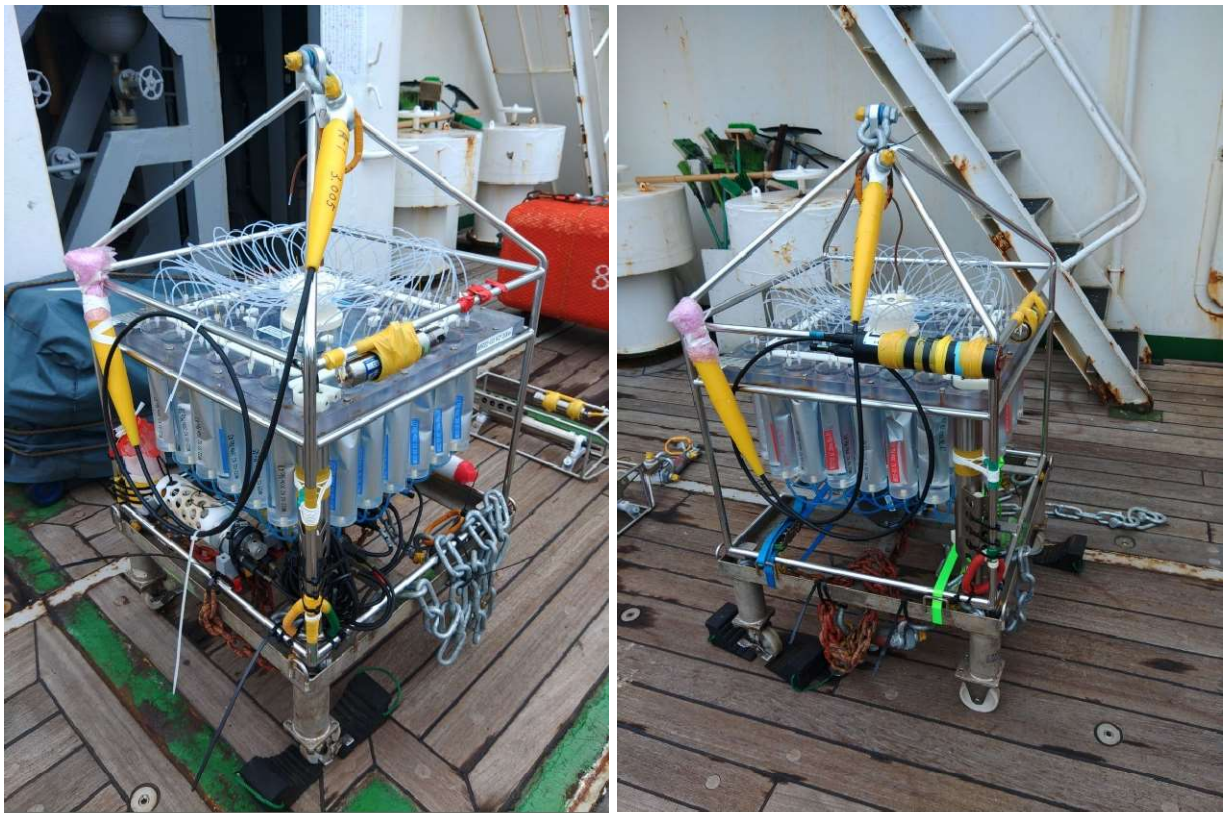

Figure 1 Remote Automatic Samplers deployed on 200m (left) and 300m (right).

Table 1 Sampling schedule of RAS in 200m and 300m on Hybrid mooring at Station K2.

	RAS 200m		**RAS 300m**	
RAS No.	ML11241-09		ML11241-07	
	Interval 10days		Interval 10days	
#	mm/dd/yyyy	Time(UTC)	mm/dd/yyyy	Time(UTC)
1	05/10/2022	1:00:00	05/10/2022	1:00:00
2	05/10/2022	1:40:00	05/10/2022	1:40:00
3	05/20/2022	1:00:00	05/20/2022	1:00:00
4	05/30/2022	1:00:00	05/30/2022	1:00:00
5	06/09/2022	1:00:00	06/09/2022	1:00:00
6	06/19/2022	1:00:00	06/19/2022	1:00:00
7	06/29/2022	1:00:00	06/29/2022	1:00:00
8	07/09/2022	1:00:00	07/09/2022	1:00:00
9	07/19/2022	1:00:00	07/19/2022	1:00:00
10	07/29/2022	1:00:00	07/29/2022	1:00:00
11	08/08/2022	1:00:00	08/08/2022	1:00:00
12	08/18/2022	1:00:00	08/18/2022	1:00:00
13	08/28/2022	1:00:00	08/28/2022	1:00:00
14	09/07/2022	1:00:00	09/07/2022	1:00:00
15	09/17/2022	1:00:00	09/17/2022	1:00:00
16	09/27/2022	1:00:00	09/27/2022	1:00:00
17	10/07/2022	1:00:00	10/07/2022	1:00:00
18	10/17/2022	1:00:00	10/17/2022	1:00:00
19	10/27/2022	1:00:00	10/27/2022	1:00:00
20	11/06/2022	1:00:00	11/06/2022	1:00:00
21	11/16/2022	1:00:00	11/16/2022	1:00:00
22	11/26/2022	1:00:00	11/26/2022	1:00:00
23	12/06/2022	1:00:00	12/06/2022	1:00:00
24	12/16/2022	1:00:00	12/16/2022	1:00:00
25	12/26/2022	1:00:00	12/26/2022	1:00:00
26	01/05/2023	1:00:00	01/05/2023	1:00:00
27	01/15/2023	1:00:00	01/15/2023	1:00:00
28	01/25/2023	1:00:00	01/25/2023	1:00:00
29	02/04/2023	1:00:00	02/04/2023	1:00:00
30	02/14/2023	1:00:00	02/14/2023	1:00:00
31	02/24/2023	1:00:00	02/24/2023	1:00:00
32	03/06/2023	1:00:00	03/06/2023	1:00:00
33	03/16/2023	1:00:00	03/16/2023	1:00:00
34	03/26/2023	1:00:00	03/26/2023	1:00:00
35	04/05/2023	1:00:00	04/05/2023	1:00:00
36	04/15/2023	1:00:00	04/15/2023	1:00:00
37	04/25/2023	1:00:00	04/25/2023	1:00:00
38	05/05/2023	1:00:00	05/05/2023	1:00:00
39	05/05/2023	1:40:00	05/05/2023	1:40:00
40	05/15/2023	1:00:00	05/15/2023	1:00:00
41	05/25/2023	1:00:00	05/25/2023	1:00:00
42	06/04/2023	1:00:00	06/04/2023	1:00:00
43	06/14/2023	1:00:00	06/14/2023	1:00:00
44	06/24/2023	1:00:00	06/24/2023	1:00:00
45	07/04/2023	1:00:00	07/04/2023	1:00:00
46	07/14/2023	1:00:00	07/14/2023	1:00:00
47	07/24/2023	1:00:00	07/24/2023	1:00:00
48	08/03/2023	1:00:00	08/03/2023	1:00:00

2.5.5 Hybrid pH sensor

Yoshiyuki NAKANO JAMSTEC

(1) Objective

We have developed newly stable and accurate *in situ* system for pH measurement using hybrid technique (potentiometric and spectrophotometric). In this cruise, we aim at testing the Hybrid pH sensor (HpHS) in the open sea. We recovered two HpHS at K2 which were deployed at MR21-01 with Hybrid profiling buoy system (150m and 200m).

(2) Method

The HpHS is constituted two types of pH sensors (i.e., potentiometric pH sensor and spectrophotometric pH sensor). The spectrophotometric pH sensor can measure pH correctly and stably, however it needs large power consumption and a lot of reagents in a long period of observation. On the other hand, although the potentiometric pH sensor is low power consumption and high-speed response (within 20 seconds), drifts in the pH of the potentiometric measurements may possibly occur for a long period of observation. The HpHS can measure in situ pH correctly and stably combining advantage of both pH sensors. The HpHS is correcting the value of the potentiometric pH sensor (measuring frequently) by the value of the spectrophotometric pH sensor (measuring less frequently). It is possible to calibrate in situ with standard solution (Tris buffer) on the spectrophotometric pH sensor. Therefore, the drifts in the value of potentiometric pH measurements can be compensated using the pH value obtained from the spectrophotometric pH measurements. Thereby, the sensor can measure accurately the value of pH over a long period of time with low power consumption.

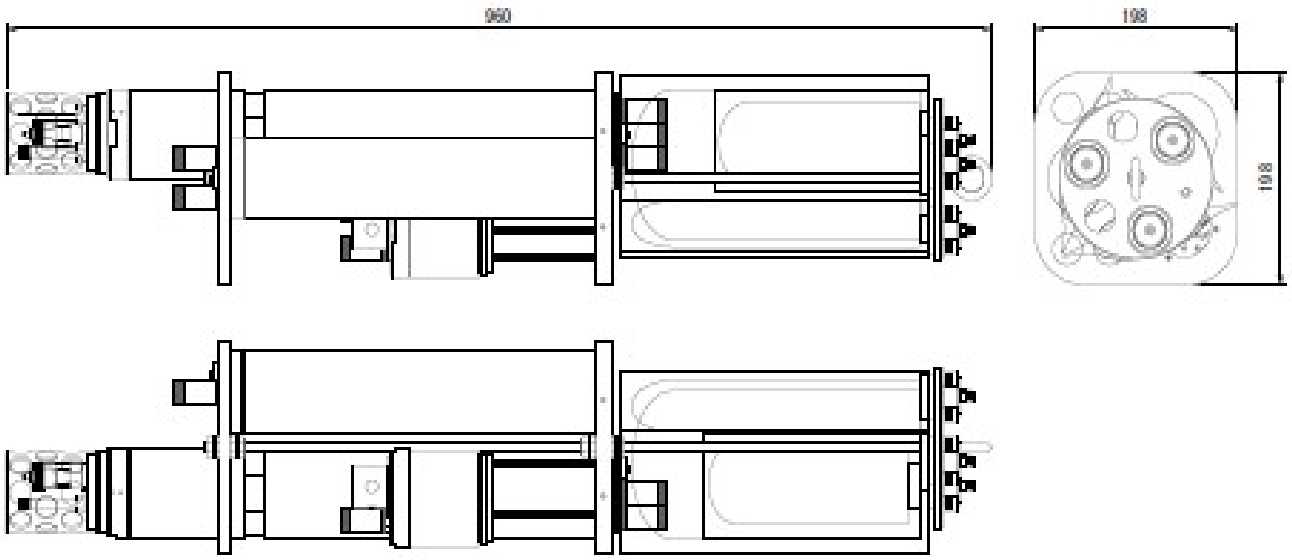

Fig. 2.5.5-1. Side view of HpHS.

Table 2.5.5-1. Specification of HpHS

	Potentiometry	Spectrophotometry
Range	6.0～8.3 pH	7.2～8.2 pH
Initial Accuracy	0.01 pH	0.002 pH
Analytical Method	Glass Electrode	m-cresol purple
Response speed	20 sec (90%, 25 deg C)	1 min (90%)
Resolution	0.001 pH	
Sample rate	1 sec	
Temperature range	0～40 deg C (Resolution: 0.01 deg C)	
Dimension	198×198×960 mm	
Weight	10 kg（in air）	
Depth rating	3,000 m	

(3) Preliminary results

We succeeded in recovering the two HpHS with winch system and RAS in Hybrid profiling buoy system and obtaining long term (about one year) pH data every four hours.

(4) Data Archive

All data will be submitted to JAMSTEC Data Management Office (DMO) and is currently under its control.

Reference

Dickson, A.G., Sabine, C.L. and Christian, J.R. (Eds.) (2007) Guide to best practices for ocean CO_2 measurements. PICES Special Publication 3, 191 pp.

Liu, X., Patsavas, M.C. and Byrne, R.H. (2011) Purification and characterization of meta-cresol purple for spectrophoto-metric seawater pH measurements. Environ. Sci. Technol., 45, pp. 4862-4868.

Takeshita, Y., Martz, T. R., Coletti, L. J., Dickson, A. G., Jannasch H. W., Johnson, K. S. (2017) The effects of pressure on pH of Tris buffer in synthetic seawater. Mer. Chem., 188, pp. 1-5.

2.2.6 Acoustic doppler current profiler (ADCP)

Minoru KITAMURA JAMSTEC

(1) Objective
An Acoustic Doppler Current Profiler (ADCP) was installed at a depth of 370 m on the K2 mooring. Purposes of this acoustic data samplings are (i) to observe seasonal change of current structure (A. Nagano and M. Wakita, JAMSTEC) and (ii) to understand zooplankton dynamics (M. Kitamura, JAMSTEC). Using the former data, we will be able to understand mixing/stratifying processes in the surface layer and nutrient supply to the surface layer due to vertical diffusion. On the other hand, ADCP have been used not only physical oceanography but also biological researches. That is, zooplankton biomass can be estimated using acoustic backscattering intensities collected from ADCP. So, we will also analyze zooplankton dynamics at K2.

(2) Specifications and sampling settings
Specifications
Model: Workhorse LongRanger (Teledyne RD Instruments, Poway, CA, USA)
S/N: 1533 (recovered ADCP), 1434 (deployed ADCP)
Frequency: 75 kHz
Max. depth: 1500m
Dimension: 1014 mm in length, 550 mm in width
Weights: ADCP; 86 kg in air and 55 kg in water and frame: 54 kg in air and 47 kg in water
Beam angle/width: 20°/4°
DC input: 20-60VDC, four internal alkaline battery packs
Voltage: 42V DC (new), 28V DC (depleted)
Velocity resolution: 1mm/s

Setting parameters for data sampling
Depth cell size: 8 m
Number of depth cells: 60
Ping per ensemble: 30
Time per ensemble: 60 min.
Time per ping: 2 min.
Mode: Broadband mode

(3) Result
In the MR22-03 cruise, the ADCP (S/N 1533) installed to the K2H210223 mooring was successfully recovered in 3 May, 2022. Although target depth was 370 m, mooring depth of the ADCP obtained from the CTD (SBE37) attached to the ADCP frame was ca 322 m. And another ADCP (S/N 1434) installed at 370 m of the K2H220507 mooring was successfully deployed in 7 May, 2022.

(4) Data archived
Obtained data will be submitted to JAMSTEC data Management Group after the cruise.

2.5.7 Sediment trap

Minoru KITAMURA **JAMSTEC**
Katsunori KIMOTO **JAMSTEC**
Yoshihisa MINO **Nagoya University**

(1) Objective

To observe long-term trend of the sinking carbon flux at K2, the sediment trap experiment is carried out. Three sediment traps (target depths; 500, 1000 and 4810 m) were successfully recovered from the K2H210223 mooring on 3 May, 2022. And three traps were installed at 500, 1000 m and 4810 m in the K2H220507 mooring which deployed on 7 may, 2022.

(2) Description of instruments

Two kinds of sediment traps were used in this study, SMD26S-6000 (NiGK Corporation, Tokyo, Japan) and MARK78H-21 (McLane Research Laboratories, INC., MA, USA). The former has 26 sampling cups while the latter has 21 cups. Target depths of the samplings were 500, 1000, and 4810 m both in the recovered and the deployed moorings. Sediment trap made by NiGK Corporation was used for the sampling at 500 m in depth, while McLane traps were used for other two depths. Deployed two MacLane traps were newly purchased just before the MR22-03 cruise, and these sediment traps had different electronics (Gen3) from the recovered ones. Specifications and serial numbers of the sediment traps are summarized in the following tables,

Table 2.2.7-1. Specifications of sediment traps

	SMD26S-6000 (NiGK Corporation)	MARK78H-21 (McLane Research Lab.)	MARK78H-21 (McLane Research Lab.)
Max. depth (m)	6000	7000	7000
Dimensions (diameter × height, cm)	104 × 160	91 ×164	91 ×164
Mouth area (m^2)	0.5	0.5	0.5
Weights (kg)	86 in air, 46 in water	72 in air, 39 in water	72 in air, 39 in water
No. of sampling bottles	26	21	21
Volume of sampling bottles (ml)	270	250	250
Battery	Alkaline/Lithium pack	14 Alkaline batteries or a Battery pack	14 Alkaline batteries
Communication cables	RMG4-USB	RMG3-Serial port-USB	SUBCOM6-USB (Cable model: M4787)
Software	N-SMD	Crosscut	MacLanePro
OS	Win 7	Win 7	Win 10

Table 2.2.7-2. Serial numbers and battery types

	Model	S/N	Battery
Recovery from			
454 m	NiGK, SMD26S-6000	26S001	Alkaline/Lithium pack
959 m	McLane, MARK78H-21	ML10558-01	14 Alkaline batteries
4810 m	McLane, MARK78H-21	ML10236-02	Battery pack
Deployed at			
500 m	NiGK, SMD26S-6000	26S029	Alkaline/Lithium pack
1000 m	McLane, MARK78H-21	ML15362-02	14 Alkaline batteries
4810 m	McLane, MARK78H-21	ML15362-01	14 Alkaline batteries

(3) Sampling schedules

Sampling schedules of the recovered and deployed sediment traps were summarized in the following tables. Internal clock of each sediment trap was set in UTC. The deployed mooring systems will be recovered during *Mirai* cruise held in 2023.

Table 2.2.7-3. Sampling schedules of the recovered sediment trap.

NGK Sediment trap_500 m

Bottle No.	Sampling (UTC, yyyy/mm/dd)		
	Start	End	Interval (days)
No.1	2021/02/24 0:00	2021/03/16 0:00	20
No.2	2021/03/16 0:00	2021/04/05 0:00	20
No.3	2021/04/05 0:00	2021/04/15 0:00	10
No.4	2021/04/15 0:00	2021/04/25 0:00	10
No.5	2021/04/25 0:00	2021/05/05 0:00	10
No.6	2021/05/05 0:00	2021/05/15 0:00	10
No.7	2021/05/15 0:00	2021/05/25 0:00	10
No.8	2021/05/25 0:00	2021/06/04 0:00	10
No.9	2021/06/04 0:00	2021/06/14 0:00	10
No.10	2021/06/14 0:00	2021/06/24 0:00	10
No.11	2021/06/24 0:00	2021/07/04 0:00	10
No.12	2021/07/04 0:00	2021/07/14 0:00	10
No.13	2021/07/14 0:00	2021/08/03 0:00	20
No.14	2021/08/03 0:00	2021/08/23 0:00	20
No.15	2021/08/23 0:00	2021/09/12 0:00	20
No.16	2021/09/12 0:00	2021/10/02 0:00	20
No.17	2021/10/02 0:00	2021/10/22 0:00	20
No.18	2021/10/22 0:00	2021/11/11 0:00	20
No.19	2021/11/11 0:00	2021/12/01 0:00	20
No.20	2021/12/01 0:00	2021/12/21 0:00	20
No.21	2021/12/21 0:00	2022/01/10 0:00	20
No.22	2022/01/10 0:00	2022/01/30 0:00	20
No.23	2022/01/30 0:00	2022/02/19 0:00	20
No.24	2022/02/19 0:00	2022/03/11 0:00	20
No.25	2022/03/11 0:00	2022/03/31 0:00	20
No.26	2022/03/31 0:00	2022/04/20 0:00	20

McLane Sediment trap_1000 & 4800 m

Bottle No.	Sampling (UTC, yyyy/mm/dd)		
	Start	End	Interval (days)
No.1	2021/02/24 0:00	2021/03/16 0:00	20
No.2	2021/03/16 0:00	2021/04/05 0:00	20
No.3	2021/04/05 0:00	2021/04/25 0:00	20
No.4	2021/04/25 0:00	2021/05/15 0:00	20
No.5	2021/05/15 0:00	2021/06/04 0:00	20
No.6	2021/06/04 0:00	2021/06/24 0:00	20
No.7	2021/06/24 0:00	2021/07/14 0:00	20
No.8	2021/07/14 0:00	2021/08/03 0:00	20
No.9	2021/08/03 0:00	2021/08/23 0:00	20
No.10	2021/08/23 0:00	2021/09/12 0:00	20
No.11	2021/09/12 0:00	2021/10/02 0:00	20
No.12	2021/10/02 0:00	2021/10/22 0:00	20
No.13	2021/10/22 0:00	2021/11/11 0:00	20
No.14	2021/11/11 0:00	2021/12/01 0:00	20
No.15	2021/12/01 0:00	2021/12/21 0:00	20
No.16	2021/12/21 0:00	2022/01/10 0:00	20
No.17	2022/01/10 0:00	2022/01/30 0:00	20
No.18	2022/01/30 0:00	2022/02/19 0:00	20
No.19	2022/02/19 0:00	2022/03/11 0:00	20
No.20	2022/03/11 0:00	2022/03/31 0:00	20
No.21	2022/03/31 0:00	2022/04/20 0:00	20

Table 2.2.7-4. Sampling schedules of the deployed sediment traps.

NGK Sediment trap_500 m

Bottle No.	Sampling (UTC, yyyy/mm/dd)		
	Start	End	Interval (days)
No.1	2022/05/09 0:00	2022/05/16 0:00	7
No.2	2022/05/16 0:00	2022/05/23 0:00	7
No.3	2022/05/23 0:00	2022/05/30 0:00	7
No.4	2022/05/30 0:00	2022/06/06 0:00	7
No.5	2022/06/06 0:00	2022/06/13 0:00	7
No.6	2022/06/13 0:00	2022/06/20 0:00	7
No.7	2022/06/20 0:00	2022/06/27 0:00	7
No.8	2022/06/27 0:00	2022/07/04 0:00	7
No.9	2022/07/04 0:00	2022/07/11 0:00	7
No.10	2022/07/11 0:00	2022/07/18 0:00	7
No.11	2022/07/18 0:00	2022/07/25 0:00	7
No.12	2022/07/25 0:00	2022/08/01 0:00	7
No.13	2022/08/01 0:00	2022/08/22 0:00	21
No.14	2022/08/22 0:00	2022/09/12 0:00	21
No.15	2022/09/12 0:00	2022/10/03 0:00	21
No.16	2022/10/03 0:00	2022/10/24 0:00	21
No.17	2022/10/24 0:00	2022/11/14 0:00	21
No.18	2022/11/14 0:00	2022/12/05 0:00	21
No.19	2022/12/05 0:00	2022/12/26 0:00	21
No.20	2022/12/26 0:00	2023/01/16 0:00	21
No.21	2023/01/16 0:00	2023/02/06 0:00	21
No.22	2023/02/06 0:00	2023/02/27 0:00	21
No.23	2023/02/27 0:00	2023/03/20 0:00	21
No.24	2023/03/20 0:00	2023/04/10 0:00	21
No.25	2023/04/10 0:00	2023/04/17 0:00	7
No.26	2023/04/17 0:00	2023/04/24 0:00	7

McLane Sediment trap_1000 and 4810m

Bottle No.	Sampling (UTC, yyyy/mm/dd)		
	Start	End	Interval (days)
No.1	2022/05/09 0:00	2022/05/23 0:00	14
No.2	2022/05/23 0:00	2022/06/06 0:00	14
No.3	2022/06/06 0:00	2022/06/20 0:00	14
No.4	2022/06/20 0:00	2022/07/04 0:00	14
No.5	2022/07/04 0:00	2022/07/18 0:00	14
No.6	2022/07/18 0:00	2022/08/01 0:00	14
No.7	2022/08/01 0:00	2022/08/22 0:00	21
No.8	2022/08/22 0:00	2022/09/12 0:00	21
No.9	2022/09/12 0:00	2022/10/03 0:00	21
No.10	2022/10/03 0:00	2022/10/24 0:00	21
No.11	2022/10/24 0:00	2022/11/14 0:00	21
No.12	2022/11/14 0:00	2022/12/05 0:00	21
No.13	2022/12/05 0:00	2022/12/26 0:00	21
No.14	2022/12/26 0:00	2023/01/16 0:00	21
No.15	2023/01/16 0:00	2023/02/06 0:00	21
No.16	2023/02/06 0:00	2023/02/27 0:00	21
No.17	2023/02/27 0:00	2023/03/20 0:00	21
No.18	2023/03/20 0:00	2023/04/10 0:00	21
No.19	2023/04/10 0:00	2023/04/24 0:00	14
No.20	2023/04/24 0:00	2023/05/08 0:00	14
No.21	2023/05/08 0:00	2023/05/22 0:00	14

(4) Preliminary result

All of the three sediment traps in the K2H210223 mooring were successfully recovered. But mooring depths of upper two sediment traps (454 and 956 m) were about 40 m shallower than the target depths.

Rotations of turntables in the sediment traps recovered from 454 and 4810 m were completed as schedules. On the other hand, that from 959 m was stopped in 11 March, 2022 due to low battery. But 19 of 22 events (rotations) were successfully conducted, mechanical behavior of this sediment trap was not so bad. However, sequential sample series of the sinking particles throughout the mooring period were not collected from all the three sediment traps. That is, particle samples were only collected until middle June at 454 m, until end of June and 19 Feb−11 Mar at 959 m, and until early August at 4810 m. Probably, too many sinking particles clogged up an end hole of the sampling cone for all the three sediment traps. Actually, muddy water could be seen in lower part of sampling cone of the recovered sediment trap from 959 m in which rotation of the turntable was abnormally stopped. Considering this trouble, sampling periods of the deployed sediment traps was shortened compared with those of the recovered ones during the productive season at K2, from April to July (see Table 2.2.7-4).

Onboard, heights of the particle samples in the collecting cups were measured with scale in order to know general view of seasonal changes of the sinking particle flux. Using base area of collecting cup (18.1 cm^2), we estimated volume flux for each collecting period (10 or 20 days). Obtained seasonal changes of the volume fluxes at the three depths were shown in the following figure.

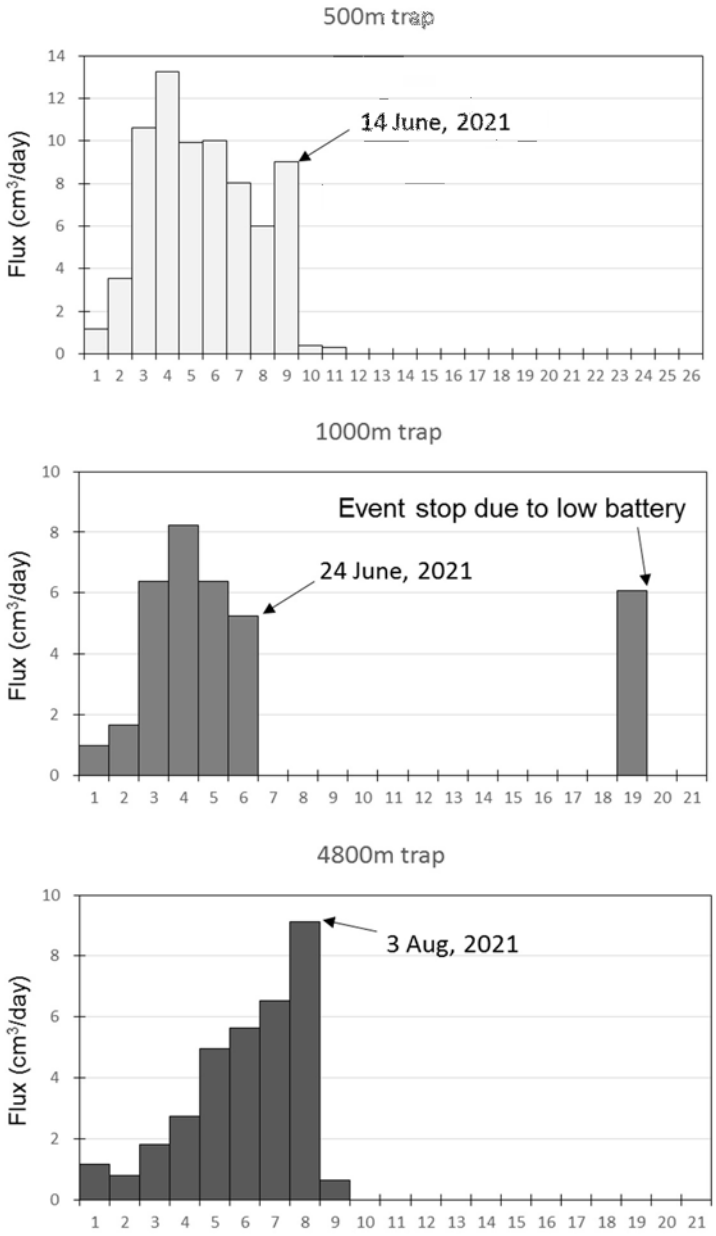

Figure 2.2.7-1. Seasonal changes of volume fluxes at 454, 956 and 4810 m, from top to bottom panels, respectively, at the Station K2.

(5) Sample archives

All samples are stored in JAMSTEC/Yokosuka. Each sample will be divided into ten aliquots and these subsamples will be distributed to co-researchers for further analysis.

2.5.8. CTD, DO sensors

Hiroshi Uchida **JAMSTEC**
Masahide Wakita **JAMSTEC**

(1) Objective
The objective of this study is to grasp variability of temperature, salinity, oxygen and FDOM at the St. K2 mooring site.

(2) Instruments and method
Pressure, temperature, and salinity are measured by CTDs (SBE37SM, Sea-Bird Scientific, Bellevue, Washington, USA). Dissolved oxygen is measured by optical oxygen sensors (Oxygen Optode model 3830, Aanderaa Data Instruments AS, Bergen, Norway, and RINKO-I [ARO-USB] or RINKO-I DSP [AROD-USB], JFE Advantech Co. Ltd., Hyogo, Japan). The Oxygen Optode sensor was attached to a datalogger with an internal battery and memory in a titanium housing (Compact-OPTODE, Alec Electronics Co., Ltd., Hyogo, Japan). Fluorescent dissolved organic matter (FDOM) is measured by an ultraviolet fluorometer (Seapoint Sensors, Inc., Exeter, New Hampshire, USA) with a data logger (RBRduo3, RBR Ltd., Ottawa, Ontario, Canada). A sampling interval was set to 1 hour for these sensors (Table 2.5.8-1).

Table 2.5.8-1 Serial number of the CTD, oxygen, and FDOM sensors deployed in the K2 mooring.

Planned depth	CTD	Oxygen	FDOM	Note
130 m	See 2.5.3	See 2.5.3	6246	POPS (See 2.5.3)
150 m	2287 (SBE37SM)	0003 (CompactOPTODE)	none	Winch
175 m	1892 (SBE37SM)	0006 (CompactOPTODE)	none	SUS frame
200 m	2239 (SBE37SM)	0050 (CompactOPTODE)	6240 (*205142)	RAS
225 m	2730 (SBE37SM)	0004 (RINKO-IDSP)	none	SUS frame
250 m	2756 (SBE37SM)	0092 (RINKO-I)	none	SUS frame
300 m	2289 (SBE37SM)	0051 (RINKO-I)	none	RAS
370 m	2288 (SBE37SM)	0009 (CompactOPTODE)	none	ADCP
500 m	2748 (SBE37SM)	0010 (CompactOPTODE)	none	Trap
780 m	2738 (SBE37SM)	0005 (CompactOPTODE)	none	SUS frame
1000 m	2285 (SBE37SM)	0007 (CompactOPTODE)	none	Trap
Bottom	2731 (SBE37SM)	none	none	Releasers

*Serial number of the RBR data logger

(3) Results
As an example, salinity obtained from the CTDs recovered in this cruise are shown in Fig. 2.2.8-1. Salinity data obtained previous mooring periods are also shown.

(4) Data archive
These obtained data will be submitted to JAMSTEC Data Management Group (DMG) after recovery of the instruments.

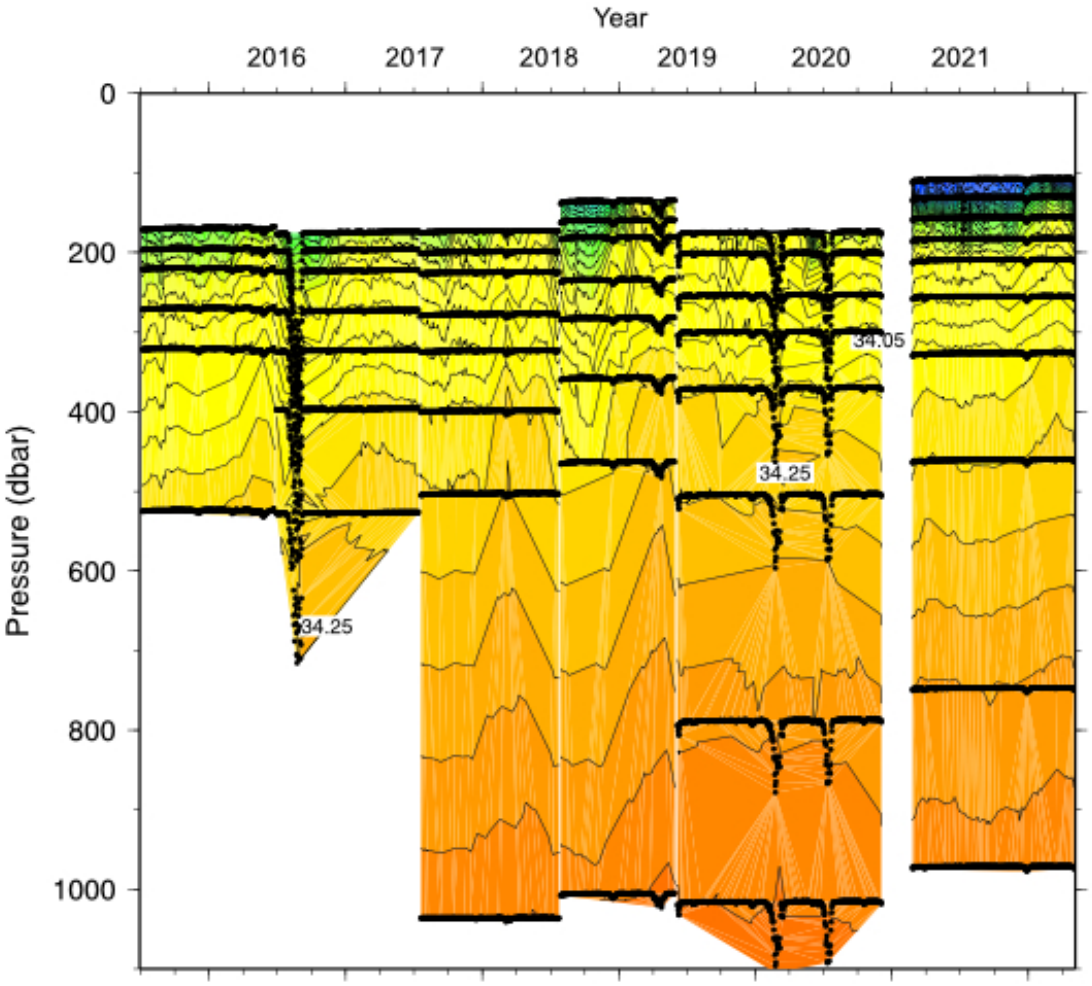

Figure 2.2.8-1. Time series of salinity obtained from the moored CTD at St. K2. Black dots show moored depth of the CTDs.

2.5.9 Experiment of pH and pCO_2 sensors

Kiminori SHITASHIMA	**Tokyo University of Marine Science and Technology**	**PI**
Miaka YAMAGUCHI	**Tokyo University of Marine Science and Technology**	
Katsunori KIMOTO	**JAMSTEC**	

(1) Objective
The objective of this study is to long-term monitoring of in-situ pH and pCO_2 by sensor.

(2) Instruments and methods
A pH/pCO_2 sensor (see 2.3.6) was installed to the top buoy of the hybrid profiling buoy, and in-situ data of pH and pCO_2 ware measured every 4 minutes during mooring observation.

(3) Parameters
In-situ pH and pCO_2

(4) Data archives
All data will be archived at Tokyo University of Marine Science and Technology after checking of data quality and submitted to Data Management Group (DMG) of JAMSTEC.

2.5.10 Backscatter

Makio HONDA JAMSTEC

1. Recovery

On 3rd May 2022, two backscatter meters installed on the K2-hybrid mooring system were recovered. Unfortunately, a backscatter meter at 175 m did not work because of malfunction. Another backscatter meter at 300 m did successfully observe time-series backscatter every 6 hours for longer than 400 days. On the land laboratory, raw data were converted to backscatter data ($bbp_{(700)}$: m^{-1}). Backscatter peaked around late May and early June 2021 and decreased toward winter (Fig.1a). This increase was, in general, synchronized with increase of total mass flux observed by sediment trap at 500 m (Fig.1 b).

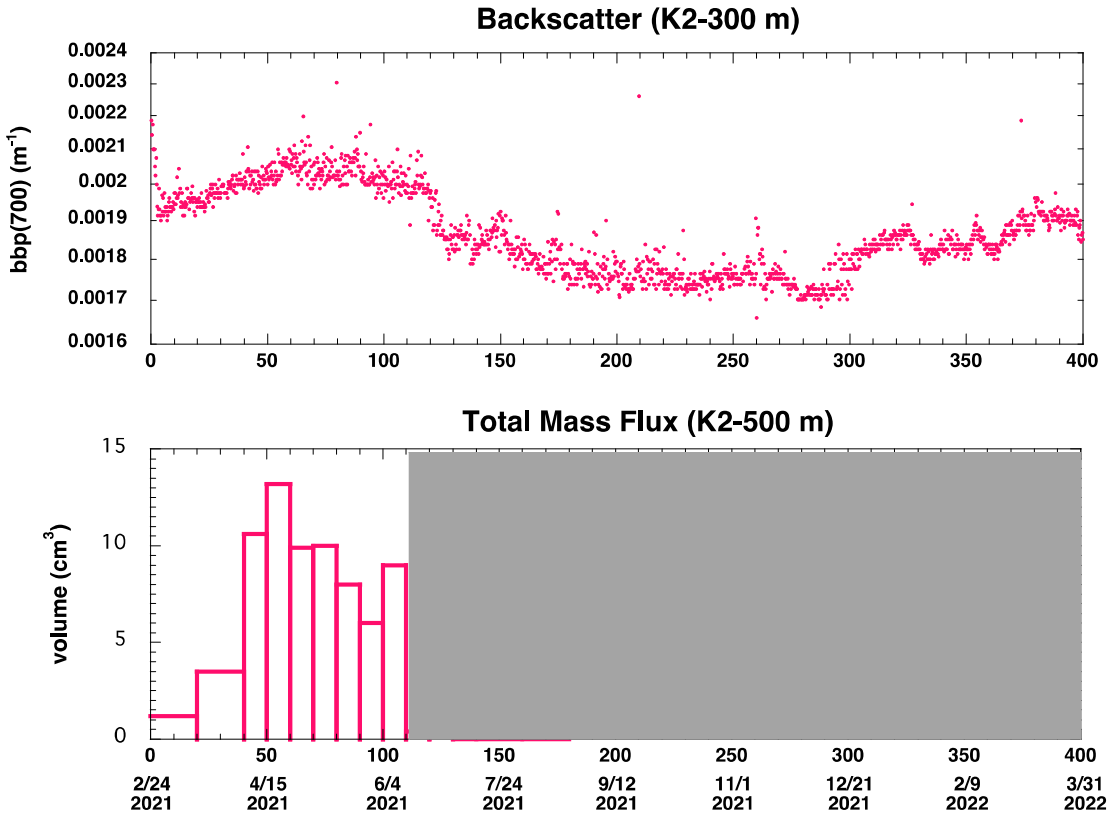

Fig. 2.5.10-1. Temporal variabilities in (a: top) backscatter at 300 m and (b: bottom) total mass flux observed by sediment trap at 500 m. Total mass flux after June 2021 are not available (shown as gray hatched area)

2. Deployment

In order to observe settling particles and/or suspended particles optically, following backscatter meters (BS) were installed on K2 “hybrid” mooring system and deployed during this cruise.

Nominal depth	Instrument	Sampling interval	Sampling time	Start (LST: JST+2 hr.)
175 m (on CTD)	BS FLBBSB #1741	6 hours	30 seconds	7 May 2022
300 m (on RAS)	BS FLBBSB #1742	6 hours	30 seconds	7 May 2022

2.6 Float observation
2.6.1 BGC Argo float

Tetsuichi FUJIKI **JAMSTEC**
Shigeki HOSODA **JAMSTEC**
Kanako SATO **JAMSTEC**
Mizue HIRANO **JAMSTEC**
Rei ITO **MWJ**
Airi HARA **MWJ**

(1) Objectives

The objective of this study is to clarify the mechanisms of climate and oceanic environment variability, to understand changes of earth system through estimations of heat and material transports, and to improve their long-term forecasts of climate changes, by monitoring in the global ocean. To achieve the objective, automatically long-term measurements of physical and biogeochemical parameters are carried out with deployment of Argo floats at the time-series stations K2 (47°N, 160°E) in the western North Pacific Ocean.

At station K2, a BGC Argo float (BGC Navis) has been deployed (Fig. 2.6.1-1), which measures biogeochemical parameters, temperature and salinity down to a depth of 2000 dbar. The purpose of the observation is to clarify changes of phytoplankton community related to environmental parameters. In collaboration with shipboard and mooring observations, long-term and spatial variability of biogeochemical process will be captured in the western North Pacific. The deployed float will also contribute to the international project of BGC Argo to construct the global array.

The BGC Argo float data will also apply to the ESTOC, which is 4D-VAR data assimilation system to estimate state of global ocean for climate changes, to investigate whole mechanism of long-term changes in the ocean.

(2) Parameters

Water temperature, salinity, pressure, dissolved oxygen, backscattering, CDOM[FDOM], chlorophyll, and pH

(3) Methods

Biogeochemical Argo profiling float deployment

We launched BGC Navis float manufactured by the Sea-Bird Scientific. The float equipped SBE41 CTD sensor, SBE63 optical DO sensor and SeaFET pH sensor manufactured by the Sea-Bird Scientific and FLBBCD backscattering, CDOM and chlorophyll sensors manufactured by WET Labs.

The float drifts at a depth of 1000 dbar (called the parking depth) until next vertical measurements, then goes upward from a depth of 2000 dbar to the sea surface. During the ascent, physical and biogeochemical values are measured every 2 dbar or at depths following depth table. During surfacing for a few ten minutes, the float sends all measured data to the land via the Iridium satellite telecommunication system with Rudics protocol. The float observations will be sustained for about a few years depending on internal battery lifetime. The status of float and its launching information is shown in Table 2.6.1-1.

Fig. 2.6.1-1. BGC Argo float deployed at Station K2.

Table 2.6.1-1 Status and launches of BGC floats

BGC Navis Float (2000dbar) (WMO ID: 2903700)

Float Type	BGC Navis float manufactured by Sea-Bird Scientific
CTD sensor	SBE41 manufactured by Sea-Bird Scientific
Oxygen sensor	SBE63 optical DO sensor by Sea-Bird Scientific
Backscatter CDOM Chlorophyll sensors	FLBBCD manufactured by WET Labs Backscattering: wavelength: 700nm CDOM[FDOM]: ex/em→ 370/460nm Chlorophyll: ex/em→ 470/695nm
pH sensor	pH sensor manufactured by Sea-Bird Scientific
Cycle	Every days (To be changed later)
Iridium transmit type	Router-Based Unrestricted Digital Internetworking Connectivity Solutions (RUDICS)
Target Parking Pressure	1000 dbar
Sampling layers	2 dbar or given depth interval from 2000 dbar to surface

Launch

Float S/N	WMOID	Date and Time of Launch (UTC)	Location of Launch	Station
F1445	2903700	2022/05/02 00:25	47-00 [N] 160-02 [E]	K2

(4) Data archive

The Argo float data with real-time quality control are provided to meteorological organizations, research institutes, and universities via Global Data Assembly Center (GDAC: http://www.argodatamgt.org/Access-to-data/Argo-GDAC-ftp-and-https-servers) and Global Telecommunication System (GTS) within 24 hours following the procedure decided by Argo data management team. For physical parameters, delayed-mode quality control is conducted within 6 months ~ 1 year, to satisfy their data accuracy for the use of research. For BGC parameters, the delayed-mode quality control is under consideration for the methods. Those data are freely available via internet and utilized for not only research use but also weather forecasts and any other variable uses.

2.6.2 Deep Ninja Argo float

Yusuke SASAKI	**Atmosphere and Ocean Research Institute, The University of Tokyo**	**PI**
Ichiro YASUDA	**Atmosphere and Ocean Research Institute, The University of Tokyo**	
Shinya KOUKETSU	**JAMSTEC**	
Ken YAMAKI	**Tsurumi Seiki Co., Ltd.**	

(1) Objective

Deep Argo float equipped with microstructure probes was deployed to measure fine scale temperature, salinity and microstructure shear in horizontal velocity and temperature for a long period (~ 1year). The purpose of this study is to explore the relationship between vertical mixing and water mass formation in the western North Pacific Ocean.

(2) Instruments and method

On the previous cruise (MR-21-04), we deployed one Deep Argo float (Deep Ninja) manufactured by Tsurumi Seiki Co., Ltd. This Deep Argo float is equipped with a Sea-Bird Electronics (SBE) 41CP CTD sensor and microstructure probes manufactured by Rockland Scientific International (RSI) Inc. The RSI system records data from microstructure shear probe, fast thermistor temperature probe (FP07) and two accelerometers. The float drifts at the parking depth for a certain period. After a drift, it sinks to the predetermined depth (which is called 'max depth'), then ascends from the max depth to the sea surface. The parking depth, max depth and interval of surfacing for each cast are shown in Table. 2.6.2-2. During the ascent, temperature, salinity, and pressure measurements are obtained from the CTD sensor at a 2dbar interval. Microstructure system is turned on when the float is rising, and microstructure shear and temperature profiles are measured at a 512Hz interval.

While at the surface, the float sends the measured CTD profile (temperature, conductivity, and pressure) and its location to the land via the Iridium communication. The location of the Deep Ninja is specified from the GPS unit (GARMIN GPS15xL). For several surfacing, however, the precise location from GPS was not obtained, probably due to rough sea surface condition. At these surfacing, the location obtained from the Iridium communication was sent to us, which was less accurate than GPS.

Microstructure data are internally recorded in the internal recorder. We downloaded these microstructure data from the instruments after the recovery of the instrument on the present cruise. We plan to examine methods for quality check of the data by comparing these microstructure data with the free fall micro shear structure data (VMP, see Section 2.2.3.3).

(3) Note for using the data

The file included in the data 'DeepNinja_MR2203.csv' shows the correspondence between the profile number and the data file name.

Table 2.6.2-1 Status of Deep Argo float, launch and recovery information

Status of Deep Argo float

Float type		Deep Ninja Tsurumi Seiki Co., Ltd
CTD sensor		SBE41CP manufactured by Sea-Bird Electronics Inc.
Microstructure probe S/N	Shear	M2249
	Fast-response thermistor (FP07)	T2165
Iridium transmit type		Short Burst Data Service (SBD)
Sampling Interval for CTD profiles		2 dbar interval

Launch information

Float S/N	Date	Time (UTC)	Latitude	Longitude
4317	2021/7/25	3:44	47-00.92N	160-01.35E

Recovery information

Float S/N	Date	Time (UTC)	Latitude	Longitude
4317	2022/5/8	19:25	47-57.16N	166-30.45E

Table 2.6.2-2 The information of each profile.

Profile number	Parking depth(dbar)	Maximum depth (dbar)	Time of surfacing		Position of surfacing		
			Date	Time	Lat	Lon	GPS or Iridium
1	NaN	1000	2021/7/25	10:52:41	47-00.5406N	160-01.6555E	GPS
2	175	1000	2021/8/4	11:40:23	47-21.1560N	160-43.0529E	GPS
3	175	1000	2021/8/14	12:16:12	48-09.8732N	161-26.0143E	GPS
4	175	1000	2021/8/24	11:39:07	49-04.6846N	162-07.2638E	GPS
5	2000	2000	2021/9/3	8:33:23	48-52.6689N	162-18.1173E	GPS
6	2000	2000	2021/9/13	9:00:59	48-38.6209N	162-23.7329E	GPS
7	2000	2000	2021/9/23	8:43:58	48-31.9993N	162-28.9680E	GPS
8	2000	2000	2021/10/3	9:32:24	48-10.9614N	162-37.2174E	Iridium
9	2000	2000	2021/10/13	9:29:26	48-07.4064N	162-45.3000E	Iridium
10	2000	2000	2021/10/23	8:50:02	48-09.9069N	162-59.0962E	GPS
11	2000	2000	2021/11/2	9:30:58	48-10.4658N	163-18.0456E	Iridium
12	2000	2000	2021/11/12	9:31:50	48-12.6564N	163-34.4406E	Iridium
13	2000	2000	2021/11/22	9:43:49	48-16.5474N	163-39.7302E	Iridium
14	2000	2000	2021/12/2	9:32:38	48-14.4822N	164-10.3818E	Iridium
15	2000	2000	2021/12/12	9:31:50	48-06.9576N	164-13.0200E	Iridium
16	2000	2000	2022/1/12	8:39:54	47-33.2472N	164-52.8096E	Iridium
17	2000	2000	2022/2/11	8:16:09	47-35.8001N	165-13.1580E	GPS
18	2000	2000	2022/3/13	7:58:48	48-00.1828N	166-05.2969E	GPS
19	2000	2000	2022/4/12	9:01:34	48-02.4918N	166-20.4828E	Iridium
20	2000	2000	2022/4/27	10:52:26	47-54.5442N	166-19.3037E	Iridium
21	2000	2000	2022/5/2	11:51:41	47-54.8888N	166-22.1595E	GPS
22	2000	2000	2022/5/7	11:54:34	47-56.3309N	166-25.1634E	GPS

2.7 Sea surface monitoring

Koji SUGIE JAMSTEC PI
Shiori ARIGA MWJ

(1) Objectives

To understand sea surface environment, data for six parameters in the surface water (water temperature, salinity, dissolved oxygen, fluorescence, turbidity and total dissolved gas pressure) were continuously collected while the ship was in motion.

(2) Instruments and Methods

The six parameters were obtained every one minute by using the Continuous Sea Surface Water Monitoring System (Marine Works Japan Co. Ltd.) which was a thermosalinograph (TSG) with Salinity, water temperature, dissolved oxygen, fluorescence, turbidity and total dissolved gas pressure sensors. This system was located in the "sea surface monitoring laboratory" and connected to shipboard LAN-system. Sea water was continuously pumped up to the laboratory from an intake placed at the approximately 4.5 m below the sea surface and flowed into the system through a vinyl-chloride pipe. The flow rate of the surface seawater was adjusted to 10 dm^3 min^{-1}. Measured data, time, and location of the ship were stored in a data management PC. Specification of this system is herein described.

a. Instruments

Software: SeaMoni Ver.1.2.0.0

Sensors

Specifications of each sensor in this system are listed below. This time Bottom of ship thermometer (SBE38) is not used because it was damaged.

Temperature and Conductivity sensor

Model:	SBE-45, SEA-BIRD ELECTRONICS, INC.
Serial number:	4557820-0319
Measurement range:	Temperature -5 ºC - +35 ºC
	Conductivity 0 S m^{-1} - 7 S m^{-1}
Initial accuracy:	Temperature 0.002 ºC
	Conductivity 0.0003 S m^{-1}
Typical stability (per month):	Temperature 0.0002 ºC
	Conductivity 0.0003 S m^{-1}
Resolution:	Temperature 0.0001 ºC
	Conductivity 0.00001 S m^{-1}

Dissolved oxygen sensor

Model:	RINKO II, JFE ADVANTECH CO. LTD.
Serial number:	35,13
Measuring range:	0 mg L^{-1} - 20 mg L^{-1}
Resolution:	0.001 mg L^{-1} - 0.004 mg L^{-1} (25 ºC)
Accuracy:	Saturation ± 2 % F.S. (non-linear) (1 atm, 25 ºC)

Fluorescence & Turbidity sensor

Model:	C3, TURNER DESIGNS
Serial number:	2300707
Measuring range:	Chlorophyll in vivo 0 μg L^{-1} – 500 μg L^{-1}
Minimum Detection Limit:	Chlorophyll in vivo 0.03 μg L^{-1}
Measuring range:	Turbidity 0 NTU - 1500 NTU
Minimum Detection Limit:	Turbidity 0.05 NTU

Total dissolved gas pressure sensor

Model:	HGTD-Pro, PRO OCEANUS
Serial number:	36-296-10
Temperature range:	-2 °C - 50 °C
Resolution:	0.0001 %
Accuracy:	0.01 % (Temperature Compensated)
Sensor Drift:	0.02 % per year max (0.001 % typical)

(3) Observation log

Periods of measurement, maintenance, and problems during this cruise are listed in Table 2.7-1. We took samples of surface water from a sampling drain of this system once a day or two days. Because of calibrate sensor data for salinity, dissolved oxygen, and chlorophyll *a*. The results of calibrations are shown in Fig. 2.7-1. All the water samples for salinity calibration were analyzed by using the Model 8400B "AUTOSAL" manufactured by Guildline Instruments Ltd. (see 2.2.2), those for dissolve oxygen were analyzed by Winkler method (see 2.3.1), and chlorophyll *a* were analyzed by using 10-AU manufactured by Turner Designs. (see 2.4.1).

(4) Preliminary data

Horizontal variabilities of sea surface temperature, salinity, dissolved oxygen and fluorescence are shown in Fig. 2.7-2.

(5) Data archives

These data obtained in this cruise will be submitted to the Data Management Group (DMG) of JAMSTEC, and will opened to the public via "Data Research System for Whole Cruise Information in JAMSTEC (DARWIN)" in JAMSTEC web site. <http://www.godac.jamstec.go.jp/darwin/e>

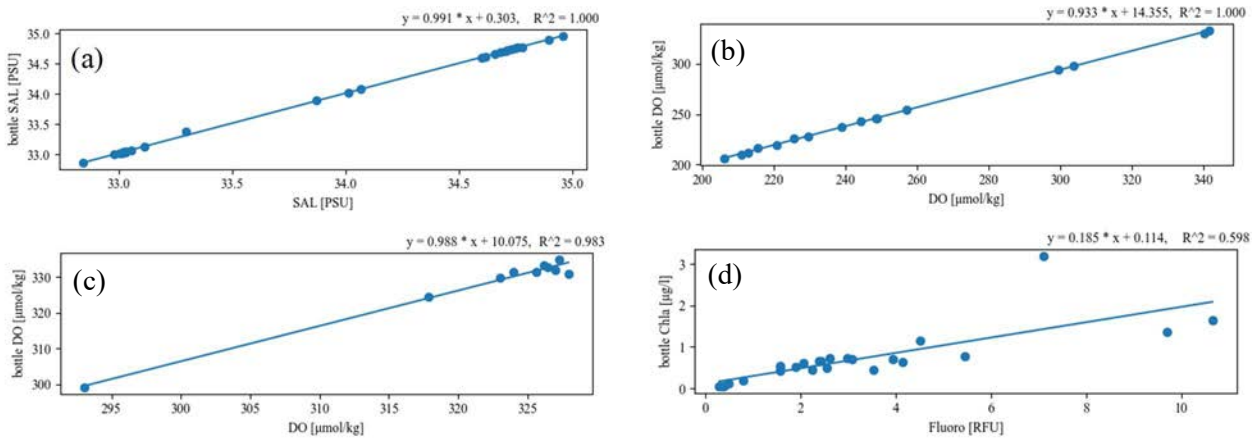

Figure 2.7-1 Results of sensor data validations for (a) salinity, (b-1) dissolved oxygen (S/N:0035), (b-2) dissolved oxygen (S/N:0013) and (c) fluorescence in MR22-03 cruise.

Table 2.7-1 Events list of the Sea surface water monitoring during MR22-03

System Date [UTC]	System Time [UTC]	Events	Remarks
2022/04/16	08:45	All the measurements started and data was available.	Start
2022/04/25	18:17-18:18	RINKOII communication interruption.	-
2022/04/25	18:40-18:41	RINKOII communication interruption.	-
2022/04/25	20:20-20:22	RINKOII communication interruption.	-
2022/04/26	01:50-01:51	RINKOII communication interruption.	-
2022/04/26	03:34-03:41	RINKOII the measurements stopped.	RINKOII Maintenance
2022/04/28	14:37-14:39	RINKOII communication interruption.	-
2022/04/30	14:58	RINKOII communication interruption.	-
2022/04/30	19:43	RINKOII communication interruption.	-
2022/04/30	21:34-21:35	RINKOII communication interruption.	-
2022/05/02	05:03	RINKOII communication interruption.	-
2022/05/02	06:56-07:00	RINKOII communication interruption.	-
2022/05/03	16:43-16:47	RINKOII communication interruption.	-
2022/05/04	02:14-03:59	All the measurements stopped.	RINKOII exchange Filter maintenance
2022/05/04	04:00	All the measurements started.	Logging restart
2022/05/14	01:53-01:59	RINKOII communication interruption.	-
2022/05/14	04:07-04:09	RINKOII communication interruption.	-
2022/05/14	04:15	RINKOII communication interruption.	-
2022/05/14	05:18	RINKOII communication interruption.	-
2022/05/16	10:02	RINKOII communication interruption.	-
2022/05/16	10:58-11:01	RINKOII communication interruption.	-
2022/05/16	11:08	RINKOII communication interruption.	-
2022/05/16	12:18-12:23	RINKOII communication interruption.	-
2022/05/16	12:47-12:48	RINKOII communication interruption.	-
2022/05/17	05:04	HGTD-Pro the measurements stopped.	-
2022/05/17	06:30	All the measurements stopped.	End

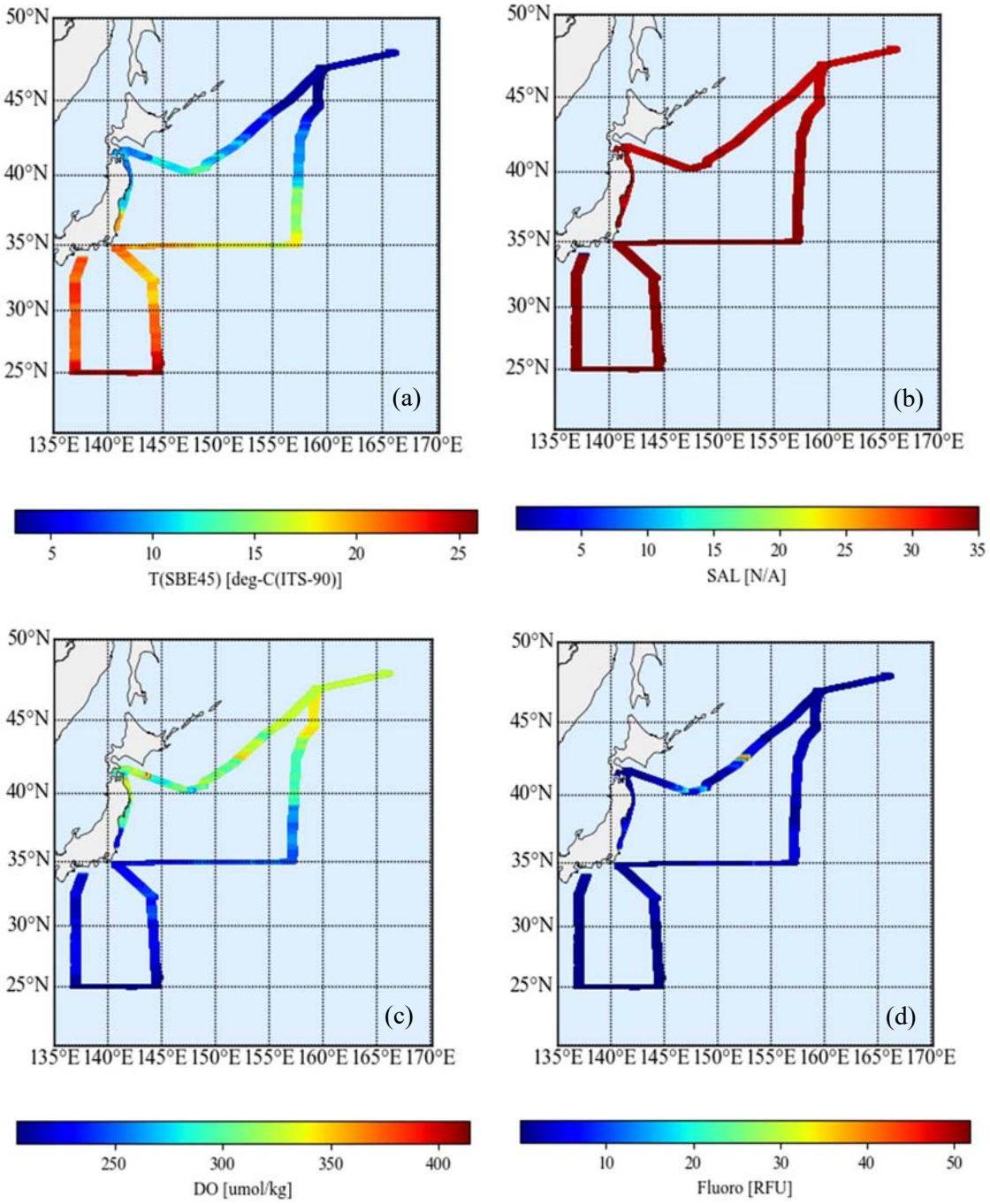

Figure 2.7-2. Horizontal variabilities of (a) temperature, (b) salinity, (c) dissolved oxygen, and (d) fluorescence in MR22-03 cruise.

2.8 Microplastic sampling

Masashi TSUCHIYA JAMSTEC
Ryota NAKAJIMA JAMSTEC
Masahide WAKITA JAMSTEC
Minoru KITAMURA JAMSTEC

(1) Objectives

The distribution of microplastics (MPs) in the open ocean of the western Pacific is largely undocumented. Substantial numbers of studies on floating MPs have been reported in the Eastern Pacific and Atlantic Ocean, yet fewer data are available in the Western Pacific. Many MPs have been observed in the vicinity of the study area of this cruise (Isobe et al., 2015) This survey was conducted in 2014, and it is important to know if there are changes over time to understand the behavior of MPs. In the present study, we conducted MPs surveys in the Tsugaru Strait (off Shiriyazaki Cape and off Kameda Peninsula) to find the MPs accumulation. The behavior of MPs reaching coastal areas can be evaluated by clarifying their relationship with eddies that occur in the Tsugaru Strait and with MPs observed in coastal areas such as Sekinehama area.

(2) Neuston net sampling for surface MPs

From May 15th to 16th 2022, a total 6 neuston net towing was conducted at stations 14 (41˚48'N, 141˚19'E) and 15 (41˚40'N, 141˚30'E). Floating MP samples were collected using a neuston net with a 333 μm opening mesh (Rigo Co., Ltd., Tokyo, Japan) and a collecting net (100 μm) at the cod-end. The net without cod-end was rinsed from the outside with seawater prior to use. At each station, the net was towed three times at 1–2 knots for 15–20 min. from the starboard side. A flow meter (Rigo) was installed at the net mouth to estimate the volume of water filtered during each tow. The collected samples were fixed with 10% formalin and stored at room temperature until analysis.

(3) Preliminary result

At St. 14, a large number of drifting algae/seaweeds were collected in the net. Also, many diatoms entered the net and may have clogged it at St. 15. MP samples collected from the neuston net will be sorted and measured size and quantities, and the type of MPs will be identified using a microscope and FT-IR. The microplastics will also be weighed for mass calculation. The distribution, density, and concentration of microplastics obtained in this study will be compared to the previous reports in the Western Pacific, Tsugaru Strait and trapped microplastics in Sekinehama.

(4) Data archive

The obtained data will be submitted to JAMSTEC Data Management Group (DMG).

2.9 Geophysical observations

2.9.1 Swath bathymetry

Koji SUGIE	**JAMSTEC**	**PI**
Yutaro MURAKAMI	**NME**	
Ryo OYAMA	**NME**	
Fumine OKADA	**NME**	
Yoichi INOUE	**MIRAI crew**	

(1) Objectives
R/V MIRAI equip with the Multi Beam Echo Sounding system (MBES; SEABEAM 3012 (L3 Communications ELAC Nautik, Germany)). The objective of MBES is collecting continuous bathymetric data along ship's track to make a contribution to geological and geophysical investigations and global data sets.

(2) Instruments and methods
The "SEABEAM 3012" on R/V MIRAI was used for bathymetry mapping during this cruise. To get accurate sound velocity of water column for ray-path correction of acoustic multibeam, we used Surface Sound Velocimeter (SSV) data to get the sea surface (6.62m) sound velocity, and the deeper depth sound velocity profiles were calculated by temperature and salinity profiles from CTD, and Argo float data by the equation in Del Grosso (1974) during the cruise. The system configuration and performance are shown in Table 2.9.1-1.

Table 2.9.1-1. SEABEAM 3012 System configuration and performance

Frequency:	12 kHz
Transmit beam width:	2.0 degree
Transmit power:	4 kW
Transmit pulse length:	2 to 20 msec.
Receive beam width:	1.6 degree
Depth range:	50 to 11,000 m
Number of beams:	301 beams (Spacing mode: Equi-angle)
Beam spacing:	1.5 % of water depth (Spacing mode: Equi-distance)
Swath width:	60 to 150 degrees
Depth accuracy:	< 1 % of water depth (average across the swath)

(3) Preliminary result
The results will be published after primary processing.

(4) Data archive
These obtained data will be submitted to JAMSTEC Data Management Group (DMG).

(5) remarks
1. The following periods, data acquisition was suspended due to operating of ANS system.
18:50UTC 02 May. 2022 - 19:58UTC 02 May. 2022
01:41UTC 07 May. 2022 - 02:00UTC 07 May. 2022

2. The following period, incorrect VRU mounting error(roll/pitch/yaw) were applied to the system.
07:28UTC 16 Apr. 2022 - 18:56UTC 10 May. 2022

2.9.2 Sea surface gravity

Koji SUGIE	**JAMSTEC**	**PI**
Yutaro MURAKAMI	**NME**	
Ryo OYAMA	**NME**	
Fumine OKADA	**NME**	
Yoichi INOUE	**MIRAI crew**	

(1) Objectives

The local gravity is an important parameter in geophysics and geodesy. We collected gravity data at the sea surface.

(2) Instruments and methods

We measured relative gravity using LaCoste and Romberg air-sea gravity meter S-116 (Micro-G LaCoste, LLC) during this cruise. To convert the relative gravity to absolute gravity at Shimizu as the reference points. Parameters of gravity meter are as follows:

Relative Gravity [CU: Counter Unit]
[mGal] = (coef1: 0.9946) * [CU]

(3) Preliminary results

Absolute gravity table is shown in Table 2.9.2

Table 2.9.2 Absolute gravity table of this cruise

No.	Date m/d	UTC	Port	Absolute Gravity [mGal]	Sea Level [cm]	Ship Draft [cm]	Gravity at Sensor *1 [mGal]	S-116 Gravity [mGal]
#1	4/15	06:42	Shimizu	979728.98	158	631	979729.69	12001.36
#2	5/20	23:00	Shimizu	979728.98	174	593	979729.65	12001.08

*1: Gravity at Sensor = Absolute Gravity + Sea Level*0.3086/100 + (Draft-530)/100*0.2222

(4) Data archive

These obtained data will be submitted to JAMSTEC Data Management Group (DMG).

(5) Remarks (Time is UTC)

The following period, gravity data (GRAVITY, SPRING TENSION) include spike noise due to rough sea condition.
14:36UTC 30 Apr. 2022 - 18:35UTC 30 Apr. 2022

2.9.3 Sea surface magnetic field

Koji SUGIE	**JAMSTEC**	**PI**
Yutaro MURAKAMI	**NME**	
Ryo OYAMA	**NME**	
Fumine OKADA	**NME**	
Yoichi INOUE	**MIRAI crew**	

(1) Objectives

Measurement of magnetic force on the sea is required for the geophysical investigations of marine magnetic anomaly caused by magnetization in upper crustal structure. We measured geomagnetic field using a three-component magnetometer during this cruise.

(2) Instruments and methods

A shipboard three-component magnetometer system (Tierra Tecnica SFG2018) is equipped on-board R/V MIRAI. Three-axes flux-gate sensors with ring-cored coils are fixed on the fore mast. Outputs from the sensors are digitized by a 20-bit A/D converter (1 nT/LSB), and sampled at 8 times per second. Ship's heading, pitch, and roll are measured by the Inertial Navigation System (INS, PHINS). Ship's position and speed data are taken from LAN every second.

(3) Principle of ship-board geomagnetic vector measurement

The relation between a magnetic-field vector observed on-board, *Hob*, (in the ship's fixed coordinate system) and the geomagnetic field vector, *F*, (in the Earth's fixed coordinate system) is expressed as:

$Hob = A * R * P * Y * F + Hp$ (a)

where, *R*, *P* and *Y* are the matrices of rotation due to roll, pitch and heading of a ship, respectively. *A* is a 3 x 3 matrix which represents magnetic susceptibility of the ship, and *Hp* is a magnetic field vector produced by a permanent magnetic moment of the ship's body. Rearrangement of Eq. (a) makes

$R * Hob + Hbp = R * P * Y * F$ (b)

where $R = A^{-1}$, and $Hbp = -R * Hp$. The magnetic field, *F*, can be obtained by measuring *R*, *P*, *Y* and *Hob*, if *R* and *Hbp* are known. Twelve constants in *R* and *Hbp* can be determined by measuring variation of Hob with *R*, *P* and *Y* at a place where the geomagnetic field, *F*, is known.

(4) Preliminary result

The results will be published after primary processing.

(5) Data archive

These obtained data will be submitted to JAMSTEC Data Management Group (DMG).

(6) Remarks (Times in UTC)

The following periods, we made a “figure-eight” turn (a pair of clockwise and anti-clockwise rotation) for calibration of the ship’s magnetic effect.

07:31 19 Apr. 2022 - 07:53 19 Apr. 2022 (25-00N, 137-29E)
07:50 28 Apr. 2022 - 08:12 28 Apr. 2022 (35-04N, 157-37E)
04:03 07 May. 2022 - 04:28 07 May. 2022 (47-01N, 160-03E)

2.10 Satellite image acquisition (MCSST from NOAA/HPRT)

Koji SUGIE	**JAMSTEC**	**PI**
Yutaro MURAKAMI	**NME**	
Ryo OYAMA	**NME**	
Fumine OKADA	**NME**	
Yoichi INOUE	**MIRAI crew**	

(1) Objectives

The objectives are to collect cloud data in a high spatial resolution mode from the Advance Very High Resolution Radiometer (AVHRR) on the NOAA and MetOp polar orbiting satellites.

(2) Instruments and Methods

We received the down link High Resolution Picture Transmission (HRPT) signal from polar orbiting satellites, which passed over the area around the R/V MIRAI. The receiving antenna (Model 1084, Sea Space Inc.) is placed on the roof of after wheel house. We processed the HRPT signal with the in-flight calibration and computed the brightness temperature (MCSST). A cloud image map around the R/V MIRAI was made from the data for each pass of satellites.

We received and processed polar orbiting satellites data throughout this cruise.

(3) Preliminary results

Fig.2.10-1 show the MCSST image in this cruise (1st to 12th May.).

(4) Data archives

These obtained data will be submitted to JAMSTEC Data Management Group (DMG).

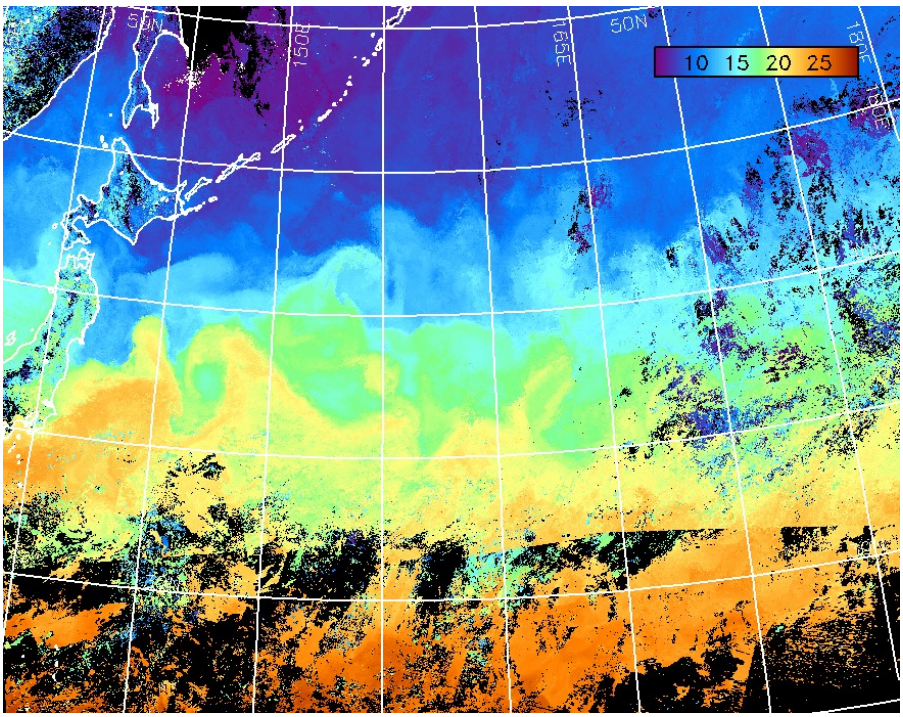

Fig.2.10-1 MCSST image in this cruise (1st to 12th May.)

3. Notice on use

This cruise report is a preliminary documentation as of the end of cruise.
This report is not necessarily corrected even if there is any inaccurate description (i.e. taxonomic classifications).
This report is subject to be revised without notice. Some data on this report may be raw or unprocessed. If you are going to use or refer the data on this report, it is recommended to ask the Chief Scientist for latest status.
Users of information on this report are requested to submit Publication Report to JAMSTEC.